Enhancing Sensitivity in the Analysis of Small Biomolecules by Surface Plasmon Resonance

A thesis presented in partial fulfilment of the requirements for the degree of

Doctor of Philosophy

in Chemistry

at Massey University, Manawatu,

New Zealand.

Gaile Suzanne Dombroski

2012

Abstract

Highly potent biological micro-pollutants in the aquatic environment can potentially have detrimental effects on marine and human health, but the development of highly sensitive test methods suitable for use in a field environment remains a challenge.

Surface plasmon resonance (SPR) is an optical-electrical phenomenon, which can be applied to the monitoring of surface binding, allowing the measurement of bio-molecular interactions in real time, without the use of radioisotope or fluorescent labeling. The technique has wide utility in the application to biological sensing, including quantitative concentration measurements and the qualitative comparison of binding partners.

The central focus of this study was to investigate quantitative techniques and improve sensitivity using various strategies, including the incorporation of linkers into one of the binding partners and exploiting the signal enhancement properties of secondary antibodies and gold nanoparticles. The use of functionalised terthiophene as an alternative scaffold for immobilising the binding partner was investigated. The effect of attaching the binding partner as a protein conjugate compared to its protein-free counterpart was explored.

Presented here is the use of SPR to investigate an estrone-antibody binding system, which has potential application in the analysis of wastewaters. The binding of a number of estrone derivatives was evaluated, with a view to being able to 'tune' the binding system so that the sensitivity range fell within a range suitable for the application. The use of secondary antibodies and gold nanoparticles to enhance the sensitivity further was also examined in the estrone system. The findings were later applied to the development of a highly sensitive test method for the detection of the shellfish toxin, domoic acid. Finally, investigations into an alternative scaffold to which one binding partner was attached to form the recognition element on the

biosensor surface were carried out with a view to creating a generic scaffold for SPR sensor surfaces.

Acknowledgements

I would like to acknowledge the many people who have contributed to this research and the thesis. Firstly, I would like to thank my supervisors, Associate Professor Ashton Partridge and Professor Peter Derrick. I am thankful for Ashton's infectious enthusiasm, particularly in the early stages of the project and for Peter's readiness to take up the supervisory reins when Ashton departed for Auckland. Peter's advice has been particularly helpful during the often arduous writing stage.

Thanks must also go to laboratory colleagues past and present for their camaraderie and willingness to help. Two members of the research group deserve particular mention. The advice and support of Dr Krishanthi Jayasundera and Dr Wayne Campbell has been invaluable in keeping me on track and both have provided clarity and encouragement when necessary.

A special mention must go to Associate Professor Len Blackwell for his practical expertise and for kindly supplying estrone antibodies and reference materials. The advice of Dr Yinqiu Wu (Plant and Food Research) was also invaluable, particularly in the early stages. Thanks also go to Professor Richard Haverkamp for carrying out the AFM, and to Professor Simon Hall and Nessha Wise for assistance with electrochemistry. I must also thank Professor Keith Gordon from the University of Otago for carrying out resonance Raman and dispersion experiments.

I would like to thank Dr Doug Mountfort and Dr Patrick Holland of the Cawthron Institute for generating the domoic acid project, and Professor Christopher Elliot and Dr Katrina Campbell of Queen's University for supplying antibody and advice.

I must acknowledge the financial contribution of the Institute of Fundamental Sciences, Massey University and the MacDiarmid Institute for Advanced Materials and Nanotechnology for my scholarship and funding.

Finally, I would like to thank family and friends for their support and encouragement, particularly Jeremy, Anna and Libby.

Table of Contents

List of Figures

List of Tables

List of Schemes

Abbreviations

AFM	atomic force microscopy
AP	alkaline phosphatase
BOC	tertiary butoxide protecting group
brs	broad singlet
BSA	bovine serum albumin
CE	counter electrode
CV	cyclic voltammetry
d	doublet
DCC	*N,N*'-Dicyclohexylcarbodiimide
DCM	dichloromethane
dil.	dilute
DME	1,2-dimethoxyethane
DMF	dimethylformamide
E1	estrone
E1G	estrone glucuronide
E2	estradiol
EDC	N-ethyl-N-(3-dimethylaminopropyl)-carbodiimide (as the hydrochloride)
EDTA	ethylenediamine tetra-acetic acid
EE2	17α-ethynylestradiol

EI	electron ionisation
ELISA	enzyme-linked immunosorbent assay
equiv.	equivalents
EtOAc	ethyl acetate
eV	electron volts
FC	flow cell
FCC	flash column chromatography
h	hour(s)
HEPES	4-(2-hydroxyethyl)-1-piperazine ethanesulfonic acid
Hex	hexane
HOAc	acetic acid
HRMS	high resolution mass spectrometry
HRP	horse radish peroxidase
IFC	integrated fluidics cartridge
LC-MS	liquid chromatography - mass spectrometry
LOD	limit of detection
m	multiplet
mAb	monoclonal antibody
MALDI	matrix assisted laser desorption ionisation
mg	milligrams
ms	milliseconds

MHz	megahertz
Milli-Q water	ultrapure water filtered through a 0.22 micron filter with a resistivity 18.2 MΩ·cm at 25 ^{o}C
min	minute
MIP	molecularly-imprinted polymer
mL	milliliters
mmol	millimoles
MS	mass spectroscopy
MW	molecular weight
nBuLi	n-butyllithium
ND	not detected
N-Glu	*N*-acetylglutamic acid
NHS	*N*-hydroxysuccinimide
NMR	nuclear magnetic resonance
NSB	non-specific binding
OEG	oligo(ethylene glycol)
OVA	ovalbumin
pAb	polyclonal antibody
PBS	phosphate buffered saline
PBS/T	phosphate buffered saline with Tween
PEG	poly(ethylene glycol)

PES	phenylether sulphone
q	quartet
RE	reference electrode
rt	room temperature
RU	response unit
SAM	self-assembled monolayer
SD	standard deviation
SEM	scanning electron microscopy
SPR	surface plasmon resonance
t	triplet
TBAP	tetrabutylammonium perchlorate
TFA	trifluoroacetic acid
THF	tetrahydrofuran
TMB	tetramethyl benzidine
TOF	time-of-flight
UV	ultra-violet
WE	working electrode

Chapter 1

Introduction

1.1 Challenges for the Aquatic Environment

The need for sensitive analytical test methods has been highlighted in recent years, as it has become apparent that low levels of some compounds can have a marked effect on human and animal health. A growing body of research indicates that these highly potent compounds are present at concentrations of toxicological concern. The quality of the aquatic environment can be affected by micro-pollutants such as the endocrine-disrupting estrogens, both natural and synthetic. Harmful algal blooms in seawater produce highly potent marine biotoxins which accumulate in shellfish. Human consumption of contaminated shellfish can result in illness or death. Developing reliable and cost-effective test methods for these highly potent compounds remains a challenge.

1.1.1 Estrogens in Wastewater

The presence of estrogenic compounds in wastewater has raised significant concerns because of their adverse effect on biological systems [1], and, by implication, the potential detrimental impact these compounds might have on human health [2, 3]. Trace amounts of these compounds can interfere with the normal functioning of the human reproductive system, resulting in changes in development, and have been linked to similar effects in other organisms in aqueous systems [4]. The natural estrogens estrone (E1) (**1**) and 17β-estradiol (E2) (**2**), and the synthetic 17α-ethynylestradiol (EE2) (**3**) widely used in oral contraceptives, are of particular interest (Figure 1), although other compounds including parabens have also shown estrogenic activity [5, 6]. These concerns have stimulated the need for highly sensitive detection at the very low levels that these compounds are found in the environment [7].

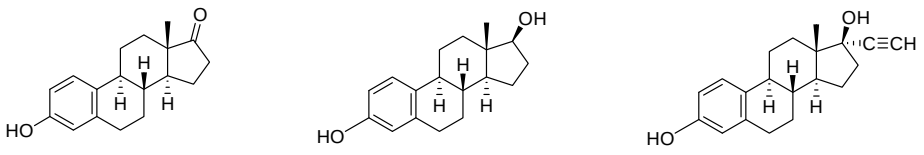

Estrone (E1) (**1**) 17 β-Estradiol (E2) (**2**) Ethynylestradiol (EE2) (**3**)

Figure 1: The natural estrogens E1 and E2, and synthetic EE2.

The most widely used method for determination of estrogenic compounds is liquid chromatography, making use of various detection techniques including ultra-violet spectrometry, fluorescence and mass spectrometry. Mass spectrometry provides the lowest detection levels, but to achieve optimum sensitivity it is necessary to pre-concentrate the samples, typically using solid phase extraction procedures [8-10].

Surface plasmon resonance biosensors offer great promise for the sensitive detection of estrogens and other compounds. While it is likely that the liquid chromatography-mass spectrometry (LC-MS) methods will remain the 'gold standard', surface plasmon resonance biosensors offer a means of screening samples and obtaining rapid results in the field, allowing a subsequent analysis of suspect samples with LC-MS in the laboratory. This two-tier system is a time- and cost-effective means of running monitoring programs.

1.1.2 Shellfish Toxins

The New Zealand coastline has been affected in recent years, by algal blooms which generate toxins. These potent toxins can accumulate in shellfish. There is no evidence that the toxins harm the shellfish, but they are harmful to human health if ingested [11, 12]. In 1993, a significant outbreak of cases of shellfish poisoning cases occurred, resulting in over 150 people being affected with neurologic and gastro-intestinal symptoms [13], and for a time shellfish harvesting along the entire New Zealand coastline was halted entirely. Since then, the country's regulatory authorities have conducted a comprehensive shellfish sampling and analysis program, the New Zealand Marine Biotoxin Monitoring Program, designed to protect the health of local consumers, and to satisfy valuable overseas markets that

New Zealand shellfish are safe and conform to regulatory limits. All shellfish exports must be tested for each of four toxin classes, *i.e.* paralytic shellfish poisoning (PSP), amnesic shellfish poisoning (ASP), neurotoxic shellfish poisoning (NSP) and diarrhetic shellfish poisoning (DSP).

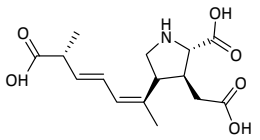

Domoic Acid (**4**)
$C_{15}H_{21}NO_6$
Mol. Wt.: 311.33

The symptoms of ASP can be attributed almost wholly to the activity of domoic acid (**4**) [14, 15]. Domoic acid is a potent neuro-excitatory toxin, which is known to bind to the glutamate receptors in the brain and interfere with neurotransmission in the central nervous system [16]. Symptoms of ASP include gastrointestinal and neurological disturbances including memory loss [17]. The scallop and mussel industries are most at risk from amnesic shellfish poisoning, so close monitoring is necessary to safeguard what has become a significant contributor to the country's economy [18]. Further, toxic blooms appear to be increasing in frequency [19, 20].

A number of analytical methods have been developed for quantitative analyses of domoic acid. Enzyme-linked immunosorbent assays (ELISA) have been used with success [21-25]. A commercial kit, the Biosense Laboratories ASP ELISA, has been developed following the work of Garthwaite *et al.* [26, 27]. Liquid chromatography has been shown to be an accurate and highly reproducible separation technique for domoic acid analysis, coupled with ultraviolet or diode array detection [28-33] or fluorescence detection [34, 35]. Liquid chromatography with mass spectrometry [36-39] is generally the method of choice, but the equipment lacks portability. Capillary electrophoresis [40, 41] requires little sample clean-up, but is the least sensitive of the methods noted here. Van Dolah [42] developed a micro-plate receptor binding assay which used tritiated ligands to aid detection. Lateral-flow immunoassay strips such as those developed by Jellett Rapid Testing Ltd have been

used, but these suffer from poorer sensitivity than the other methods. Methods which can give rapid results on-site allow for immediate response to a positive test, while samples can be sent to a laboratory for more rigorous testing.

1.2 Surface Plasmon Resonance

1.2.1 Background and Introduction to Surface Plasmon Resonance

When light is incident on the internal surface of a glass prism, it is totally internally reflected beyond a certain critical incident angle. An electrical field is generated which extends a short distance beyond the glass. If the prism is in contact with a thin film of a noble metal, the energy of the electrical field can be (under appropriate conditions) transferred to the electrons of the metal, creating a surface plasmon oscillation. At a certain incident angle and wavelength of light surface plasmons are created, and a gap or drop is observed in intensity of the reflected light. The angle at which this occurs is known as the surface plasmon resonance (SPR) angle [43]. Just as the photons create an electrical field extending beyond the interface, the plasmons generate a field extending into the media on both sides of the interface. This field is known as an evanescent wave, so-called because the amplitude of the wave decays exponentially with increasing distance from the interface. The evanescent wave travels a short distance (around 200 to 300 nm) from the noble-metal film. For this reason the depth of effective volume for the purpose of sensing is no more than 300 nm into the medium (Figure 2) [44]. A response is a change in the SPR angle when the target analyte alters the refractive index of the medium (Figure 3). This change in the SPR angle can be measured very precisely.

Observed by Wood early last century [45, 46] and probed by Lord Rayleigh [47] and Fano [48], the phenomenon was first referred to as surface plasmon resonance by Ritchie *et al*. in 1968 [49]. In the same year, Otto [50] and Kretschmann [51] separately demonstrated the optical excitation of surface plasmons by attenuated total reflection, but it was not until 1982 that the use of surface plasmon resonance for sensing was reported by Liedberg and Nylander [43, 44]. Its potential was

quickly recognised by Pharmacia, and in 1986 a company was formed to develop SPR biosensing technology. The first commercial SPR instrument, the Biacore™ (so named for its ability to perform bio-specific interaction analysis) was introduced in 1990 [52], and while Biacore™ remains the market leader [53], the number of companies entering the market indicates the growth in the use of SPR technology.

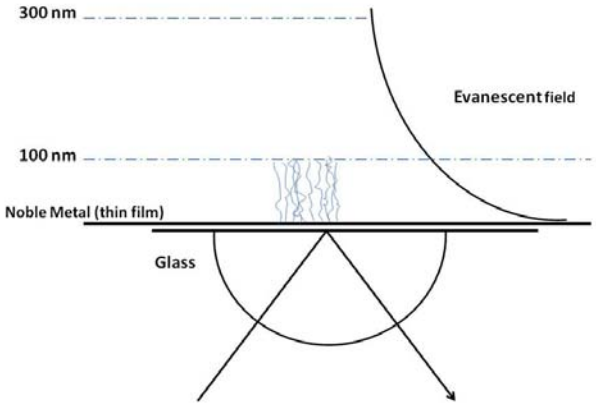

Figure 2: Schematic of the evanescent field, which decays exponentially with the distance from the sensor surface. A 100 nm carboxymethylated dextran scaffold is shown. Adapted from [54].

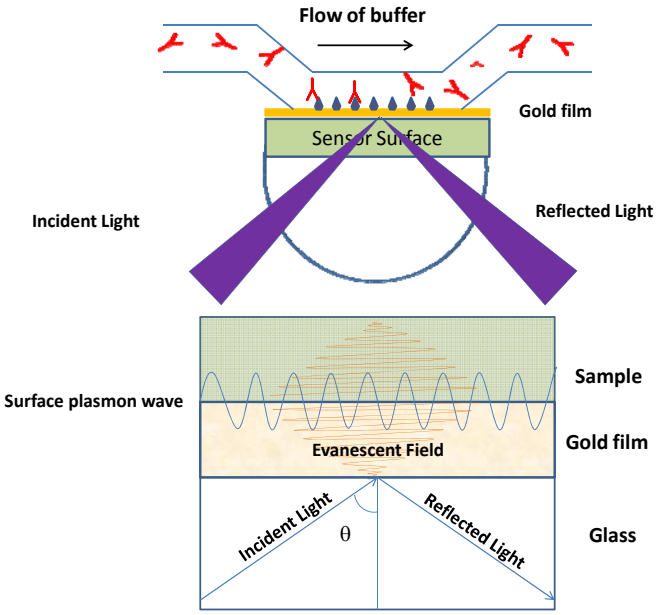

Figure 3: A schematic illustration of Surface Plasmon Resonance applied to a binding system. Here, an antibody in solution is shown binding to its binding partner immobilised on the surface of the sensor chip.

SPR has applications in areas where a high level of sensitivity is necessary. The binding chemistry can then be applied to other formats such as a strip sensor. Portable SPR units designed for use in a field setting have been utilised for the detection of several analytes [55-57]. SPR sensing also lends itself to implementation in a production environment, where it can be placed within a processing stream.

1.2.2 Surface Plasmon Resonance in Practice

The surface plasmon resonance (SPR) angle is dependent on the properties of the film in contact with the glass prism, the wavelength of incident light and the refractive indices of the media on either side of the solid/liquid interface. During a binding event, reduction in the solute concentration causes the refractive index of the liquid medium to change, and as a result the SPR angle changes (Figure 4). This phenomenon can be exploited to give a direct insight in changes of refractive index at the surface, resulting from the bio-specific interactions occurring at the interface, and allows binding to be followed in real time.

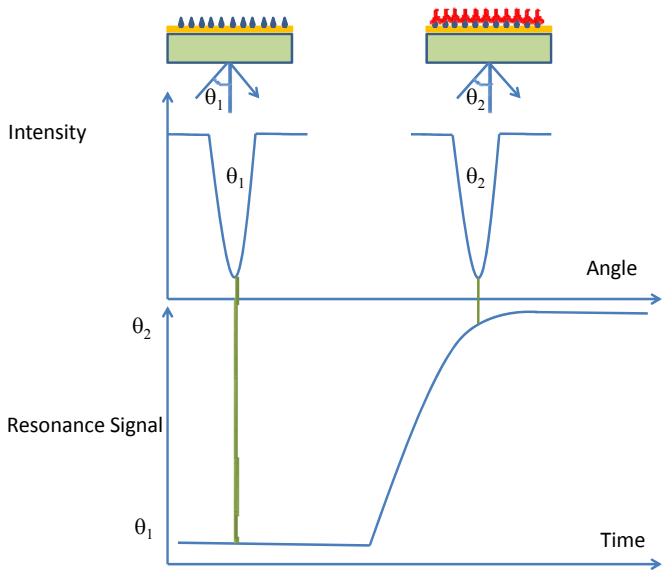

Figure 4: The change in surface plasmon resonance angle observed upon binding.

The evanescent wave penetrates the solution and conditions for the resonance effect are very sensitive to changes in the refractive index and hence in solute concentration. Changes in the refractive index can only be monitored within the penetration depth of the wave into the solution, and not beyond this distance. A number of important conclusions follow:

- SPR is relatively insensitive to changes in the bulk phase outside this depth, which gives a very high signal-to-noise ratio, and hence high sensitivity,
- Interactions occurring very close to the sensor surface will generate much higher responses that those occurring further from the surface, and,
- Since the evanescent wave penetrates the sample, it is possible to analyse turbid samples. In practice, however, the sample must be completely free of particulates, since their presence will shorten the life of the critical microfluidic liquid handling system.

All SPR instruments have three essentially distinct components – the optics, the liquid handling system and the sensor chip which contains the recognition element, *i.e.* the surface-immobilised binding partner.

The Biacore™ instruments use the Kretschmann [51] configuration in which the noble metal is in direct contact with the prism, to promote more efficient plasmon generation. The most suitable metal film is considered to be gold, with a film thickness of around 50 nm. Gold is favoured because it is largely inert in physiological buffer conditions, it can be easily functionalised, and a 50 nm thickness produces a most pronounced reflectance dip. The prism couples p-polarised light (in the plane of the interface) into the surface plasmon (metal) film, and reflects the light on to a photodiode. In developing a commercial instrument, it was also necessary to miniaturise the integrated fluid handling system to optimise the sensitivity of the technique [58].The flow cells are created when pre-formed microfluidic channels are pressed against the sensor surface, with the sensor chip forming the floor of the flow cell. The cell volume for the Biacore™ x100 is about 60 nL. The flow cell is designed with a thin channel (50 μm) to allow fast diffusion of

molecules to the sensor surface. The silicon rubber integrated fluidics cartridge (IFC) allows the liquid to pass over the sensor surface in a continuous flow, maintaining constant concentrations at the sensor surface and minimising dispersion of the sample 'plug'. A series of pneumatic valves is used to direct the flow of liquid.

Liedberg's early experiments involved protein-capture molecules directly adsorbed on to noble metal surfaces, but a more widely applicable method of immobilising the capture molecule was necessary for the technique to be viable in a commercial sense. A self-assembled alkanethiol monolayer coating acts as an adhesion layer to link the gold and the immobilisation matrix containing functional groups, protects bio-molecules from the gold and prevents non-specific binding to the sensor surface. The introduction of an immobilisation layer provides a means of attaching the sensing element - a convenient surface for groups which will readily couple to analytes and create the recognition element. A carboxymethylated dextran surface, to which capture molecules could be attached covalently, has been developed by Biacore™ as an immobilisation layer. Dextran is a flexible, hydrophilic, unbranched carbohydrate polymer sufficiently inert for most SPR applications. In commercial Biacore™ CM5 sensor surface 'chips', the dextran is covalently bound to the alkanethiol layer. The carboxyl functionality is then introduced [59], affording a range of coupling chemistries [60, 61]. The Biacore™ CM5 sensor surface used in this work was a carboxymethylated dextran surface.

In the Biacore™ instruments, the shift in the SPR angle is expressed in 'Response Units' (RU) [62]. With the wavelength used in the Biacore™ range of instruments, 1 RU corresponds to an accumulated mass of 1 pg of protein/mm^2 [61].

1.3 Bridging Linkers

Many workers in the area of biosensing have used a linker to act as a spacer between the bio-molecule and the surface to which it is bound [63-66]. Recently (2011), Watanabe *et al.* investigated the effects of three linkers of varying lengths

and rigidities to determine which gave the optimum binding response in their surface plasmon resonance binding system [67].

Wu *et al.* investigated the effect of increasing linker length on the sensitivity of SPR and ELISA assays [68], using an aliphatic linker between a steroid (progesterone) and ovalbumin. For conjugates with similar ratios of progesterone to ovalbumin, those with a longer linker gave a higher response with an antibody-immobilised sensor in surface plasmon resonance. When the assay format was altered and the conjugates were immobilised on the sensor surface, the longest-linker conjugate failed to attach to the surface. However, for those conjugates that were able to be attached, the longer linker again demonstrated superior response. Wu's later work on a progesterone ELISA [69] demonstrated improved sensitivity with increased linker length, in keeping with other workers' observations for enzyme immunoassays [70]. Wu *et al.* also suggested that the optimum linker length for a bio-conjugate might depend on the relative size difference between the two molecules joined by the linker. They also saw the format of the assay as being important *e.g.* an end-point assay such as the ELISA, compared with a flow-through format of surface plasmon resonance.

The sensitivity and specificity of immunoassays can be manipulated by site-, bridge- and hapten- heterology (a hapten is a small molecule which will not itself generate an immune response in an animal, but can be made to do so by first conjugating it to a carrier protein). In this way, a more sensitive immunoassay can be developed by using a different immunogenic conjugate to produce the antibody than is used in the immunoassay's sensing surface [71]. The conjugates differ at the hapten attachment position and the linker (bridge), and, less commonly, the hapten itself may differ, resulting in a more sensitive immunoassay [72-75]. Investigation of these factors is beyond the scope of the work presented in this thesis. The estrone derivatives described here are all derivatised at the 3-position of the steroid (Figure 5).

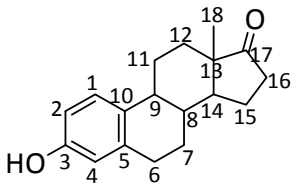

Figure 5: Estrone with the steroid numbering included.

Introducing a hydrophilic oligo(ethylene glycol) (OEG) linker into the progesterone system has been shown to produce a dramatic improvement in the ratio of steroid molecules per protein in the bio-conjugate used for surface plasmon resonance [76]. The production of the higher density conjugate was attributed to the increased solubility of the steroid-linker derivative in the polar solvents used in conjugating the steroid-linker to the protein [76]. Later work used the attachment of the (protein-free) steroid-linker derivative directly to a self-assembled monolayer, and further developed the linker technology by incorporating a gold-nanoparticle-linker-antibody conjugate to enhance the surface plasmon resonance signal [77].

The more steroid-dense steroid-OEG-linker conjugate was beneficial in the context of concentration analyses because it would provide a more sensitive detection surface. This OEG linker has been used in the analysis of a number of steroidal and non-steroidal analytes. Sensitive detection of estriol in a surface plasmon resonance assay and in a lateral flow immunoassay [78, 79] was achieved using an estriol-OEG linker-ovalbumin conjugate, with gold nanoparticle signal enhancement in the case of the SPR assay. Estradiol [80], testosterone [81] and cortisol [82] have been detected in the same way as progesterone above, *i.e.,* the steroid-OEG linker derivative was attached directly to the carboxymethylated dextran surface *via* the linker terminus rather than as a protein conjugate. The testosterone assay incorporated gold-nanoparticles for signal enhancement; the cortisol and estradiol used secondary antibodies alone for enhancement.

The same strategy has been applied to non-steroidal analytes. The antibiotic chloramphenicol was attached both as an oligoethylene glycol linker protein

conjugate [83] and as an oligo(ethylene glycol) linker derivative [84], to form sensing surfaces for surface plasmon resonance analysis. The mycotoxin ochratoxin A [85] was detected by covalently attaching two conjugates to the sensing surface, one an ochratoxin A-oligoethylene glycol linker-ovalbumin conjugate and the second an ochratoxin A-bovine serum albumin conjugate without a linker. The binding responses of the two surfaces were compared.

1.4 Signal Enhancement: Secondary Antibodies and Gold Nanoparticles

In surface plasmon resonance analysis of small molecules, the approach most often used involves detection of the antibody binding to the sensor surface. Decreasing the concentration of antibody improves the assay's sensitivity, because smaller amounts of analyte inhibit antibody binding. The amount of antibody binding to the sensor surface must, however, be sufficiently large to generate a significant SPR response. Methods to amplify the SPR signal can be used to increase assay sensitivity by permitting the use of small amounts of antibody, which without signal enhancement, would be too low.

Since SPR signals are determined by the mass of material bound, binding a secondary antibody couples the binding event with larger mass changes, and therefore increases signal size. The use of colloidal gold nanoparticles can, however, provide a superior signal increase for several reasons. Since colloidal gold is very dense, it produces a very large signal increase. Gold is generally compatible with the bio-molecules used in SPR, and the diameter of the gold nanoparticle can be varied by altering the preparation conditions [86].

In much the same way as the incident light induces a surface plasmon (charge density oscillation) which propagates along the gold surface, localised surface plasmons can be excited within gold nanoparticles. Plasmon coupling can occur, resulting in amplification of the SPR signal which occurs on binding. Gold was first used in surface plasmon resonance as an agent to enhance signal by Lyon *et al.* [87,

88], who observed a 25-fold increase in signal on binding of antibody-10 nm gold conjugate *cf.* the 'free' antibody. They applied the concept to an immunoassay for human IgG.

Larger nanoparticles have been shown to give a more pronounced increase in signal [89, 90], however increasing size also broadens the plasmon resonance peak, making a shift in the peak more difficult to detect. Mitchell observed that gold nanoparticles larger than 25 nm are more prone to aggregation and settling over time [91]. The shape of the nanoparticle [92], and the distance between the nanoparticle and the gold substrate [93, 94] impact upon the enhancement effect. Effects of gold nanoparticle size and the surface plasmon resonance coupling on the signal amplification have been investigated by Hong and Hall [95].

Gold nanoparticles tethered to the surface of the gold film provide label-free signal amplification [96, 97], but using the gold nanoparticle as a label is common [98-103], and is particularly useful where a high level of sensitivity is required. The preparation of antibody-gold nanoparticle conjugates is well-established, since they have long been used in immunographic test strips to generate a distinct red colour, the intensity of which correlates with concentration [104-107].

The streptavidin-biotin binding system has been applied to gold nanoparticle signal enhancement for the detection of progesterone. In this case the monoclonal antibody was biotinylated, and the streptavidin labeled with 10 and 20 nm gold nanoparticles [76].

1.5 The Scaffold Layer for SPR

SPR scaffold alternatives to dextran have been investigated. The most widely used alternative scaffold is the self-assembled monolayer, defined as an ordered molecular assembly of an active surfactant on a solid surface [108]. A highly ordered monolayer can be formed by the co-ordination of disulphides, sulphides or thiols on to the gold surface [109]. Incorporation of an appropriate terminal group for attachment of a sensing molecule creates a scaffold suitable for use in surface

plasmon resonance. Scaffolds of this type have been used with considerable success [110-114], but the sensing surface is typically less stable than a comparable carboxymethyldextran sensor. The monolayer is, however, often more cost-effective to generate, and it can be removed allowing the gold surface to be re-used. A lower limit of detection was achieved for progesterone using a self assembled monolayer immobilisation scaffold than with a carboxymethylated dextran surface [77].

Sasaki [115] *et al.* fabricated a gold surface functionalised with an organic silica compound (γ-aminopropylethoxysilane) and attached an antibody to the surface using a conventional coupling method to detect the herbicide atrazine. A paralyne polymer film (a polymer of p-xylene) modified with primary amine groups was used by Jeon *et al.* [116]. To demonstrate the suitability of the polymer as a scaffold, horse radish peroxidase was covalently attached through the amine groups. An interesting linking layer prepared *via* electro-copolymerisation of pyrrole linked to oligonucleotides created a DNA sensing layer. This surface was designed for surface plasmon resonance imaging, but it was proposed that the chemistry could be applied to peptide immobilisation [117].

Thiophene has been used by a number of workers to create scaffolds. A polythiophene with a pendant linker functionalised with *N*-hydroxysuccinimide ester groups was used in the detection of a protein marker used for clinical diagnosis [118]. Very recently, polythiophene with a carboxy-functionalised linker has been used for adsorption of avidins, forming a binding layer suitable for the detection of biotinylated antibodies [119]. The latter method was also employed for the detection of clinical markers. Polythiophene has also been used with success in the surface plasmon resonance detection of C-reactive protein which serves as a clinical marker in the prediction of cardiovascular diseases [120]. This scaffold was a polymer formed by the ferric chloride oxidation of thiophene with a pendant *N*-hydroxysuccinimide ester moiety. The resulting polymer was dissolved in

dimethylsulphoxide and a gold SPR chip surface immersed in the solution. An antibody was then immobilised on the scaffold in the usual manner.

Molecularly imprinted polymers (MIP) formed on the gold sensor surface can act as a sensing layer suitable for surface plasmon resonance. A MIP is formed by the polymerisation of one or more monomers in the presence of a template molecule producing an analyte shaped cavity. The template molecule is then removed, leaving a recognition cavity with highly specific molecular recognition capability, effectively forming a custom-made synthetic receptor [121]. The technology was advanced by Wulff [122], and has found application in biosensing. The use of MIPs is limited in SPR when the binding events involve small molecules, making detection at low concentrations difficult [123]. Nonetheless, Pernites *et al*. [124] describe the detection of theophylline, naproxen and paracetamol using an electrochemically polymerised carboxyl-functionalised terthiophene to create a molecularly imprinted polymer. This sensing layer gave sensitive detections of these three important drugs. Sharma has recently reviewed the use of electrochemically synthesised polymers used in the generation of molecularly imprinted polymers for sensing [125].

Chapter 5 details efforts to develop an SPR scaffold based on terthiophene, which would use the same coupling chemistry as the commercially available dextran surfaces. The introduction of an oligo(ethylene glycol) linker on the terthiophene was thought to improve binding of a detecting molecule such as an antibody, by allowing the binding moiety to extend slightly away from the sensor surface into the flow of buffer. The use of one pendant linker on each terthiophene was designed to act as a self-spacing mechanism along the sensing surface.

1.6 Aims

Surface plasmon resonance has the potential to improve upon the performances of other techniques currently available for quantitative analysis of biomolecules in aqueous environments, particularly when addressing environmentally relevant

concentrations in those applications in which a very low level of sensitivity is mandatory. The interest driving this study was to help realise this potential.

Much work must be done to establish threshold levels where the concentration of estrogens begins to generate harmful effects to the environment, and to the organisms within it, but the level of estrone in wastewater in the pg/mL range is known to induce estrogenic responses in fish [1]. SPR provides a tool to characterise a binding system, and this can then be used to produce strip sensors, which have application in a field situation – an enormous advantage for use in wastewater treatment plants. Portable SPR units are available for on-site testing. Surface plasmon resonance has the potential to deliver reliable and cost-effective test methods for screening of samples in the field, especially valuable for samples derived from an aquatic environment.

The aim of the work discussed in Chapter 3 was to investigate the effects of the length and characteristics of linkers on binding response and sensitivity in an estrone binding system. The intention was to probe signal enhancement using secondary antibody binding and gold nanoparticles in the estrone system and develop an SPR method with a limit of detection in the pg/mL range, with a potential application in the analysis of estrone in wastewaters.

In Chapter 4, work focused on application of the signal enhancement strategies used in Chapter 1 to the detection of the shellfish toxin domoic acid. The aim then became to develop an SPR assay for domoic acid with a limit of detection which would have potential application in testing for levels of the toxin which would exceed regulatory limits. One objective was to investigate whether use of an intermediate linker would improve sensitivity.

In Chapter 5, the aim was to develop an SPR scaffold based on linker-functionalised terthiophene, with a view to increasing sensitivity by ensuring the binding event was in the more sensitive region for SPR detection. It was also intended to investigate the effect of attachment of the analyte to protein in the preparation of the sensing surface and compare the sensitivity to a non-protein surface.

Chapter 2

Experimental Terms and Techniques

Those established biochemical terms and approaches referred to in this thesis are discussed briefly in this chapter. Other procedures which relate to biosensing with surface plasmon resonance are also described briefly.

2.1 Immunoassays

Tests that use one or more binding reactions of antibodies are called immunoassays, a reference to the fact that antibodies are produced in living organisms by the immune system.

Antibodies

Antibodies are certainly the most widely used binding partners in surface plasmon resonance (SPR), at least at present. The selection of an antibody with the most suitable binding characteristics is very important to the success of any immunoassay. For all the work described in this thesis, antibodies were used as the detecting molecule, *i.e.*, that part of the binding pair whose binding generates an SPR signal.

Antibodies are large Y-shaped glycoproteins that are produced by a host's immune system to identify and neutralise foreign bodies. The antibody binds specifically to the foreign body, also referred to as an antigen. Most higher mammals have five classes of the immunoglobulin (Ig) antibodies: IgG, IgM, IgA, IgD and IgE, but it is the IgG antibodies that are used almost exclusively in immunoassays. Compared with the other immunoglobulins, IgG is the most abundant class of antibody in serum, produces the highest yield in response to immunisation, binds with high affinity to its binding partner, is stable during isolation and purification, and has several convenient sites which can be used for chemical coupling with only minimal loss of

activity. All antibodies used in the experimental work described in this thesis are of the IgG class, with a molecular mass of approximately 150 kDa.

The structure of an IgG antibody consists of two identical heavy (H) polypeptide chains with two identical light (L) chains, configured in a characteristic Y-shape (Figure 6). IgG antibodies consist of one Y unit. The areas in the antibody are divided into segments, (referred to as domains) of approximately 110 amino acids. The heavy chains comprise three constant domains (C_H) and one variable domain (V_H). The C_H and C_L domains are relatively constant in sequence, but the V_H and V_L domains are more variable, and it is within these variable domains that three complementarity determining regions (CDRs) form the antibody's binding sites, one on each arm of the 'Y'. The complementarity determining regions of the antibody are specific for a particular epitope (binding site) on its antigen. The epitope is also referred to as the antigenic determinant, because it is the part of the antigen that is recognised by the antibody.

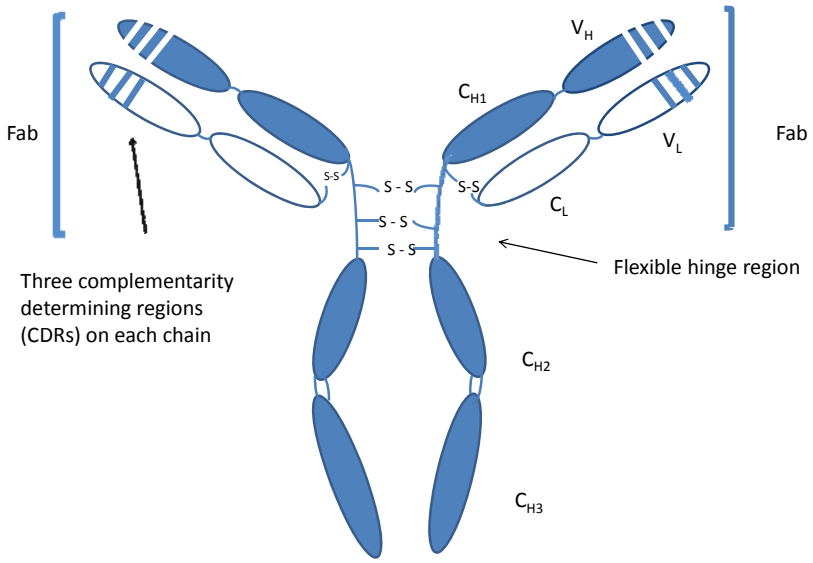

Figure 6: Antibody Structure (IgG1). The heavy chains consist of three constant domains (C_H1, C_H2 and C_H3) and one variable domain (V_H), linked to a light chain consisting of one constant domain (C_L) and one variable domain (V_L). The variable domains on both the light and heavy chains have highly variable complementarity determining regions (or CDRs) which bind to the antigen.

Antibody fragments can be generated by treating intact antibodies with protease enzymes. Antibody treatment with the enzyme papain yields two antigen binding fragments (Fab) (one antigen binding site on each fragment), whereas pepsin cleaves below the hinge region, giving a single $F(ab')_2$ fragment containing both antigen binding sites (Figure 6). These antibody fragments have found application in immunoassays where their relatively small size is an advantage. All the antibodies used in this work are intact.

Monoclonal and Polyclonal Antibodies

Monoclonal antibodies are highly specific antibodies originating from a single cloned antibody-producing cell and bind to the same epitope on the antigen, whereas polyclonal antibodies originate from different antibody-producing cells, and are therefore more diverse [126]. The anti-estrone glucuronide antibodies W and C used in Chapter 3 are monoclonal antibodies, as is the anti-progesterone antibody used in Chapter 5. The anti-domoic acid antibody used in the SPR assay of domoic acid is polyclonal.

Hapten

Small molecules which will not themselves generate an immune response in an animal can be made to do so by first conjugating them to a carrier protein such as keyhole limpet haemocyanin, bovine serum albumin or ovalbumin. The small molecules used in this way are known as haptens [127].

Aptamers

Aptamers are short single-stranded oligonucleotides which can bind biomolecules with high affinity and specificity. Aptamers offer great potential as the binding partners in a biosensor. They can be readily synthesised in a particular sequence, conferring a high degree of specificity, and are more stable than antibodies. Because the technique used to isolate aptamers is *in vitro*, the use of animals is not necessary, and aptamer production is more reproducible than antibody production. Aptamers' generally smaller masses *cf.* an IgG antibody, mean that they are most

often immobilised on to a sensor surface and used in a sandwich assay method [128], or biotinylated aptamers are bound to a streptavidin sensor surface [129, 130]. While not widely used in surface plasmon resonance at present, aptamers are an exciting new development in the broader context of biosensors.

2.2 Immobilisation

Attaching the binding partner to the sensor surface on a sensor chip is a crucial step in surface plasmon resonance. Conditions for this 'immobilisation' step must be selected so that the final immobilisation level is sufficient for the application, and preferably readily reproducible for the preparation of subsequent surfaces. Steric issues may need to be considered to ensure that the immobilised binding partner is sufficiently accessible to the detecting molecule, and the surface produced must be robust enough to withstand the regeneration conditions necessary to dislodge the detecting molecule after each injection.

2.2.1 Immobilisation Chemistry

The coupling methods for immobilisation in this study employed covalent activation chemistry. The commercial immobilisation matrix used for much of the following work was a CM5 chip with a carboxymethylated dextran surface. The amine coupling of the carboxylated surface as a means of immobilising a binding partner to the sensor surface is a technique which has been widely used and studied, and which is considered to be robust and easy to use [62]. Typically, the carboxyl groups are converted to an active ester intermediate, which then reacts with lysine residues on a protein or peptide, or with the terminal amino group of a binding pair to be immobilised. Again, this is well-established chemistry [131, 132]. The carbodiimide used in immobilisation steps was the water-soluble *N*-ethyl-*N*-(3-(3-dimethylaminopropyl)-carbodiimide as the hydrochloride (EDC) (**5**), and its urea by-product is also water-soluble, making it suitable for use in the SPR instrument. The reaction is mediated by the addition of *N*-hydroxysuccinimide (NHS) (**6**) producing an active ester with a sufficiently long lifetime to be useful for activating sensor surfaces in the SPR instrument (Scheme 1).

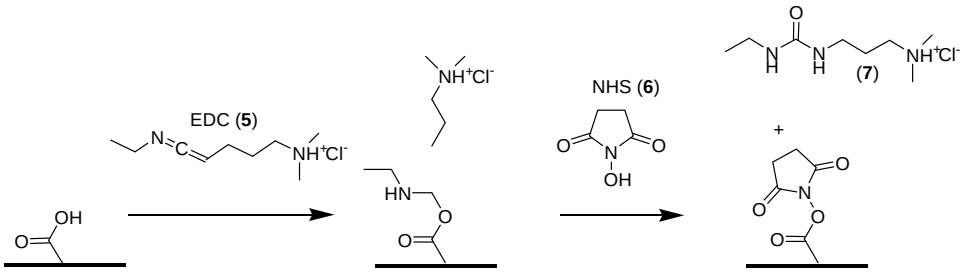

Scheme 1: Activation of the surface of a carboxymethylated dextran sensor chip with *N*-ethyl-*N*-(3-dimethylaminopropyl)-carbodiimide as the hydrochloride (EDC) (5) and *N*-hydroxysuccinimide NHS (6) to give reactive succinimide esters. The activated esters react spontaneously with nucleophilic groups such as amines, allowing direct immobilisation of molecules containing such groups.

In general, the protein conjugates used in this work were immobilised at pH 4.0, following activation of the sensor surface with *N*-ethyl-*N*-(3-(3-dimethylaminopropyl)-carbodiimide as the hydrochloride (EDC) and *N*-hydroxysuccinimide (NHS). After multiple injections to produce a satisfactory level of binding partner on the surface, the remaining active esters were 'capped' using ethanolamine.

In the shellfish toxin work, the domoic acid itself (*i.e.,* not conjugated to a protein) was coupled to the sensor surface in a step-wise fashion. First, a linker with an amino-terminus was attached to the EDC/NHS-activated surface, and then the surface was capped using ethanolamine as before. Domoic acid was activated using EDC/NHS chemistry outside the SPR instrument, and then introduced to the sensor surface with the linker already attached.

2.3 Regeneration

Regeneration should remove all (non-covalently bound) analyte from the sensor surface in readiness for the next cycle, but without affecting the binding activity of the immobilised binding partner. Poor regeneration can result in a drifting baseline, which will decrease the binding response. For protein surfaces, suitable regeneration conditions are low pH (10 mM glycine pH 1.5 – 3.0), high pH (1 – 100 mM NaOH), 50 – 100 % ethylene glycol, high ionic strength (0.5 – 5 mM NaCl or 1 – 4 mM $MgCl_2$) or 0.02 – 0.5 % sodium dodecylsulphate [61]. The choice of appropriate regeneration conditions (regeneration time and solution) is a critical

step in the development of a satisfactory assay. The regeneration conditions should be only as strong as is necessary to remove all the bound analyte without destroying the activity of the surface. In general, the usable life-time of a sensor surface is dependent upon the severity of the regeneration conditions.

2.4 Concentration analysis in Surface Plasmon Resonance

For all concentration assays described here, it was possible to increase the signal by increasing the time that the assay solution was in contact with the sensor surface. This requires more sample solution, and increases the assay throughput time.

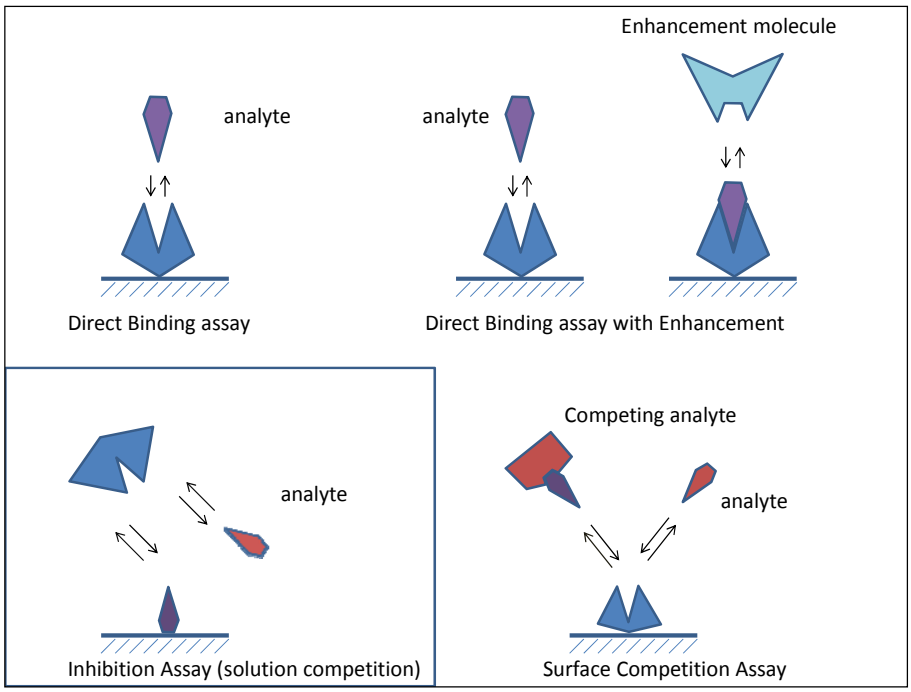

Figure 7: Immunoassay formats commonly used in surface plasmon resonance measurements.

2.4.1 Direct-Binding Assay:

The sample containing the analyte is injected directly over the surface of the sensor in a direct binding assay, and the analyte binds to the surface-bound antibody. Because the SPR response is proportional to the mass of the material bound, this type of assay is more suitable for macromolecules (>5000 Da). Where this method is used for smaller molecules, it is often in combination with a signal enhancement

strategy (Figure 7), to bring the response up to an acceptable range. A secondary antibody can act as the enhancing agent by binding to the analyte in a second binding event.

2.4.2 Inhibition or Competition Assay:

The inhibition or competition type of assay is suitable for small molecules (<1000 Da), because it is the detecting molecule (usually an antibody), and not the analyte which is responsible for generating the signal. In a solution competition (inhibition) assay (Figure 7) a known, fixed amount of the detecting molecule was mixed with the analyte solution, and the binding reaction incubated before injection into the SPR. The remaining free unbound antibody then bound to the sensor surface, generating a response. This response was inversely proportional to the level of analyte in the original solution. This was the method used for all analyses in this study.

In a surface competition assay (Figure 7) the analyte and a high molecular weight analogue (often a protein conjugate) compete for binding to the sensor surface. Again, the response is inversely proportional to the concentration of analyte.

2.5 Assay Design

Concentration measurements in this study are based on the interaction of the analyte and the detecting molecule. The size of the SPR signal is proportional to the mass of the material bound. The analytes in this work were all small molecules (<1000 Da), hence when the assay was designed, it was as an inhibition (solution competition) format. The binding response is proportional to the amount of the binding pair immobilised on to the surface, so that a higher level of immobilisation made for a more sensitive method, with lower detectable analyte concentrations. By contrast, if the (relatively large) antibody had been immobilised and the (relatively small) un-conjugated steroid allowed to bind to the surface, the sensitivity of the (direct competition assay) would have been relatively low even with high levels of immobilisation.

The assay standard curves were fitted to a 4 parameter logistic (dose-response curve with variable slope), using Prism™ or OriginPro™ curve-fitting software, generating a sigmoidal calibration curve. The quantity on the y-axis in a dose-response curve is the biological response (with surface plasmon resonance the units are response units). The logarithm of the dose or concentration is on the x-axis. The slope of the curve is defined by the Hill slope or slope factor. The error bars shown on the graphs represent one standard deviation (SD) of the mean.

The range of the immunoassay is determined by the affinity of the antibody for its binding partner in solution, and by the concentration of the antibody used in the assay. An antibody with a higher affinity for its antigen can allow the detection of lower analyte concentrations. For an antibody of a given affinity, lowering the antibody concentration can move the calibration curve to a more sensitive operating range, *i.e.* lower analyte concentration (Figure 8). The size of the signal response is, however, proportional to the antibody concentration, so the concentration must be sufficiently large for a signal to be detected in the sample medium.

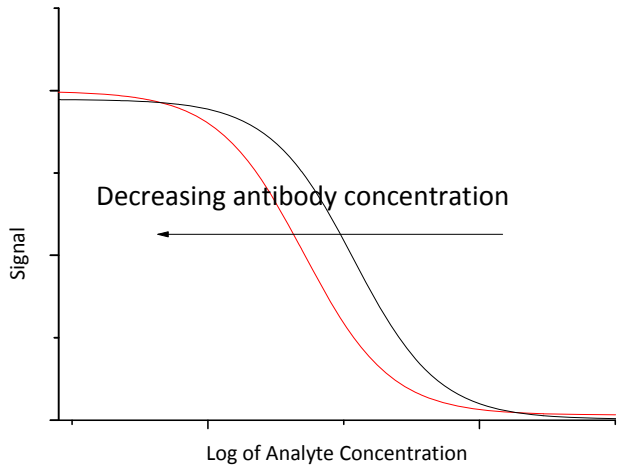

Figure 8: Effect of antibody concentration on assay sensitivity

2.6 Antibody Sensitivity:

The sensitivity of an antibody, *i.e.,* the size of the surface plasmon resonance response for a given concentration impacts on the assay in terms of its cost, and in how low a concentration may be used in the assay - an antibody with a relatively high response in the surface plasmon resonance may allow the use of lower concentrations in the assay, potentially moving the standard curve to a more sensitive region.

2.7 Assay Sensitivity:

The sensitivity of an assay can be considered in two ways: the position of the dose response curve, *i.e.* the concentrations the working range encompasses, and the limit of detection. An assay with a small working range but a lower limit of detection may have less application than an assay with a higher limit of detection, but a broader working range.

The IC_{50} was defined as the concentration of analyte (inhibitor) that reduced the response to 50 % of the maximum response. The maximum response was defined as the signal for the detecting molecule only, with no analyte present.

The working range was defined as the generally linear portion of the assay, between the IC_{20} and IC_{80}.

The limits of detection (LOD) given in this work were calculated as the IC_{90}, *i.e.,* the concentration of analyte that reduced the response to 90 % of the maximum response. An alternative method of calculating the limit of detection by subtracting two or three standard deviations from the blank response and interpolating that response into the corresponding concentration has been used by other workers [133], but this method was not used in this study. In general, the data points had very little scatter.

2.8 Choice of Binding Partners:

The binding partner to be immobilised should be sufficiently robust under the immobilisation conditions so as to retain most binding capacity. The binding reaction should occur with sufficient selectivity, depending on the requirements of the assay. The binding event should occur sufficiently rapidly so as to be amenable to the time scales used in surface plasmon resonance. For reasons of practicality, the binding between the analyte and the binding partner should be relatively fast. Incubation time needs to be minimised, and rapid throughput of solutions is required.

The binding should be stable enough to allow measurement shortly after the binding event to allow for reliable measurement. Dissociation must be relatively slow, because the measurement of binding is taken shortly after sample injection has ceased and the buffer is introduced into the flow cells. In this way any difference in response between the baseline (before the sample is introduced) and the report point at which binding is measured can be attributed to the bound analyte, and not the "bulk effect". The "bulk effect" describes the difference in refractive index between the running buffer in the analyte solution, and the running buffer flowing over the sensor surface. This effect is marked when using gold nanoparticle enhancement strategies, where other agents (*e.g.* polyethylene glycol) are used to stabilise the gold nanoparticle-antibody conjugate.

Further, the detecting molecule should be readily removable from the sensor surface, using regeneration solutions which are quick acting and sufficiently gentle so as not to degrade the immobilised surface. The antibody itself needs to be stable over the period of analysis (usually several hours).

Enhancement using secondary antibodies can provide a cost-effective strategy for improving assay cost. The requirements of a signal enhancement agent, usually a secondary antibody (possibly conjugated to a gold nanoparticle), are similar to those for the primary antibody, with respect to binding, dissociation speed and the

regeneration of the surface. The binding of a secondary antibody to a primary antibody must occur at a different site from that involved in binding the analyte. As for the binding of the secondary antibody to the already-bound primary, this too needs to be relatively rapid, certainly within the time-frame of the contact time and flow rate selected. Secondary antibodies used as signal enhancement reagents are large molecules, and, as is the case with the analysis described later, may be capable of binding to more than one site on the (already-bound) primary antibody.

2.9 Enzyme Linked Immunosorbant Assay (ELISA)

An ELISA also exploits the binding reaction between binding partners, one of which is labelled to allow detection. Many immunoassays are based on the reaction between enzymes such as horseradish peroxidase (HRP) or alkaline phosphatase (AP), and a substrate, *e.g.* tetramethyl benzidine (TMB) or p-nitrophenylphosphate. The reaction leads to the formation of a coloured product which can be readily detected spectrophotometrically. Other enzymes have been developed which give fluorescent products, and the fluorescence intensity is measured instead. The amount of analyte present in the sample can be determined by reading off a calibration curve generated using a series of standard solutions. ELISA assays can be very sensitive.

The commercial ELISA kit used in this work for the detection of domoic acid was an inhibition assay, where free domoic acid in the sample competed with domoic acid-conjugated protein coated on to a solid phase, typically a plastic well, for binding to anti-domoic acid antibody (a polyclonal ovine anti-domoic acid antibody) free in solution. The solution containing domoic acid was incubated in the wells with the anti-domoic acid antibody-horseradish peroxidase conjugate. The wells were washed, and the amount of antibody bound to the well was measured by incubation with a substrate which gave a blue product upon reaction with the horseradish peroxidase enzyme. Addition of acid stopped the reaction and induced a colour change in the product which could be measured spectrophotometrically.

Chapter 3

Surface Plasmon Resonance of Estrone Analogues

The main focus and central theme of this study has been to probe means of improving the sensitivity of surface plasmon resonance (SPR) assays. One aim of the work described in this chapter was to investigate the effect of the linker length and characteristics on binding response using estrone as a model compound. The oligo(ethylene glycol) linker was appended to estrone glucuronide, and to a short acyclic linker already appended to estrone, and the binding response and sensitivity of the two estrone derivatives compared to the estrone derivatives without the oligo(ethylene glycol) linker. A second aim was to probe signal enhancement by secondary antibodies and gold nanoparticles, using estrone as a model system and, using these strategies, to develop an assay which could detect the steroid in the pg/mL range necessary for analyses of wastewaters. Estrogenic compounds were chosen, because the steroid estrone (E1) is an important reproductive hormone and because highly sensitive methods of detection are required for analyses of wastewaters.

The sensitivity of a surface plasmon resonance (SPR) with an inhibition immunoassay is limited by the amount of antibody used – an assay with a lower antibody concentration added to analyte solutions will have a lower limit of detection. The level of antibody added to an analyte solution must be high enough so that sufficient un-bound (so-called “residual”) antibody remains in solution, which can then bind with the binding partner immobilised on the sensor surface and generate a signal. Methods which enhance the size of the signal allow the use of smaller amounts of antibody, producing a lower limit of detection.

One potential method of sensitivity improvement probed with the estrone system was signal enhancement using secondary antibodies and gold nanoparticles.

Estrone is a relatively small molecule, which generates a modest surface plasmon resonance response upon binding to a sensor surface, so a competitive inhibition assay (refer to Chapter 2) was designed. In this type of assay, a known, constant amount of anti-estrone antibody is added to a solution of estrone (in the glucuronide form) and the residual un-bound antibody in solution binds to the estrone derivative attached to the sensor surface. In this way, the higher molecular-weight antibody binds to the sensor surface rather than the very much smaller steroid, and a larger surface plasmon resonance response is generated. Using a second binding event, where a secondary antibody binds to the primary antibody already bound to the sensor surface will generate a second response.

Gold nanoparticles have been attached to the antibodies to amplify the surface plasmon resonance signal. The signal enhancement is thought to be due to two effects – not only does the high mass of the nanoparticle increase the signal size, but also the nanoparticle itself undergoes surface plasmon resonance and reinforces the signal. Gold nanoparticle signal enhancement has been used in several surface plasmon resonance assays [83, 84, 114, 134, 135]. Some earlier workers have attached a gold nanoparticle to a primary antibody to obtain signal amplification. In this work the nanoparticle was attached to the secondary antibody in the expectation of exploiting both of the enhancement effects mentioned above.

Inserting an oligo(ethylene glycol) (OEG) linker between a steroid and the sensor surface (or between a steroid and the protein which is then attached to the sensor surface) has been shown to improve greatly antibody binding in the case of progesterone [76]. Oligo(ethylene glycol) (OEG) linkers are hydrophilic, so much so that their use in a conjugate to elicit an immune response for antibody generation has been found to reduce the antibody production, by effectively covering the protein with a hydrophilic shell of oligo(ethylene glycol) [136, 137]. In biosensing, OEG linkers can prevent protein absorption, avoiding fouling of the sensor surface [138-140]. This ability to hinder unwanted protein adsorption has been used to good effect in self-assembled monolayers [141-143]. Linker insertion is thought to

aid antibody binding by orientating the steroid into the flow of aqueous buffer. The assumption has been that intermediate linkers diminish potential steric obstruction when a relatively large antibody binds to much smaller surface-bound partner. Insertion of a linker and gold nanoparticle signal enhancement of primary antibody binding has been exploited in the analysis of estradiol [78] and insertion of a linker and secondary antibody signal enhancement was used to enhance sensitivity in the analysis of the steroid hormone cortisol [82]. Many workers have prepared gold nanoparticles using the classical methods of Frens [144] and Turkevich [145]. Commercial gold nanoparticles were used in all work described here to minimise the possibility of aggregation of the gold. Aggregation could potentially compromise the performance of the micro-fluidics in the surface plasmon resonance instrument.

In this chapter, the investigations of effects of gold nanoparticle enhancement and linker chemistry on the surface plasmon resonance detection of estrone glucuronide are described. The estrone sensing elements used were in the form of ovalbumin protein conjugates immobilised on to carboxymethylated dextran surfaces (Figure 9).

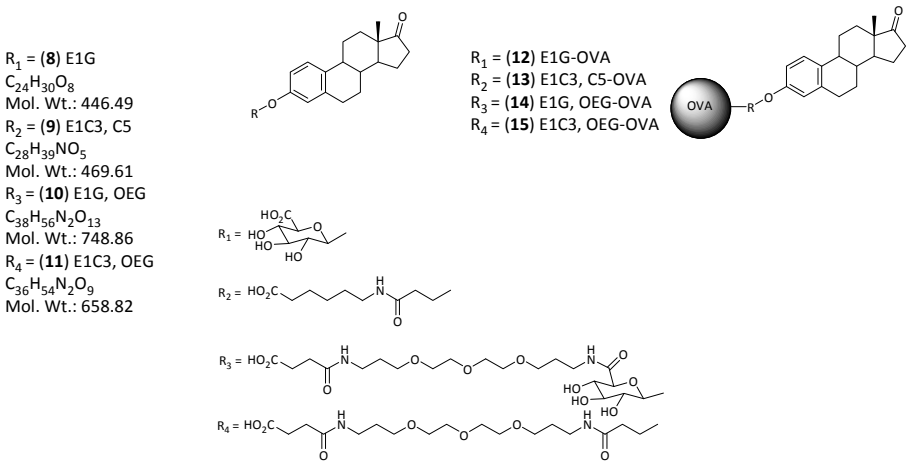

Figure 9: The estrone derivatives and their corresponding ovalbumin conjugates used in sensor surfaces for surface plasmon resonance.

3.1 Materials and Methods

Two different primary mouse monoclonal antibodies W [146] and C [147], estrone glucuronide (E1G) and estrone sulphate (ES) were kindly supplied by Associate Professor Len Blackwell of Massey University. The estrone analogues (**8** – **11**) were synthesised and their conjugates (**12** – **15**) (Figure 9) were prepared by Dr Krishanthi Jayasundera. Details of the synthesis and conjugation are provided in the Appendix. A Biacore™ X-100 system (GE Healthcare, Uppsala, Sweden) was the instrument used for all surface plasmon resonance measurements. Reagents and sensor chips, including the CM5 sensor surface chips, the amine coupling kit (0.1 M *N*-hydroxysuccinimide (NHS), 0.4 M *N*-ethyl-*N*-(3-dimethylaminopropyl)-carbodiimide (EDC), and 1 M ethanolamine hydrochloride pH 8.5 and the HBS-EP+ running buffer pH 7.4 (10 mM HEPES (pH 7.4), 150 mM NaCl, 3 mM EDTA, and 0.05 % surfactant P-20) were supplied by Biacore™ AB (Uppsala, Sweden). 20 nm (EM.GC 20) and 40 nm (EM.GC 40 nm) gold colloids and goat anti-mouse IgG/nanogold 40 nm (BA.GAM 40) were purchased from British Biocell International (Cardiff, U.K.). Secondary anti-mouse antibodies were obtained from Sigma: M7023 (Anti-Mouse IgG (whole molecule) produced in rabbit, IgG fraction of antiserum), A9044 (Anti-Mouse IgG (whole molecule) peroxidase antibody produced in rabbit, IgG fraction of antiserum) and M8890 Anti-Mouse IgG (whole molecule) produced in Goat, IgG fraction of antiserum). Bovine serum albumin was purchased from Gibco, (Invitrogen Corporation) and polyethylene glycol 400 by Fisher Scientific (Leceistershire, U.K.). 50 mL polypropylene 'Oak Ridge Tubes' were obtained from Tarsons (Kolkata, India). Maxymum™ recovery tubes were sourced from Axygen Inc., (Union City, CA, U.S.A.).The water used for all reagent preparation was ultra pure Milli-Q (Millipore Corporation, Billerica, MA, USA). A Sorvall Evolution RC centrifuge fitted with an SS-34 rotor and an Eppendorf Mini-Spin centrifuge were used in the preparation of the gold-antibody conjugates.

The estrone derivative-ovalbumin conjugates (**12** – **15**) were analysed by matrix-assisted laser desorption/ionization time-of-flight (MALDI-TOF) mass spectrometry

on an AutoFlex II MALDI-TOF mass spectrometer (Bruker Daltonics), at the University of Waikato Mass Spectrometry facility. The matrix used was a mixture of 2,5-dihydroxybenzoic acid and 5-methoxysalicylic acid, at 5 mg/mL in 2:1 0.1 % TFA/acetonitrile. A protein calibration mix supplied by Bruker Daltonics was used for calibration.

3.2 The Sensor Surface:

Sensor surfaces were prepared by covalently immobilising each estrone-ovalbumin conjugate (**12** – **15**) on the surface of a separate CM5 sensor chip. The carboxyl groups on the surface of the CM5 chip were activated by 70 μL injections of Biacore™ coupling solutions 390 mM EDC/100 mM NHS (mixed in 1:1 ratio) at 10 μL/min. All conjugates were diluted in 10 mM sodium acetate solution pH 4.0 and filtered through a 0.45 μm Phenomenex PES syringe filter to remove any insoluble material. Repeated injections of the conjugate solution at 5 μl/min were made until a satisfactory immobilisation level was reached (at least 1000 RU). Any remaining activated carboxyl groups were deactivated by injecting 70 μL of 1 M ethanolamine hydrochloride pH 8.5. The reference flow cell 1 was then immobilised in a similar manner, using as a target the final immobilisation level (in RU) obtained for the conjugate flow cell. In this way, a sensor surface was produced with two flow cells containing well-matched immobilisation levels.

One sensor surface was prepared in a similar manner using the E1G-ovalbumin conjugate with a relatively low loading of conjugate material, *i.e.* less than 1000 RU. This sensor surface was used to test for differences in antibody-binding behaviour, when compared with a higher-load surface.

Regeneration conditions were optimised by injecting a solution of monoclonal antibody W on to the surface of an E1G-OVA chip, and observing the effects of the regeneration solutions. Three solutions were trialed: glycine solutions with two different pHs (pH 2.0 and pH 2.5) and 50 mM NaOH. Each solution was passed over the surface at 5 μL/min, with two different contact times (30 s and 120 s).

Before use in binding studies, the surfaces of both flow cells was conditioned with ten successive injections of running buffer followed by a 20 μL injection of 50 mM NaOH (regeneration solution) at 10 μL/min.

3.3 SPR Antibody Binding Studies

A plot of response versus antibody concentration was prepared by diluting monoclonal antibody W in HBS-EP+ running buffer to produce a concentration series, and injecting three 20 μL individual replicates of each concentration. For E1G-OVA and E1G,OEG-OVA sensor surfaces, the antibody concentrations were 0, 0.1, 0.2, 0.3, 0.4, 0.5, 0.6, 0.7, 0.8, 0.9, 1.0, 1.25 and 1.5 μg antibody/mL, and for E1C3,C5-OVA and E1C3,OEG-OVA surfaces the concentrations were 0.2, 0.4, 0.6, 0.8, 1.0, 1.2, 1.4, 1.6, 1.8, and 2.0 μg antibody/mL. The flow rate for all injections was 30 μL/min. There was a 180 s delay prior to regeneration of the sensor surface using 50mM NaOH, (20 μL, 10 μL/min).

The concentrations used for monoclonal antibody C on the E1G-OVA sensor surface were in the range 0 to 50 μg/mL *i.e.* 0, 5, 10, 15, 20, 25, 30, 35, 40, 45 and 50 μg/mL. Solutions were injected as above, except that two regeneration pulses of 20 % v/v CH_3CN in 100 mM NaOH were required to produce satisfactory regeneration of the surface.

3.4 Inhibitive Immunoassays (Standard Curves)

The monoclonal antibodies W and C had high specificity for estrone glucuronide and acted as the high molecular weight detecting molecule. A constant amount of an antibody was added to an analyte (E1G or estrone sulphate) solution, prior to injection over the sensor surface. The expectation was that the E1G present in the solutions would be bound to the antibody, and the residual antibody would bind to the estrone-OVA conjugate immobilised on the sensor surface.

To obtain calibration ('standard') curves, series of standard estrone glucuronide solutions covering two different concentration ranges were prepared in HBS-EP+

buffer. Each individual standard solution was mixed with an equal volume of monoclonal antibody W (1 μg/mL) in HBS-EP+ buffer, giving a final concentration of 0.5 μg monoclonal antibody W/mL. This solution (60 μL) was passed over the chip surface for 120 s at a flow rate of 30 μL/min. The sensor surfaces were regenerated with two pulses of 50 mM NaOH (one of 20 μL and one of 5 μL, at 10 μL/min). The same procedure was carried out five times for each solution. Concentrations of the standard estrone glucuronide in the final solutions were 0, 2.5, 5, 10, 25, 50, 100, 250, 500, and 1250 ng/mL in the higher-range curve and 0, 0.25, 0.5, 0.75, 1.00, 1.25, 1.5, 2.0, 2.5 and 5.0 ng/mL in the lower-range curve.The solutions were injected over each of the four estrone-OVA conjugate sensor surfaces.

Diluted ascites fluid used in place of the antibody W was also investigated, using the same estrone glucuronide concentrations. Single injections were made of each standard solution. The solutions were injected over the E1G-OVA surface.

To obtain a standard curve for estrone glucuronide using monoclonal antibody C estrone glucuronide solutions were prepared in HBS-EP+ buffer and mixed with an equal volume of antibody C solution (30 μg/mL), giving an antibody concentration of 15 μg monoclonal antibody C/mL. This solution (60 μL) was passed over the chip surface for 120 s at a flow rate of 30 μL/min. As with the antibody C binding curve determination, two regeneration pulses of 20 % v/v CH_3CN in 100 mM NaOH were used to regenerate the sensor surface prior to subsequent injections. Five replicates were measured for each concentration. A single range of standard solutions was prepared with concentrations of estrone glucuronide of 0, 1, 1.5, 2, 2.5, 3, 4, 5, 6, 10 ng/mL. The solutions were injected over the E1G-OVA sensor surface.

To observe the behaviour of antibody W in solution with a different estrone derivative, the standard curves for estrone sulphate standard material with monoclonal antibody W on an E1G-OVA sensor surface were prepared. Two series of standard estrone sulphate solutions of different concentration ranges were prepared in HBS-EP+ buffer. The final antibody concentration was 1 μg antibody W/mL. The solutions (60 μL) were passed over the E1G-OVA chip surface for 120

seconds at a flow rate of 30 μL/min. Regeneration was by a two pulses of 50 mM NaOH (one of 60 μL and one of 5 μL, at 10 μL/min).

The procedure was carried out in triplicate. Concentrations of the standard estrone sulphate material in the final solutions were 0, 10, 25, 50, 100, 500, 1000, 2500, 5000, 10000 and 52600 ng/mL in the higher-range curve, and 0, 0.1, 0.25, 0.50, 0.75, 1.00, 1.25, 2.50, 5.0, 7.5, 10 and 25 ng/mL in the lower-range curve. The solutions were injected over the E1G-OVA sensor surface.

With a new stock of antibody W, SPR antibody binding studies (binding curves) were repeated as before but with antibody W concentrations in the range 0 to 4.5 μg/mL. The standard curves with estrone glucuronide were repeated on each of the four estrone-OVA conjugate sensor surfaces as described earlier, using the new stock of monoclonal antibody W, but with an antibody W concentration of 1.0 μg/mL in the final solutions.

3.5 SPR Signal Enhancement – Experimental Details

Three Sigma anti-mouse antibodies, M8890, A9044 and M7023 were separately assessed for their suitability as secondary antibodies, by making duplicate injections of antibody W mAb (1μg/mL in running buffer) (60 μL, 30 μL/min) immediately followed by the anti-mouse antibody, M8890 (9.2 μg/mL), A9044 (53 μg/mL) or M7023 (12 μg/mL). Regeneration of the surface was made by two pulses of 50 mM NaOH (20 μL and 5 μL, at 10 μL/min). This process was repeated using HBS-EP+ running buffer in place of the antibody W mAb to assess the level of non-specific binding. The solutions were injected over the E1G-OVA sensor surface.

The effects of adding modifiers to the running buffer HBS-EP+ (10 mM HEPES (pH 7.4) 150 mM NaCl, 3 mM EDTA, and 0.05 % surfactant P-20) was investigated by repeating the above procedure with the following modifiers added to the running buffer:

0.5 % v/v PEG 400

0.05 % v/v PEG 400

0.5 % v/v Triton-X

0. 5% surfactant P-20

0.5 M NaCl

0.05 % w/v bovine serum albumin

0.05 % w/v ovalbumin.

To optimise loading of A9044 secondary antibody-peroxidase, antibody W mAb 1 μg/mL, 60 μL in running buffer, 30 μL/min) was injected immediately followed by A9044 secondary antibody-peroxidase conjugate in running buffer (60 μL, 10 μL/min) at 0, 10.6, 21.2, 42.4, 106, 138, 212, and 424 μg/mL concentrations. Regeneration was by two pulses of 10 % v/v acetonitrile in 50 mM NaOH (5 and 10 μL at 10 μL/min). The solutions were injected over the E1G-OVA sensor surface.

3.5.1 Signal Enhancement with Secondary Antibodies

3.5.1.1 Enhanced Binding Curves (106 and 212 μg/mL) A9044 secondary antibody-peroxidase) on E1G-OVA Sensor Surface

Solutions of antibody W were prepared with concentrations of 0.2, 0.4, 0.6, 0.8, 1.0, 1.2, 1.4, 1.6, 1.8, and 2.0 μg/mL. Triplicate 60 μL injections were made at 30 μL/min, followed immediately by A9044 secondary antibody-peroxidase solution 106 μg/mL (60 μL, 10 μL/min). Regeneration was by two pulses of 10 % v/v acetonitrile in 100 mM NaOH (60 μL, 5 μL at 10 μL/min).

A higher concentration (212 μg/mL) of A9044 secondary antibody-peroxidase was also investigated in an identical fashion.

3.5.1.2 Enhanced Inhibitive Immunoassays (Standard Curves): Estrone Glucuronide and Antibody W on E1G-OVA Sensor Surface

To investigate enhancement of inhibitive immunoassays, two series of standard estrone glucuronide solutions of different concentration ranges were prepared in HBS-EP+ buffer. Each standard solution was mixed with an equal volume of antibody W solution (2 μg/mL) in HBS-EP+ buffer, to give a final antibody W concentration of 1 μg/mL. The mixture (60 μL) was passed over the chip surface for 120 seconds at a flow rate of 30 μL/min, immediately followed by A9044 secondary antibody-peroxidase solution 106 μg/mL (60 μL, 10 μL/min). Regeneration was by two pulses of 10 % v/v CH_3CN in 100 mM NaOH (2 x 5 μL, 10 μL/min).

Five replicates were injected. Concentrations of the standard estrone glucuronide material in the final solutions were 0, 2.5, 10, 50, 100, 250, 1250 and 2500 ng/mL in the higher-range curve, and 0, 0.1, 0.25, 0.50, 0.75, 1.00, 1.50, 2.5 and 5.0 ng/mL in the lower-range curve.

A 0.5 μg/mL concentration of antibody W with 212 μg/mL of A9044 secondary antibody-peroxidase was also investigated. Five replicates were injected. Concentrations of the standard estrone glucuronide material in the final solutions were 0, 10, 50, 100, 250, 1 250 and 2 500 ng/mL in the higher-range curve, and 0, 0.1, 0.25, 0.50, 0.75, 1.00, 1.50, 2.5 and 5.0 ng/mL in the lower-range curve.

A 0.1 μg/mL concentration of antibody W with 212 μg/mL of A9044 secondary antibody-peroxidase was also investigated as above. Regeneration was by a single pulse of 10 % CH_3CN in 100 mM NaOH (5 μL, 10 μL/min). The procedure was carried out in triplicate. Concentrations of the standard estrone glucuronide material in the final solutions were 0, 0.5, 1, 2, 5, 10, 20, 50, 100, 250 and 500 ng/mL in the higher-range curve, and 0, 0.02, 0.04, 0.06, 0.08, 0.10, 0.15, 0.20, 0.25, 0.50 and 1.0 ng/mL in the lower-range curve.

A lower concentration of antibody W (0.05 μg/mL) with 212 μg/mL of A9044 secondary antibody-peroxidase was also investigated with the same concentrations

of estrone glucuronide as for the 0.1 μg/mL antibody concentration assay described above.

3.5.2 Signal Enhancement with Gold nanoparticles: 40 nm Gold-IgG-Peroxidase Conjugate

Signal enhancement using a 40 nm then a 20 nm gold nanoparticle conjugated to the A9044 secondary antibody was investigated.

The 40 nm gold-IgG-peroxidase conjugate was prepared according to the method of Kumar [148]. A 1.5 mL aliquot of 40 nm colloidal gold and 150 μL of A9044 secondary antibody-peroxidase were combined in a Maxymum^{TM} recovery Eppendorf tube by manual inversion for 20 minutes. The tube was allowed to stand for one to two hours. The tube was then centrifuged at 2000 *x* g for 10 minutes at 4^{o}C and the supernatant liquid removed. The supernatant liquid itself was again centrifuged as before, and the supernatant liquid from this second centrifugation was discarded. The fluid pellets from both centrifugations were pooled and reconstituted in 150 μL of phosphate buffered saline (PBS) pH 7.4 containing 0.2 % w/v bovine serum albumin (BSA) and 3 % v/v polyethylene glycol 400 (PEG). The conjugate was filtered through a Phenomenex 'Phenex' 0.45 μm Polyethersulphone (PES) or Advantec 0.2 μm cellulose acetate disposable syringe filter immediately before use.

To optimise loading of 40 nm gold-IgG-peroxidase conjugate, antibody W in running buffer (1 μg/mL) was injected (60 μL, 30 μL/min) followed immediately by neat 40 nm gold-IgG-peroxidase conjugate (60 μL, 10 μL/min). Regeneration was by injections of 10 % (v/v) acetonitrile in 50 mM NaOH (5 μL then 10 μL at 10 μL/min). The injection was repeated with the conjugate diluted 1:1 with 10 % v/v PEG 400 in Milli-Q water. To assess non-specific binding to the surface, the injection was repeated using running buffer in place of the antibody W mAb solution.

3.5.2.1 40 nm Gold Conjugate: Enhanced Binding Curve

Signal enhancement with the 40 nm gold nanoparticle conjugated to the A9044 secondary antibody was investigated as for 3.5.1.1, but with neat 40 nm gold-IgG-peroxidase conjugate (60 μL, 10 μL/min) used in place of the A9044 secondary antibody-peroxidase solution. Regeneration was by a single pulse of 10 % v/v CH_3CN in 100 mM NaOH (10 μL, 10 μL/min).

3.5.2.2 40 nm Gold Conjugate: Enhanced Inhibitive Immunoassays (Standard Curves): Estrone Glucuronide and Antibody W (1 μg/mL)

To investigate enhancement of inhibitive immunoassays with 40 nm gold nanoparticles conjugated to the A9044 secondary antibody, standard curves were prepared as for 3.5.1.2 but with neat 40 nm gold-IgG-peroxidase conjugate (60 μL, 10 μL/min) used in place of the A9044 secondary antibody-peroxidase solution. Regeneration was by two pulses of in 10 % v/v CH_3CN in 100 mM NaOH (2 x 5 μL, 10 μL/min).

The procedure was carried out in triplicate. Concentrations of the standard estrone glucuronide material in the final solutions were 0, 0.5, 2.5, 5, 10, 50, 100, 250, 1250, 2500 ng/mL in the higher-range curve, and 0, 0.25, 0.50, 1.00, 1.50, 2.0 and 5.0 ng/mL in the lower-range curve.

3.5.3 Signal Enhancement with Gold nanoparticles: 20 nm Gold-IgG-Peroxidase Conjugate

Signal enhancement using 20 nm gold nanoparticles when preparing a gold nanoparticle: secondary antibody conjugate was investigated. The conjugation method was also altered.

The 20 nm gold-IgG-peroxidase conjugate was prepared using the method of Mitchell and Wu [54], *i.e.*, two 25 mL aliquots of 20 nm colloidal gold were dispensed into separate 50 mL polypropylene 'Oak Ridge Tubes' and 750 μL of polyethylene glycol (3 % v/v) was added to each tube before centrifuging at 14000 x

g for 30 minutes. The supernatant was removed from the liquid pellet and reconstituted in 5 mL of Milli-Q water with the aid of sonication. The contents of the tube were mixed using a vortex mixer during the addition of 500 μL of A9044 secondary antibody-peroxidase solution (8 mg/mL in Milli-Q water) then shaken on a mechanical rotator for ten minutes. The solution was stored overnight at 4^{o}C before adding 550 μL of a freshly prepared solution of bovine serum albumin (20 % v/v in Milli-Q water). The resulting conjugate solution was mixed on a mechanical rotator for ten minutes and refrigerated at 4^{o}C for four hours, then filtered as for the 40nm conjugate before use in the surface plasmon resonance instrument.

3.5.3.1 20 nm Gold Nanoparticle-IgG-Peroxidase Conjugate Enhanced Binding Curve

The effect of a secondary binding event using a smaller gold nanoparticle was investigated with the 20 nm gold nanoparticle-IgG-peroxidase conjugate. The binding curve was carried out as for 3.5.1.1 with antibody W solutions in the concentration range 0.1, 0.2, 0.3, 0.4, 0.5, 0.6, 0.7, 0.8, 0.9 and 1.0 μg /mL. 20 nm gold-IgG-peroxidase conjugate diluted 1:1 with 1 % v/v PEG 400 (60 μL, 10 μL/min) was used in place of A9044 secondary antibody-peroxidase solution. Regeneration was by one pulse of 20 % v/v acetonitrile in 100 mM NaOH (60 μL, 10 μL/min).

3.5.3.2 20 nm Gold Nanoparticle-IgG-Peroxidase Conjugate: Enhanced Inhibitive Immunoassays (Standard Curves): Estrone Glucuronide vs Antibody W (1 μg/mL and 0.05 μg/mL))

To investigate enhancement of inhibitive immunoassays with 20 nm gold nanoparticles conjugated to the A9044 secondary antibody, standard curves were prepared as for 3.5.2.2, but with 20 nm gold-IgG-peroxidase conjugate diluted 1:1 with 1 % v/v PEG (60 μL, 10 μL/min) used in place of 40 nm gold-IgG-peroxidase. Regeneration was as for the binding curve.

Standard curves were also generated as above using a lower antibody W concentration (0.05 μg/mL) and with lower concentrations of the standard estrone

glucuronide 0, 0.25, 0.5, 1.0, 2.5, 5.0, 10, 25, 50, 125, 250 ng/mL in the higher-range curve, and 0, 0.005, 0.01, 0.02, 0.03, 0.04, 0.050, 0.075, 0.10, 0.125, 0.25 and 0.50 ng/mL in the lower-range curve.

3.6 Results and Discussion

Effects of Linker Length on Sensitivity

Previous SPR studies with progesterone [68] had suggested that antibody binding was enhanced by the incorporation of a linker between the steroid and the protein used for conjugation. Introducing a linker of the type proposed might enhance binding by orientating the steroids, so that they project away from the sensor surface and into the flow of buffer. One other consideration is that this type of linker is known to suppress binding of protein to the sensor surface [78], effectively reducing non-specific binding.

Degrees of conjugation of each of the four estrone-ovalbumin conjugates, *i.e.* E1G-OVA, E1G, OEG-OVA, E1C3, C5-OVA and E1C3, OEG-OVA were determined by matrix-assisted laser desorption/ionization time-of-flight (MALDI-TOF) mass spectrometry using the method of Carroll [149]. The centroid of a typically broad conjugate peak was taken as the molecular mass of the estrone-OVA conjugate. Deducting the weight of ovalbumin, the average number of the conjugated estrone molecules was calculated (Table 1).

Table 1: Results of the determination of mass spectrometry of hapten ratio (estrone to ovalbumin) in the estrone conjugates, and the corresponding level of conjugate immobilisation on sensor surfaces. Flow cell 1 was immobilised with ovalbumin only, to act as a reference, and flow cell 2 with the respective estrone-ovalbumin conjugate.

Estrone Conjugate	MW	Steroid MW	Hapten Number	Flow Cell 2 (RU)	Flow Cell 1 (RU)
Ovalbumin	44327				
E1G-OVA	45418	446.49	2.4	4513	3939
E1G,OEG-OVA	48171	748.86	5.1	815	1680
E1C3,C5-OVA	45084	469.61	1.6	2294	2420
E1C3,OEG-OVA	46546	658.82	3.4	2644	2561

The conjugation of the estrone derivatives to ovalbumin was carried out using exactly the same procedure in all cases, but the hapten values varied from 1.6 (E1C3, C5-OVA) to 5.1 (E1G, OEG-OVA). When using the Immobilisation Wizard on the Biacore^{TM} instrument, the target level was set at 5000 RU, but those conjugates with OEG linkers were more difficult to immobilise than those without the linker. The level obtained for the E1G, OEG-OVA chip was obtained only after further dilution in 10 mM sodium acetate solution pH 4.0 (when compared with the non-linker conjugates) and repeated injections over the surface.

The EDC/NHS activation of the carboxymethylated dextran CM5 surface was carried out at 10 μL/min, and the solution injected until the change in response units was at least 200 RU, which was taken to indicate a satisfactory level of surface activation. The final step, namely the capping of remaining the activated esters using ethanolamine reduced the response level by around 300 – 500 RU for the conjugate, and a little less for the ovalbumin surface (200 – 300 RU). Conditioning the surface with ten blank injections (no antibody) through both flow cells provided a sufficiently stable sensor by removing traces of unbound material.

Regeneration injections of 50 mM NaOH gave far superior surface regeneration. Values for flow cell 2 values dropped only slightly over repeated injections, and sample response increased and then stabilised, indicating that the bound material was sufficiently removed without loss of surface activity. The contact time for regeneration was decided on the basis of how large the signal produced during binding – a smaller binding signal required only a modest regeneration period.

When using secondary antibodies and gold-antibody conjugates, a slightly harsher regeneration cocktail was necessary to restore the baseline to initial conditions. In these cases the concentration of NaOH was increased to 100 mM, and acetonitrile was employed (up to 20 % v/v). Two regeneration pulses were often required with these assays.

When comparing the E1-OEG-OVA conjugates to their (non-OEG linker) counterparts, it is apparent that the incorporation of the OEG linker improved the hapten ratio approximately two-fold *i.e.* 2.4 for E1G-OVA, *cf.* 5.1 for E1G, OEG-OVA and 1.6 for E1C3, C5-OVA *cf.* 3.2 for E1C3, OEG-OVA. Yuan *et al*.[77] observed a similar pattern in their progesterone work, and attributed the increase to the higher solubility of the OEG conjugates in polar solvents used in the conjugation step. However, the hapten ratios for these E1-OEG linker conjugates are still much lower than their progesterone analogues with a similar linker length. The 23-atom linker progesterone-ovalbumin conjugate used by those workers had a hapten ratio of 11 progesterone-linker molecules/protein, very much higher than the estrone analogues discussed here. The reasons for this are unclear.

Certainly the signals produced by antibody binding to both the E1-OEG-OVA surfaces are higher when compared to their E1 analogues without a linker (Figure 10), but it is difficult to attribute to steric advantages improving antibody binding, since those conjugates with a higher hapten number will have a higher concentration of the E1 analogue on the sensor surface. Whilst the linkers have enhanced the binding to some degree, in the sense that the SPR response for a given antibody concentration is higher (Table 2), in a practical sense the difficulty in immobilising these conjugates to the sensor surface outweighed the potential improvements. Accordingly, sensor surfaces produced with E1G-OVA were used for later work on signal enhancement.

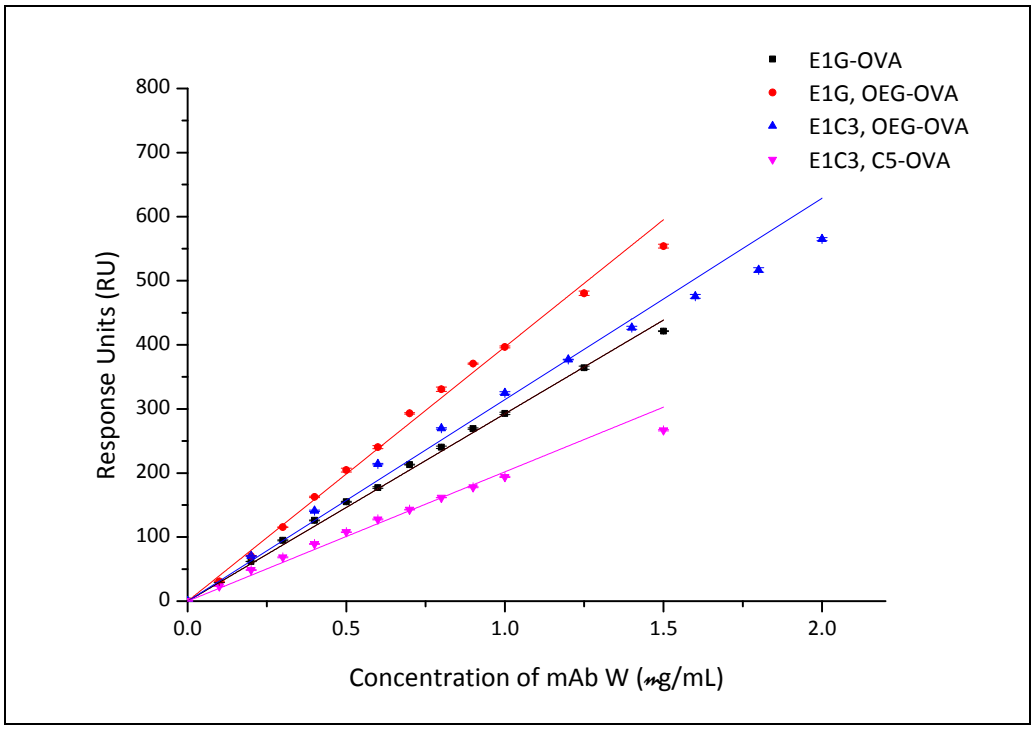

Figure 10: Antibody response (binding) curves for CM5 sensor surfaces prepared using ovalbumin conjugates of the estrone derivatives: estrone glucuronide, E1G-OEG, E1C3,C5, and E1C3, OEG. Antibody is monoclonal antibody W. Error bars shown on the graphs represent one standard deviation (SD) of the mean.

Table 2: The Limits of detection and IC_{50} for the calibration curves of the four estrone derivatives. Data given is for the 'low' concentration series only.

Estrone Conjugate	Primary antibody concentration (µg/mL)	LOD (pg/mL)	IC_{50}(pg/mL)	RU.mL/µg
E1G-OVA	0.5	520 ± 30	1300 ± 40	290 ± 5
E1G,OEG-OVA	0.5	460 ± 20	1200 ± 30	400 ± 5
E1C3,C5-OVA	0.5	710 ± 40	1400 ± 40	200 ± 5
E1C3,OEG-OVA	0.5	440 ± 20	1100 ± 30	310 ± 5

3.6.1 New Monoclonal Antibody W Stock:

After initial studies proved promising, a second stock of the antibody W was sourced, but proved to be less active in surface plasmon resonance binding than

the original material supplied. In order to obtain a similar signal size in surface plasmon resonance, about twice the concentration was necessary. The reasons for this reduction in signal are not clear, but may result from a change in activity due to a difference in storage conditions. Accordingly, the binding curve was repeated, and the standard curves used 1 μg monoclonal antibody W/mL (Table 3), *cf.* the original curves prepared using 0.5 μg/mL. The second stock supplied was used for all remaining work. Table 3 lists the LOD and IC_{50} values for two assays, one with a 'high' range concentration of estrone glucuronide and the other a 'low' concentration range. The reasons for this are discussed in the next section.

Table 3: Limits of detection and IC_{50} values for an estrone glucuronide assay using the second batch of antibody W stock, at 1.0 μg antibody W/mL on an E1G-OVA sensor chip. Values given for both (H) high and (L) low concentration ranges of estrone glucuronide. The signal size of this second batch is given by RU.mL/μg.

Estrone Conjugate	Primary antibody concentration (μg/mL)	LOD (pg/mL)	IC_{50}(pg/mL)	RU.mL/μg
E1G-OVA	1.0	440 ± 15 (L)	980 ± 15 (L)	120 ± 5
	1.0	9700 ± 350 (H)	84000 ± 1200 (H)	

3.6.2 'Double-Curve' Inhibition Assays

The standard curves for the four estrone conjugates were measured and showed irregular features (Figures 11, 12, 13 and 14). For clarity, the axes have the same scaling for all of the estrone derivative conjugates. Initial testing with the higher range of estrone glucuronide concentrations generated curves with the expected sigmoidal shape, but the responses for the points at the lower concentrations of estrone glucuronide were much lower than expected, when compared on the basis of the response for the antibody-only concentration in the binding curve. The experiment was repeated and similar results obtained. A second series of solutions with much lower estrone glucuronide concentrations ('low concentration') was analysed on each of the four chips, revealing a second curve at a lower concentration and generating the 'double curve' shown in the Figures 11, 12, 13

and 14. In each case, a discontinuity occurs in the graph, when the two concentration sets were run separately. (There was no discontinuity in a single run where both concentration sets were run in quick succession – data not shown). For the purposes of calculating the LOD and IC_{50} values, the two curves were treated separately.

A standard curve using a second antibody (antibody C) with the E1G-OVA sensor surface chip (Figure 15) showed no second curve at lower concentrations (the RU values at low E1G concentrations were as expected when compared with the binding curve values for that antibody concentration). This antibody gave an inhibition assay with a limit of detection of 1900 ± 90 pg/mL, and required a high concentration of antibody (15 μg/mL) to produce an SPR signal around 100 RU, whereas 1 μg/mL of antibody W gave a signal around 120 to 150 RU. A high concentration of primary antibody would make this a relatively high-cost assay, but it served to confirm that in all probability that the two-curve effect was related to the antibody used. The typical single curve assay using antibody C was obtained on the same E1G-OVA sensor surface as the antibody W assays which gave double curves.

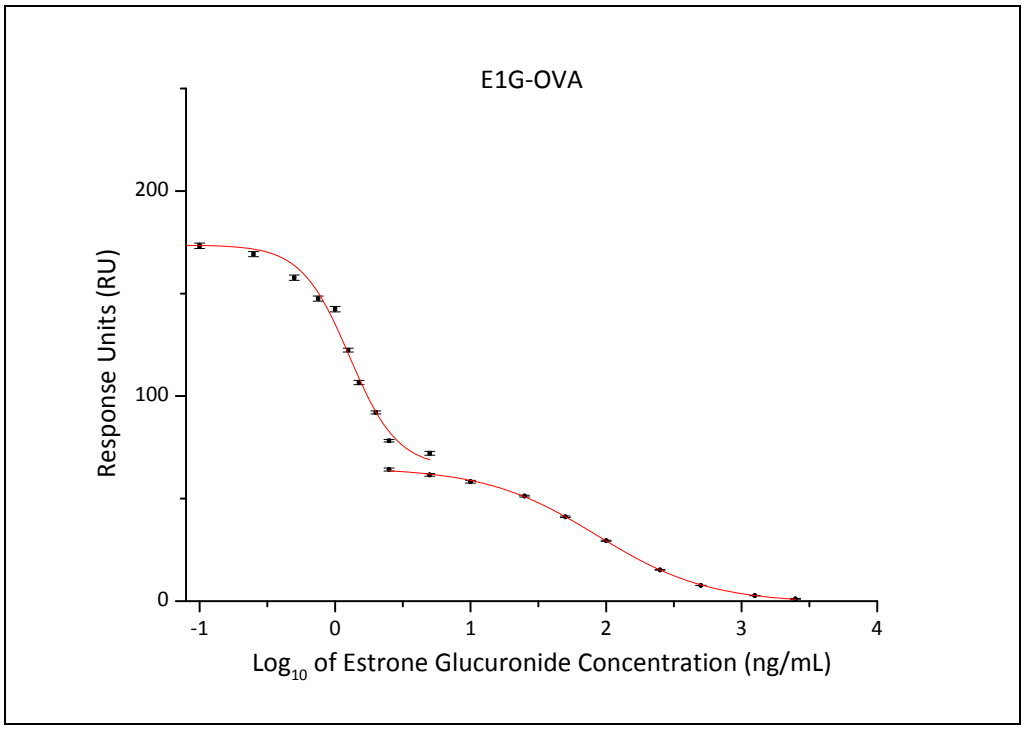

Figure 11: Inhibition assay standard curve for estrone glucuronide on a CM5 sensor surface immobilised with E1G-OVA. Antibody W mAb used for this assay. SPR Response Unit (RU) against the logarithm of concentration (in ng/mL) of estrone glucuronide. Error bars shown on the graph represent one standard deviation (SD) of the mean.

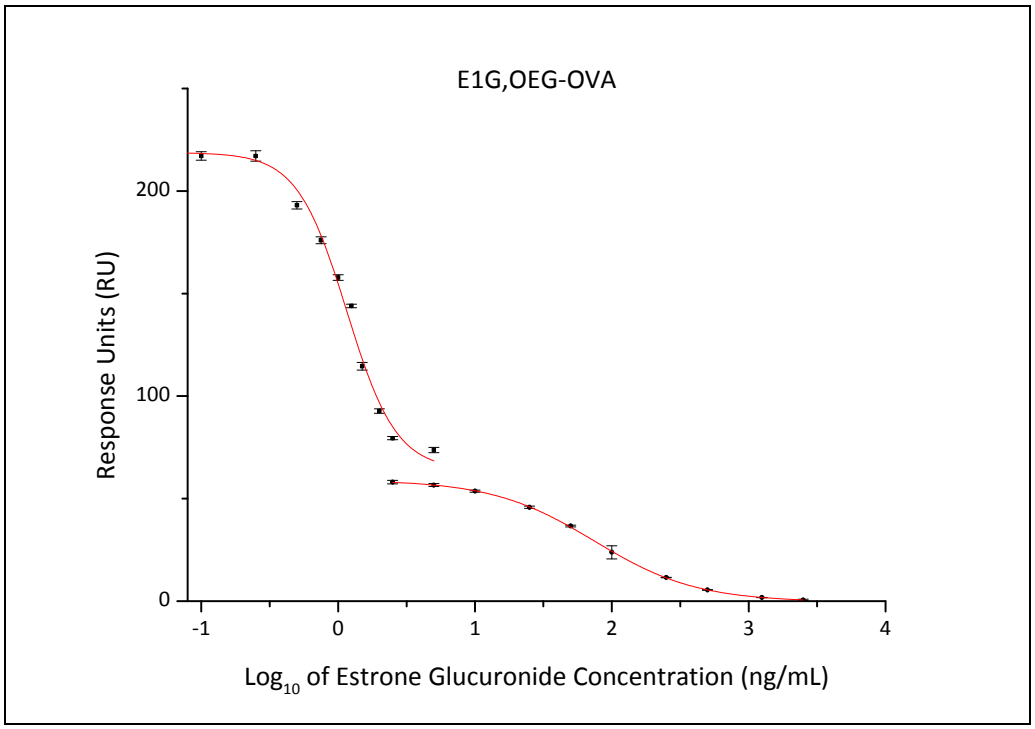

Figure 12: Inhibition assay standard curve for estrone glucuronide on a CM5 sensor surface immobilised with E1G, OEG-OVA. Antibody W mAb was used for this assay. SPR Response Unit (RU) against the logarithm of concentration (in ng/mL) of estrone glucuronide. Error bars shown on the graph represent one standard deviation (SD) of the mean.

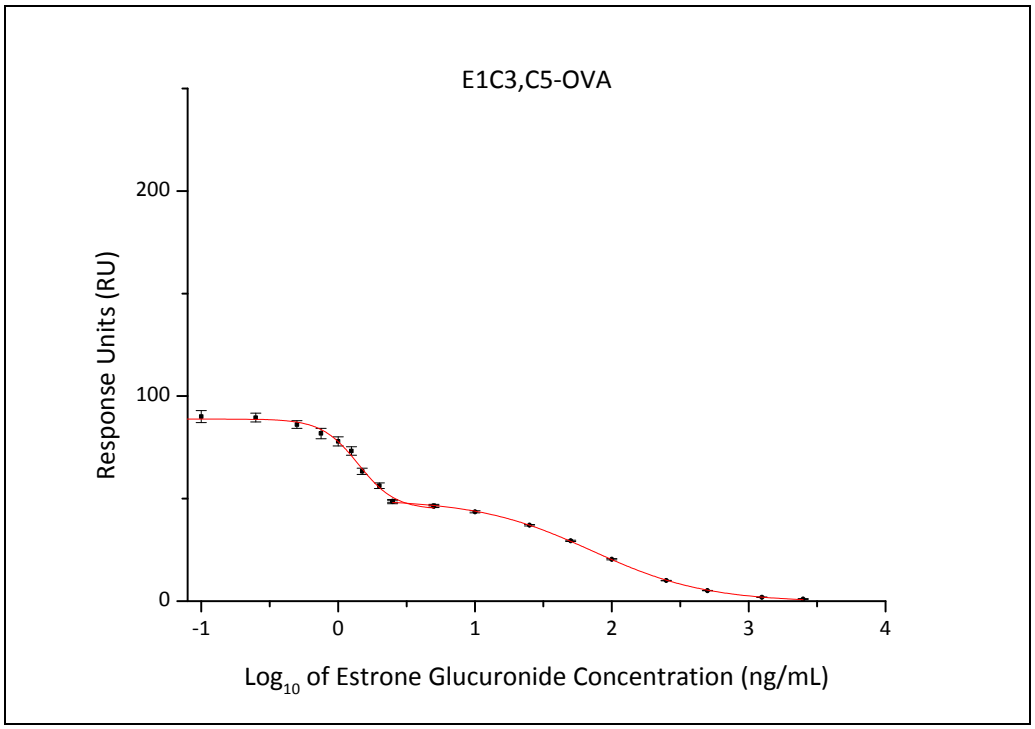

Figure 13: Inhibition assay standard curve for estrone glucuronide on a CM5 sensor surface immobilised with E1C3, C5-OVA. Antibody W mAb used for this assay. SPR Response Unit (RU) against the logarithm of concentration (in ng/mL) of estrone glucuronide. Error bars shown on the graph represent one standard deviation (SD) of the mean.

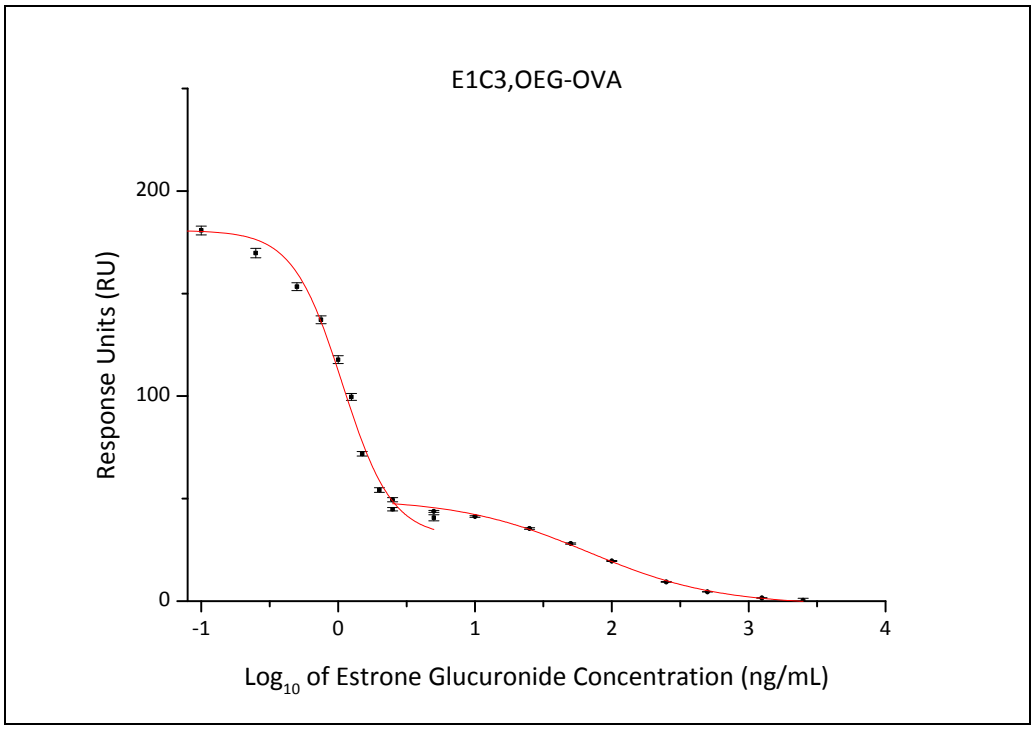

Figure 14: Inhibition assay standard curve for estrone glucuronide on a CM5 sensor surface immobilised with E1C3, OEG-OVA. Antibody W mAb used for this assay. SPR Response Unit (RU) against the logarithm of concentration (in ng/mL) of estrone glucuronide. Error bars shown on the graph represent one standard deviation (SD) of the mean.

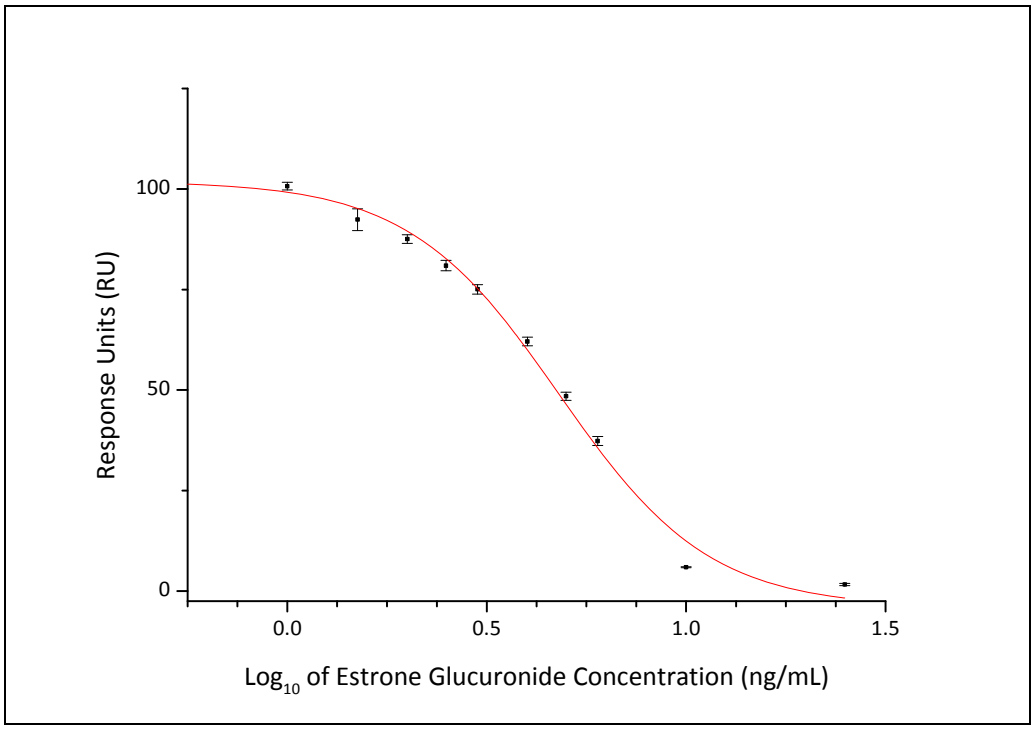

Figure 15: Inhibition assay standard curve for estrone glucuronide on a CM5 sensor surface immobilised with E1G-OVA. Monoclonal antibody C used for this assay. SPR Response Unit (RU) plotted against the logarithm of concentration (in ng/mL) of estrone glucuronide. Error bars shown on the graph represent one standard deviation (SD) of the mean.

The binding events occurring at a lower loading of estrone glucuronide conjugate on the sensor surface were investigated by preparing a CM5 chip with approximately 1000 RU of E1G-OVA immobilised on the surface *cf.* approximately 4000 to 5000 RU on a typical E1G-OVA chip. The results were similar (other than an overall decrease in signal), in that two curves were apparent in the standard curve (data not shown). Two curves were still produced, albeit with lower responses, as expected of a lower-loaded surface. Secondly, changing the standard material from estrone glucuronide to estrone in the sulphate form was designed to probe for differences in antibody binding behaviour occurring in solution. (The antibody W was raised against estrone sulphate, and exhibited cross-reactivity with estrone glucuronide, so was expected to bind to estrone sulphate). Again, two curves were apparent when estrone sulphate was used as a standard material (Figure 16).

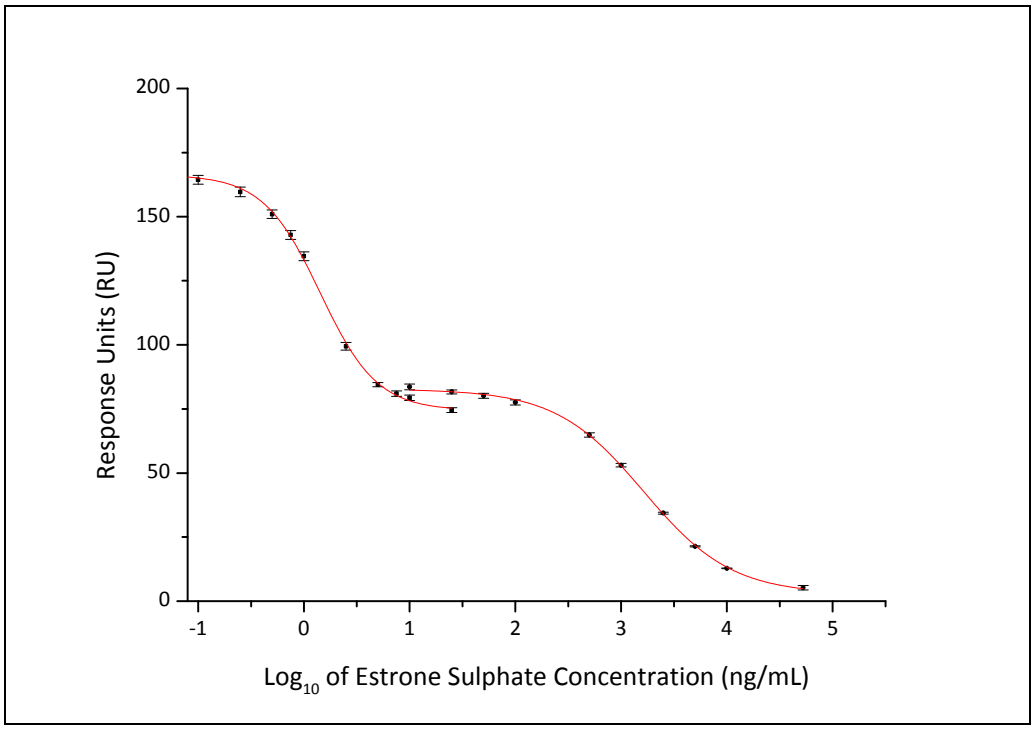

Figure 16: Inhibition assay standard curve for estrone sulphate on a CM5 sensor surface immobilised with E1G-OVA. Antibody W mAb used for this assay. SPR Response Unit (RU) against the logarithm of concentration (in ng/mL) of estrone sulphate. Error bars shown on the graph represent one standard deviation (SD) of the mean.

The results of this standard curve indicate that the binding event in solution occurred in a similar fashion for both the glucuronide and the sulphate, and that the effect was restricted to the monoclonal antibody W. To determine whether antibody W had been somehow affected during its purification, the ascites fluid (peritoneal cavity fluid drawn from the immunised animal) was used without further treatment to determine if it exhibited the same behaviour during an SPR inhibition assay. The ascites fluid was diluted to give a response around 130 RU, and an inhibition assay run as for the estrone glucuronide assay with antibody W. Single injections were run over both of the concentration ranges used in the estrone glucuronide assay. An estrone glucuronide-ovalbumin conjugate sensor surface was employed. The results are given in Figure 17, showing the same distinctive double curve standard curve observed in the assays with antibody W.

The possibility exists that the antibody supplied contained two clones, each with a different binding behaviour, but to confirm this would have involved exhaustive investigation.

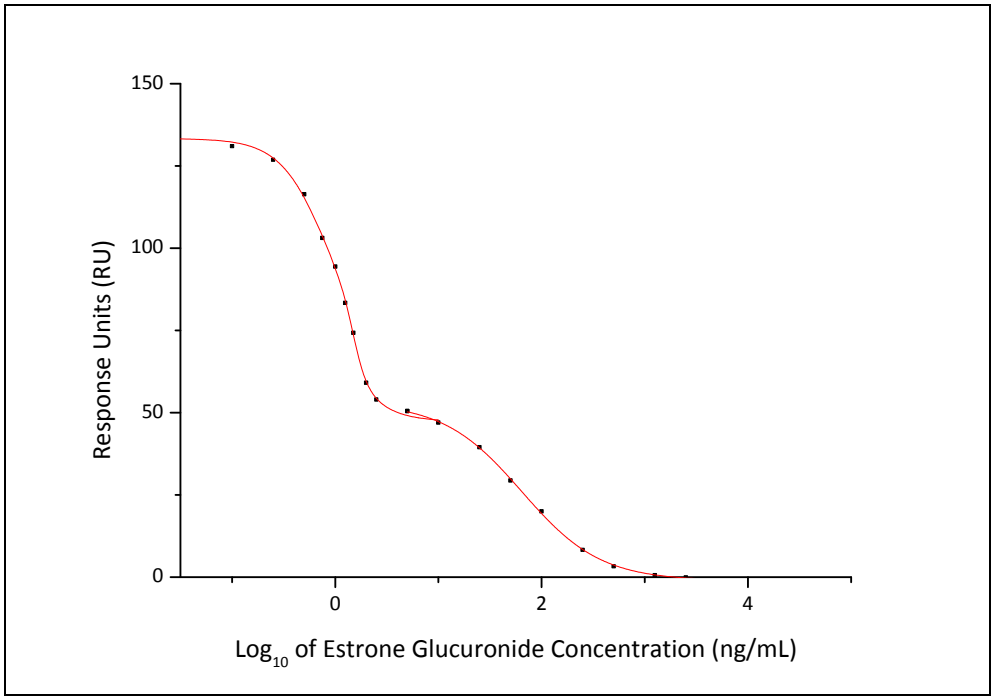

Figure 17: Inhibition assay standard curve for estrone glucuronide on a CM5 sensor surface immobilised with E1G-OVA. Ascites fluid was used for this assay. SPR Response Unit (RU) is plotted against the logarithm of concentration (in ng/mL) of estrone glucuronide.

The Effect of Signal Enhancement on Sensitivity

Introducing a sequential binding event by binding a secondary antibody to a surface-bound primary antibody has been found to be a straight-forward means of increasing signal and thereby improving assay sensitivity. Typically, use of a secondary antibody for signal amplification in this way can improve signal size many times, depending on the antibody selected. The use of a secondary antibody for signal enhancement can allow the use of much less primary antibody, reducing the cost of the analysis.

To explore the possibility of enhancing sensitivity, three anti-mouse secondary antibodies, Sigma M8890, A9044 and M7023 were trialed for their suitability. The performances of the three secondary antibodies in running buffer were

investigated, and then the addition of various buffer modifiers was examined. The results for the three secondary antibodies trialed are given in Table 4. The criteria considered to be important in assessing the secondary antibody and the buffer modifier were: the size of the primary antibody signal, level of enhancement by the secondary antibody, and the degree of non-specific binding. The addition of modifiers such as surfactants or protein was intended to minimise non-specific binding, but some of the modifiers depressed the responses for both antibodies when compared to unmodified HBS-EP+ running buffer *i.e.* 10 mM HEPES (pH 7.4), 150 mM NaCl, 3 mM EDTA, and 0.05 % surfactant P-20.

Table 4: Assessment of secondary antibodies on the signal enhancement of the primary antibody signal, and the effect of buffer modifiers on the primary antibody signal size and the degree of non-specific binding. The non-specific binding level (*i.e.* the response when the secondary antibody is injected in the absence of the primary antibody) is expressed as a percentage of the total primary and secondary binding (to 1 significant figure).

		HBS-EP+	% NSB	+0.5M NaCl	% NSB	+0.05%w/v BSA	% NSB	+0.05%w/v OVA	% NSB	+0.05%w/v PEG	% NSB	+0.5%w/v PEG	% NSB	+0.05%w/v Triton X*	% NSB	+0.05%w/v Tween 20**	% NSB	HBS-EP+ pH 8.4	% NSB
M8890	1° only	168		25		169		136		134		157		93		140		63	
		170		26		171		146		136		158		90		140		63	
	1°+ 2° Ab	305		57		299		280		255		302		218		292		178	
		309		57		305		289		262		306		227		293		183	
	2° Ab only	163	**50**	38	**70**	146	**50**	152	**50**	142	**60**	156	**50**	165	**80**	170	**60**	129	**70**
		159	**50**	37	**60**	143	**50**	148	**50**	139	**50**	151	**50**	154	**70**	166	**60**	127	**70**
A9044	1° only	172		27		172		147		139		160		90		141		66	
		166		27		170		146		139		159		87		140		67	
	1°+ 2° Ab	363		127		368		346		315		348		276		334		185	
		365		126		370		348		318		349		283		334		188	
	2° Ab only	173	**50**	89	**70**	157	**40**	162	**50**	150	**50**	158	**50**	205	**70**	172	**50**	115	**60**
		163	**50**	86	**70**	149	**40**	154	**40**	143	**50**	148	**40**	178	**60**	163	**50**	111	**60**
M7023	1° only	163		27		167		146		139		158		92		141		69	
		160		27		168		145		138		157		82		139		68	
	1°+ 2° Ab	220		73		209		216		200		226		179		218		125	
		222		73		212		219		203		228		191		220		128	
	2° Ab only	122	**50**	55	**80**	106	**50**	120	**60**	112	**60**	123	**60**	157	**90**	129	**60**	87	**70**
		115	**50**	54	**70**	101	**50**	114	**50**	107	**50**	116	**50**	142	**80**	124	**60**	84	**70**

Sigma A9044 antibody was selected for closer investigation because of its slightly higher signal enhancement and relatively low non-specific binding level (*i.e.* its lower level of undesirable binding to the sensor surface in the absence of the primary antibody). The A9044 antibody was an IgG-peroxidase conjugate, slightly larger than the other two antibodies, which might explain its higher level of enhancement when compared with the other secondary antibodies trialed. The results with the buffer modifiers suggested that the addition of 0.5 % w/v bovine serum albumin (BSA) gave slightly lower levels of non-specific binding than unmodified buffer, but the difference was minimal, and the use of BSA in the running buffer was found to shorten the life of the sensor surface, so unmodified buffer was used for all subsequent work. The optimum dilution level for the A9044 secondary antibody was determined by plotting the signal against concentrations of secondary antibody for a constant concentration of primary mAb (1 μg/mL), shown in Figure 18.

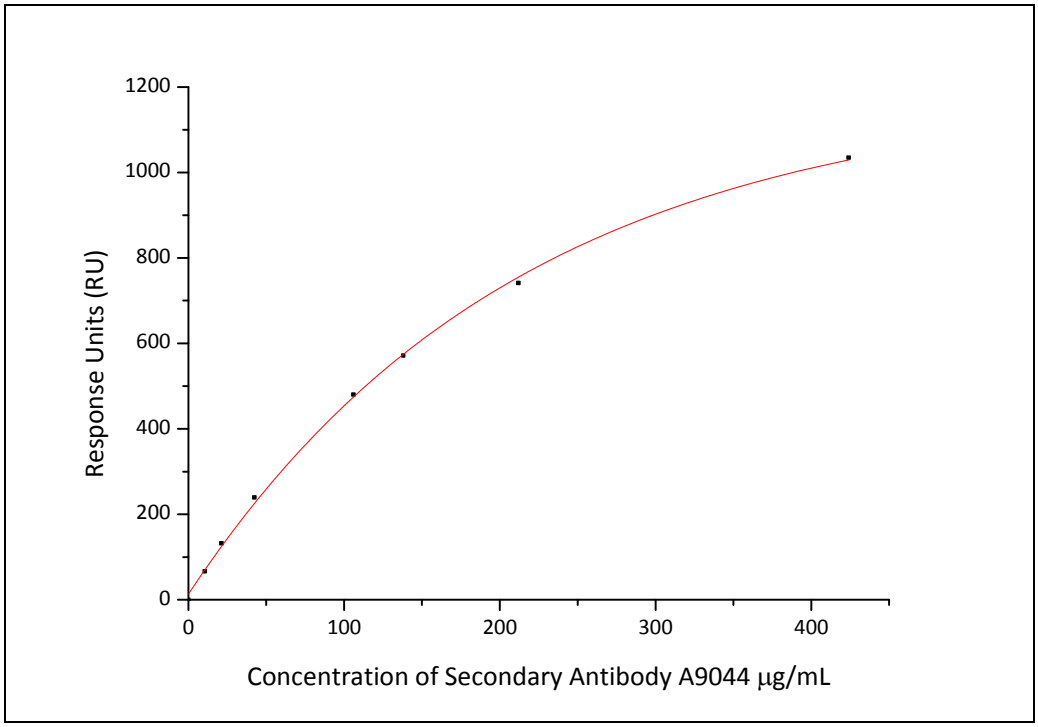

Figure 18: Optimisation of secondary antibody loading.

The secondary antibody concentration plot (Figure 18) suggested that a suitable concentration was approximately 200 μg/mL, where good signal enhancement was obtained without using excessive amounts of antibody. In this way a sensitive assay could be produced, with assay costs kept to a minimum.

Early assays used relatively higher concentrations of monoclonal antibody W; later assays reduced the amount of primary antibody to produce the most sensitive assay with this binding system.

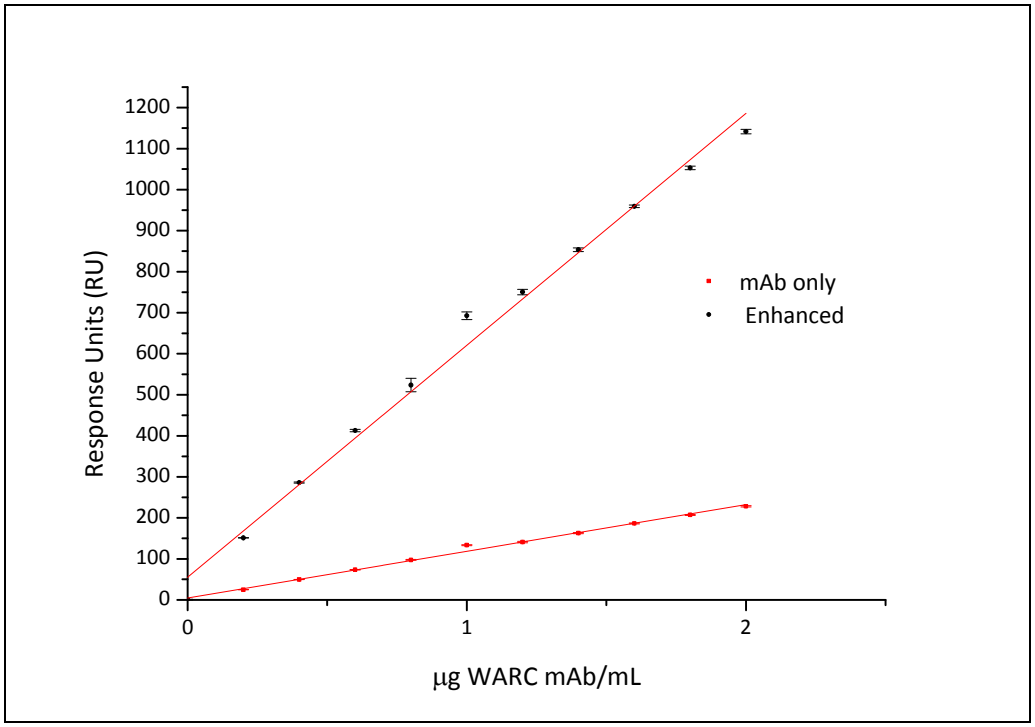

Figure 19: Antibody binding response plot for primary monoclonal antibody only and secondary antibody-enhanced binding. Secondary antibody concentration A9044 is 212 μg/mL. Signal enhancement 5.0. Error bars shown on the graph represent one standard deviation (SD) of the mean.

The level of enhancement was calculated by dividing the slope of the enhanced antibody binding plot by the slope of the monoclonal (un-enhanced) antibody plot. Using the A9044 secondary antibody at a relatively high concentration (212 μg/mL for up to 2 μg antibody W/mL) gave 5-fold signal amplification (Figure 19). This high level of signal enhancement is in keeping with the findings of Mitchell [76], who speculated that the enhancement might be due to binding of multiple secondary antibodies to a single primary antibody. The A9044 secondary antibody was slightly

larger in mass than the primary antibody, since it was an antibody-peroxidase conjugate, but the difference in mass is too small to account for enhancement by a factor of 5.

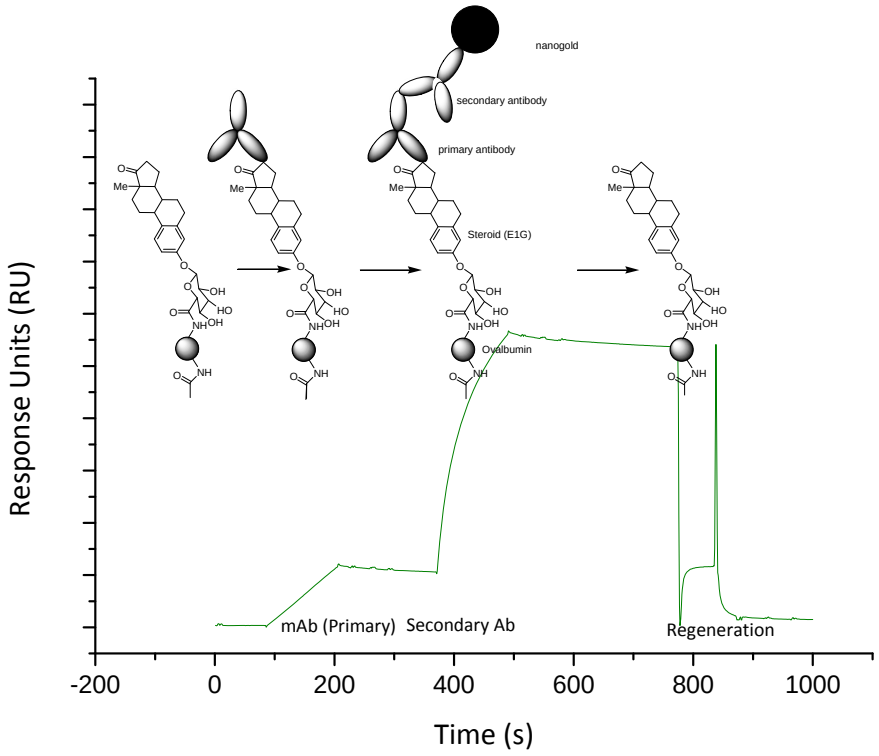

Figure 20: The sensorgram of the primary antibody binding event, the secondary antibody binding event, and the regeneration step. The secondary antibody shown here is conjugated to a gold nanoparticle.

Whether labeling a secondary antibody with gold nanoparticles might further raise the signal enhancement (and therefore the sensitivity of the assay) was investigated. A typical sensorgram showing the primary and secondary binding events and regeneration step is shown in Figure 20. Initially a commercially supplied 40 nm gold-secondary antibody conjugate (goat anti-mouse IgG/nanogold 40 nm) was trialed. No enhancement was observed when compared to primary monoclonal antibody only binding signal. A small signal increase (approximately 100 RU) was observed for all solution concentrations, including those with no antibody present. The increase was attributed to 'bulk effects', *i.e*. the difference in refractive index

between the solution injected and the running buffer. When corrections had been made for this difference in refractive indices, it was apparent that no enhancement had occurred. The reasons for this absence of enhancement are not clear, but it is likely that the secondary antibody had degraded.

Commercially available 40 nm gold nanoparticle was conjugated to the A9044 secondary antibody using the method of Kumar [148]. The conjugate was prepared by adsorbing the secondary antibody molecules on the gold nanoparticle surface, and then blocking off the remaining sites on the gold nanoparticle with protein (bovine serum albumin). The UV-visible spectrum of the conjugate prepared in this way exhibited a peak shift (5 nm), when compared with the a solution of untreated 40 nm gold nanoparticles diluted with phosphate buffered saline (PBS) pH 7.4 containing 0.2 % w/v bovine serum albumin (BSA) and 3 % v/v polyethylene glycol (PEG) 400. This shift was taken to indicate formation of an antibody layer around the nanoparticles. Other than the peak due to the gold nanoparticle (around 525 nm), the UV-visible spectrum did not exhibit any other peaks, which was consistent with an absence of aggregation [148]. The signal enhancement was modest, 3.6 fold. Gold was visible on the 'Maxymum^{TM} recovery' tubes (Figure 21), which was taken to indicate losses of the gold during preparation of the conjugate.

In order to gauge the degree to which this modest enhancement could be attributed to the secondary antibody itself, the secondary antibody-enhanced binding curve and assays were carried out using a (lower than optimum) concentration of A9044 secondary IgG-peroxidase (106 μg/mL) without gold attached. The 106 μg/mL concentration of secondary antibody was comparable to that used in the preparation of the 40 nm gold conjugate. The enhancement was around 4.3-fold, in line with the value expected on the basis of the secondary antibody enhancement plot. This enhancement (4.3) was larger than that with the 40 nm gold conjugate (3.6). In Kumar's method of conjugation, there was a concentration step at the end of the procedure, with remaining unbound antibody removed during centrifugation. It is therefore entirely possible that a lower

enhancement would be found with the gold antibody-conjugate compared to the antibody-only. Other factors contributing to reduction in signals would be losses of gold on to the surfaces of the tubes, and the failure of the conjugate to remain completely in solution, even for the relatively brief time frame required for these assays. Difficulties with aggregation of 40 nm gold nanoparticles occurring over time have been reported by other workers. Mitchell and Wu [54] considered that a gold nanoparticle size around 25 nm was optimum, and so the focus was moved to a 20 nm nanoparticle, also commercially sourced. The method of conjugation was altered to that of Mitchell and Wu [54], in which the centrifugation step occurs prior to the addition of antibody. With this method even unbound remaining antibody would contribute to the signal enhancement.

Figure 21: Maxymum™ recovery tubes used in the conjugation of A9044 anti-mouse antibody to a commercially available 40 nm gold nanoparticle. Note residual gold deposited on the walls of the tubes.

Two batches of 20 nm-A9044 antibody conjugates were prepared separately, with signal enhancement values of 8.4 and 8.5 (Figure 22). It was concluded that the Mitchell and Wu method produced a reproducible conjugate. Only minor losses of

gold were noted on the walls of the Oak Ridge tubes used. The enhancement was an appreciable improvement on that obtained for the secondary antibody only, even given that the secondary antibody concentration used was higher.

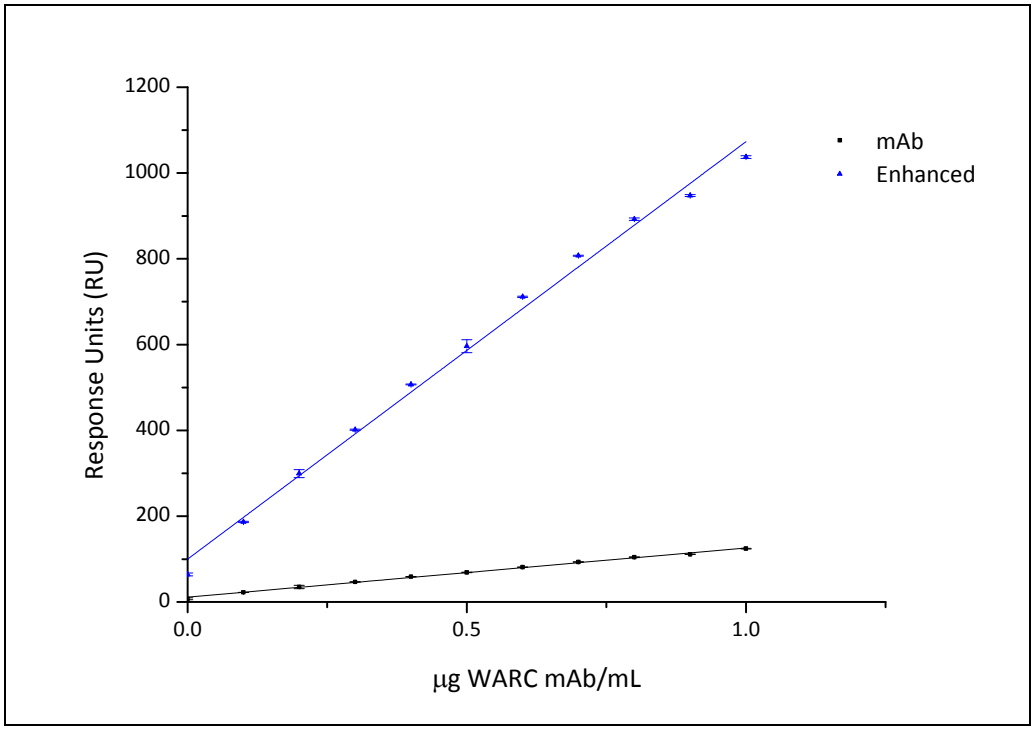

Figure 22: Antibody binding response plot for primary monoclonal antibody only and 20 nm gold:A9044 secondary antibody conjugate enhanced binding. Signal enhancement 8.5. Error bars shown on the graph represent one standard deviation (SD) of the mean.

The first 20 nm gold enhanced assay using monoclonal antibody W concentration of 0.5 µg/mL gave results with good enhanced signal size for both the high and low concentration ranges of estrone glucuronide. The assay was repeated with the second batch of conjugate, using a much lower concentration of primary antibody (0.05 µg/mL), with a view to obtaining an assay with maximised sensitivity and reduced limits of detection. The variation obtained in the enhanced measurements was high, however and the level of non-specific binding was significant, such that the relatively small changes in signal made generating an assay curve impossible.

The secondary-antibody-only assay gave a lower signal enhancement (5.0 *cf*. 8.5 for the gold-antibody complex), but good signal reproducibility, so the use of secondary-antibody-only enhancement using the same concentration of primary

mAb (0.05 µg/mL) was trialed, with success. Interestingly, the unenhanced primary-antibody-only assay gave sufficiently precise results to be used in a standard curve, despite a very low signal. A similar phenomenon was reported in Mitchell's testosterone assay [81]. Mitchell attributed a reduction in signal variability to the absence of a second binding event. The LOD was low for the primary-antibody only assay, *i.e.* 10 pg/mL (for the lower concentration range of estrone glucuronide). The standard curve is shown in Figure 23. The use of an assay with such low signals would however be limited, because while this assay worked well in buffer, the presence of a sample matrix would be likely to limit application in real-world samples. The secondary antibody enhanced signal gave an LOD only slightly higher (13 pg/mL), but its higher signal range would make use in samples such as wastewater more feasible.

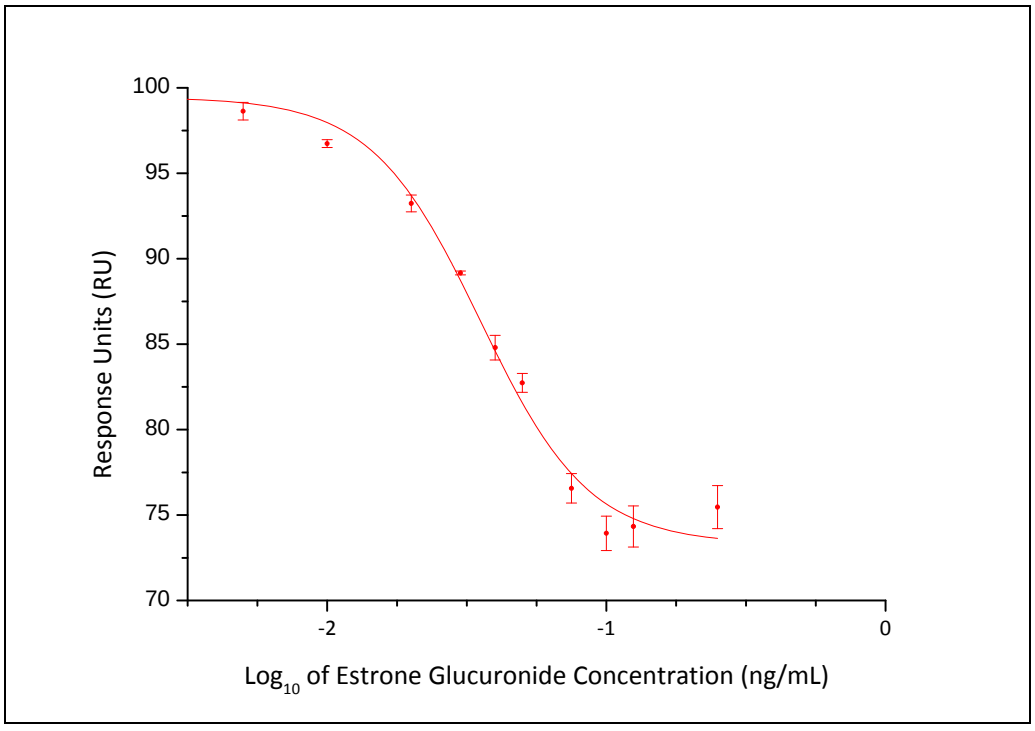

Figure 23: Secondary antibody enhanced assay – low concentration range of estrone glucuronide. LOD is 13 pg/mL. Error bars shown on the graph represent one standard deviation (SD) of the mean.

The E1G-OVA sensor surface proved to be stable for at least 300 injections and similar surfaces have proven to perform acceptably for at least 1000 cycles. The results of all assays are summarised in Table 5.

Table 5: IC_{50} and LOD values in are given in ng/mL, unless otherwise stated. All errors quoted are standard errors. (H) and (L) refer to high- and low- concentration ranges of estrone glucuronide. 20 and 40 nm refer to the size of gold nanoparticle used to prepare the secondary antibody-gold nanoparticle conjugate. The limit of detection (LOD) is the IC_{90} value, and the sensitivity in (RU.mL/μg) is the size of the antibody signal relative to amount of antibody in solution, determined from the binding curve. "Not Valid" signifies that the signal variation was large, and no curve was produced.

Assay format	Primary mAb	Secondary Conc	IC_{50}		LOD		Sensitivity (RU.mL/μg)		Enhance-ment
			Primary mAb	Enhanced	mAb only	Enhanced	mAb only	Enhanced	
(H)	0.5	212	78 ± 2	62 ± 5	11 ± 1	5.3 ± 1	110 ± 3	570 ± 15	5.0
(L)	0.5	212	510 ± 10 pg/mL	504 ± 10 pg/mL	220 ± 10 pg/mL	220 ± 10 pg/mL			
(H)	0.1	212	70 ± 20	65 ± 15	11 ± 5	15 ± 5			
(L)	0.1	212	100 ± 5 pg/mL	90 ± 2 pg/mL	33 ± 2 pg/mL	30 ± 1 pg/mL			
(H)	0.05	212	180 ± 40	80 ± 10	12 ± 2	14 ± 2			
(L)	0.05	212	40 ± 2 pg/mL	35 ± 2 pg/mL	10 ± 1pg/mL	13 ± 1 pg/mL			
(H)	1.0	106	58 ± 1	40 ± 5	8.7 ± 0.5	9.2 ± 3	130 ± 2	570 ± 15	4.3
(L)	1.0	106	940 ± 20 pg/mL	920 ± 20 pg/mL	370 ± 20 pg/mL	360 ± 20 pg/mL			
40 nm (H)	1.0	106	60 ± 2	50 ± 5	7.8 ± 0.4	8.0 ± 2	160 ± 1	560 ± 20	3.6
40 nm (L)	1.0	106	830 ± 30 pg/mL	840 ± 30 pg/mL	270 ± 20 pg/mL	300 ± 20 pg/mL			
20 nm (H)	0.5	360	82 ± 2	70 ± 4	11 ± 0.5	18 ± 2	120 ± 1	1030 ± 30	8.4
20 nm (L)	0.5	360	440 ± 20 pg/mL	460 ± 20 pg/mL	186 ± 20 pg/mL	230 ± 30 pg/mL			
20 nm (H)	0.05	360	70 ± 20	Not valid	16 ± 5	Not valid	115 ± 1	970 ± 15	8.5
20 nm (L)	0.05	360	53 ± 4 pg/mL	Not valid	18 ± 2 pg/mL	Not valid			

3.7 Summary

Ultra-sensitive detection of estrone glucuronide was achieved through signal enhancement. The insertion of an intermediate linker between the steroid and the protein was found to enhance binding less in the estrone system than was the case with the progesterone system studied by Wu *et al.* [68]. The linker did increase the ratio of steroid to protein in the conjugate, *i.e*. raised the hapten ratio. For a given level of immobilisation, a higher steroid content within a conjugate created a higher density of the steroid binding partner on the sensor surface, and thereby generated a more sensitive assay. The linker conjugates were, however, more difficult to immobilise and did so to a lower level than those without a linker. The improvement from a higher hapten ratio was therefore off-set by a lower level of immobilisation on the sensor surface.

It should be noted that linker attachment positions alternative to the 3-position on estrone were not investigated in this study. It is possible that improvements in sensitivity comparable to those observed by Wu *et al.* for progesterone [68] might have been possible by using site-heterology [71] *i.e*., the combination of an antibody raised against a conjugate prepared through the 3-position and a sensor surface with a steroid-linker-conjugate with a linker attachment at a position other than the 3-position. The antibody could then be paired with the conjugate which gave the optimal response as a sensor surface in surface plasmon resonance. It may be that varying linker length and characteristics would have a more pronounced effect when attached at a different position.

A second possibility for the difference observed between the two steroids is their difference in polarity. Progesterone is less polar than estrone, and might have benefited more from the incorporation of a linker orienting the steroid into the buffer flow.

For the estrone glucuronide-ovalbumin conjugate, an ultra-sensitive assay was obtained using secondary-antibody binding for signal enhancement. The highest signal enhancement was obtained through attaching the secondary antibody to a

gold nanoparticle, but, at the very low concentrations of primary antibody necessary to develop the most sensitive assay, the signal variations observed upon binding of the gold-secondary antibody conjugate were unacceptably high. The secondary antibody without gold was used for signal amplification in the final ultra-sensitive assay. Interestingly, the assay using primary antibody without enhancement gave a satisfactory limit of detection, but the un-enhanced signals would most likely be swamped by the matrices of real-world samples because the signals were small.

The level of detection required for estrone in wastewaters is in the pg/mL range, and the SPR assay meets that requirement. For the assay to be useful for screening of samples in the field would require its application to a portable SPR unit and further testing for matrix effects in wastewater samples. A lateral flow immunoassay developed using the same binding system might also provide a suitable level of sensitivity for detection of high levels of estrone. Assays of this type are particularly useful for on-site testing, because they require little expertise and provide rapid results.

Chapter 4

Domoic Acid

The first recorded incidence of amnesic shellfish poisoning was in Canada in 1987, where three people died, and over a hundred were affected by gastro-intestinal and neurological symptoms including permanent short-term memory loss. The causative agent was determined to be domoic acid (**4**) [15], a water-soluble tri-carboxylic acid (Figure 24) which accumulates harmlessly in shellfish but acts as a potent neurotoxin in animals that ingest the contaminated shellfish [16].

Surface plasmon resonance (SPR) detection has been used for the analysis of domoic acid by a number of workers. A gold-coated sensor surface functionalised with a mixed oligo(ethylene glycol) self-assembled monolayer [150] has been used to obtain a limit of detection of 0.1 ng/mL. Molecularly imprinted polymer techniques have also been used in SPR analysis of domoic acid, giving a limit of detection of 5 ng/mL [151]. Surface plasmon resonance is a technique which exhibits exceptional promise in screening for domoic acid, because portable SPR units are available, offering potential for use in a field setting [55, 152]. The analysis of small molecules such as domoic acid (MW 311) using surface plasmon resonance does, however, provide its own set of difficulties due to the correspondingly small signals generated.

In this chapter, the aim was to apply the strategies investigated with the estrone analogues in the previous chapter, such as the use of linkers and gold nanoparticle enhancement strategies to another small molecule binding system and develop an SPR assay for the sensitive detection of the shellfish toxin domoic acid.

Immobilisation of domoic acid on to the surface of an SPR sensor chip has been carried out by Traynor [153] and Le Berre [154], and provided a basis for this work. The effectiveness of the immobilisation of the domoic acid on the sensor surface was probed by passing a solution of anti-domoic acid antibody over the chip

surface, and examining the resulting SPR sensorgram for evidence of binding. An increase in response indicated that binding had occurred. Two anti-domoic acid antibodies were used in this work, one sourced from the commercial Biosense Laboratories ASP ELISA test kit, (AOAC method 2006.02), and the other R866 from Queen's University, Belfast, U.K.

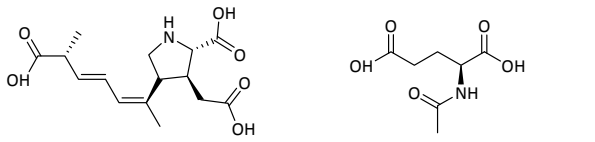

Domoic Acid (**4**)
$C_{15}H_{21}NO_6$
Mol. Wt.: 311.33

N-Acetyl-L-Glutamic Acid (**16**)
$C_7H_{11}NO_5$
Mol. Wt.: 189.17

Figure 24: The neurotoxin domoic acid and *N*-acetylglutamic acid.

Several sensor surfaces were trialed in this study. The domoic acid was attached directly to the chip surface using a short ethylene diamine linker, first using a conventional in-line procedure where the sensor surface was activated using the EDC/NHS protocol (see 2.2.1). The sensing element in the form of activated domoic acid was covalently attached and finally the remaining activated esters deactivated with a pulse of ethanolamine. A second surface using a longer oligo(ethylene glycol) (OEG) diamine linker in place of ethylenediamine was prepared in a similar way. Thirdly, the method used for the first sensing surface was repeated, but instead of performing the procedure in the instrument, a 'dry' immobilisation procedure was used. The binding partner to be immobilised was placed on the chip surface as a solution, then dried in *vacuo*, to bring the reactive groups closer to the sensor surface, potentially increasing the efficiency of the immobilisation step. Finally, the use of a domoic acid-ovalbumin conjugate was studied. Domoic acid is expensive and not readily available, so the conjugation procedure was optimised first with *N*-acetyl glutamic acid (*N*-Glu) (**16**) in place of domoic acid, using the method of Kawatsu [155]. The conjugates were examined with mass spectrometry and by observing the SPR response during immobilising onto a sensor surface.

Signal enhancement with a gold nanoparticle-secondary antibody conjugate was applied to the domoic acid-ovalbumin chip, and a binding curve and standard curve prepared.

4.1 Materials and Methods

Anti-domoic acid rabbit antibody R866 was supplied by Queen's University, Belfast. The freeze-dried anti-domoic acid rabbit antibody (R866) was reconstituted in 1 mL Milli-Q water, filtered through a Phenomenex PES 17 mm syringe filter 0.45 μm and frozen in 20 μL aliquots until required for use. Secondary antibody goat anti-rabbit IgG conjugated to 20 nm gold was sourced from BBInternational (EM.GAR20). The antibody:gold conjugate was diluted with PEG-400 (1 % v/v in Milli-Q water) and filtered through a 0.2 μm cellulose acetate filter (Advantec ISMIC-03) before use.

The Biacore™ X-100 SPR instrument, sensor chips including the CM5 sensor surface chips, the amine coupling kit and HBS-EP+ running buffer were all supplied by GE Healthcare, Uppsala, Sweden as detailed in Chapter 3. The ASP ELISA kit was supplied by Biosense Laboratories AS (Bergen, Norway). The domoic acid was supplied by BioVectra, (Charlottetown PE, Canada). The water used for all reagent preparation was ultra pure Milli-Q (Millipore Corporation, Billerica, MA, USA). Ethylenediamine (Merck, KGaA, Darmstadt, Germany) and dimethylsulphoxide (UniVar, Ajax Chemicals PTY, Auburn, Australia) were purified according to the methods of Perrin and Armareggo [156].

Matrix-assisted laser desorption/ionization mass spectrometry with time-of-flights (MALDI-TOF) were recorded on a Bruker Daltonics Autoflex spectrometer at the University of Waikato as described in Chapter 3.

4.2 Immobilisation to CM5 Chip Surfaces

The carboxyl groups on the surface of a CM5 chip were activated in the Biacore™ by exposure to two 80 μL injections of Biacore™ coupling solutions 390 mM EDC/100 mM NHS (mixed in a 1:1 ratio) at 5 μL/min. Four 90 μL pulses of 1 M

ethylenediamine pH 8.5 were passed over the sensor surface to form the linker. Finally, a solution containing activated domoic acid was injected over the sensor surface in four pulses (475 μL, 5 μL /min). Domoic acid (1 mg) was activated by dissolving in 250 μL of dimethylformamide solution (4 % w/v) and mixing with 225 μL of a solution containing 5 mg of EDC and 2 mg of NHS in 10 mM sodium acetate solution pH 4.5. The activated domoic acid solution was incubated for fifteen minutes prior to injection to ensure full activation.

In other experiments, the short ethylenediamine linker was replaced with a longer oligo (ethylene glycol) linker with a BOC-protected amine terminus (**17**) (refer to Scheme 7 in the Appendix). The OEG linker was used in a 1:9 ratio with ethanolamine. The sensor surface was activated in the Biacore™ instrument as above, and 180 μL of this 1:9 (molar) ratio of OEG linker (**17**) and ethanolamine was injected over the sensor surface at 5 μL/min (in three separate pulses). The removal of the BOC group using formic acid was carried out externally from the instrument ('off-line'). The chip was flushed with Milli-Q water and returned to the instrument. The domoic acid was activated as before, and the solution was injected over the chip surface.

'Dry' immobilisation was also explored. The surface of the chip was cleaned with 2 M NaCl and 10 mM NaOH, washed with Milli-Q water, and dried first with a stream of argon, and then in *vacuo*. A 50 μL aliquot of Biacore™ coupling solutions 390 mM EDC/100 mM NHS (mixed in a 1:1 ratio) was dropped on to the corner of the surface of a CM5 chip, and the chip dried in *vacuo* for twenty minutes. This activation step was repeated with a second 50 μL aliquot. A 50 μL aliquot of 1 M ethylenediamine pH 8.5 was similarly added to the chip surface, and dried under vacuum for one hour before washing with Milli-Q water, drying with a stream of argon, and in *vacuo* as before. Three 50 μL aliquots of activated domoic acid solution (the domoic acid was activated as before in the other immobilisation procedures, except that the activation was allowed to proceed for three hours) were applied to the chip surface, drying in *vacuo* between applications. Finally the

surface was washed with Milli-Q water and the chip docked in the surface plasmon resonance instrument to wash the surface with HBS-EP+ running buffer before use.

4.2.1 Immobilisation of Ovalbumin Conjugates

Three ovalbumin conjugates of the domoic acid model compound, *N*-acetyl glutamic acid were prepared to optimise the conjugation procedure. A single domoic acid conjugate was then prepared.

Each ovalbumin conjugate was covalently immobilised on the surface of a CM5 sensor chip. The carboxyl groups on the surface of the CM5 chip were activated by 70 μL injections of Biacore™ coupling solutions 390 mM EDC/100 mM NHS (mixed in 1:1 ratio) at 10 μL/min. The conjugates were diluted to an approximate protein concentration of 500 μg/mL, by dilution in 10 mM sodium acetate solution pH 4.0 and filtered through a 0.45 μm Phenomenex phenylether sulphone (PES) syringe filter. Repeated injections of the conjugate solution at 5 μl/min were made until a satisfactory immobilisation level was reached (at least 2000 RU). Any remaining activated carboxyl groups were deactivated by injecting 70 μL of 1 M ethanolamine hydrochloride pH 8.5.

For the domoic acid conjugate, a reference flow cell was then immobilised in a similar manner but with ovalbumin in place of the domoic acid conjugate, using as a target level the final immobilisation level (in RU) obtained for flow cell with the conjugate. This allowed for correction for any non-specific binding of the antibody to ovalbumin in the reference flow cell.

Prior to use in binding studies, the surface of both flow cells was conditioned with ten successive injections of HBS-EP+ running buffer followed by a 20 μL injection of 50 mM NaOH then 50 mM HCl (regeneration solutions) at 10 μL/min. The RU obtained in flow cell 1 was subtracted from that in flow cell 2 for analysis of results to eliminate non-specific binding data.

4.3 Preparation of the Ovalbumin Conjugates

Three *N*-acetyl glutamic acid-ovalbumin conjugates were prepared at three different ratios of hapten to ovalbumin (10:1, 20:1 and 26.5:1) according to Scheme 2, as follows. To a solution of *N*-acetyl glutamic acid (1.30 mg, 6.9 μmol) in dimethylsulphoxide (50 μL) were added 20 μL of *N*-ethyl-*N*-(3-dimethylaminopropyl)-carbodiimide (EDC), 80 mg/mL in dimethylsulphoxide (8.2 μmol) and 10 μL *N*-hydroxysuccinimide (NHS) 95 mg/mL in dimethylsulphoxide (8.2 μmol). The solution was stirred at room temperature for 90 minutes, then ovalbumin (OVA) solution (20 mg/mL, 0.45 μmol/mL in 0.085 M borate buffer containing 0.06 M NaCl, pH 8.2), was added. 1530 μL was added for the 10:1 ratio of hapten to conjugate, 760 μL for the 20:1 and 580 μL for the 26.5:1 respectively. The reaction was stirred overnight at room temperature (26.5:1 conjugate) or 4^{o}C (10:1 and 20:1 conjugates) to achieve optimum conjugation.

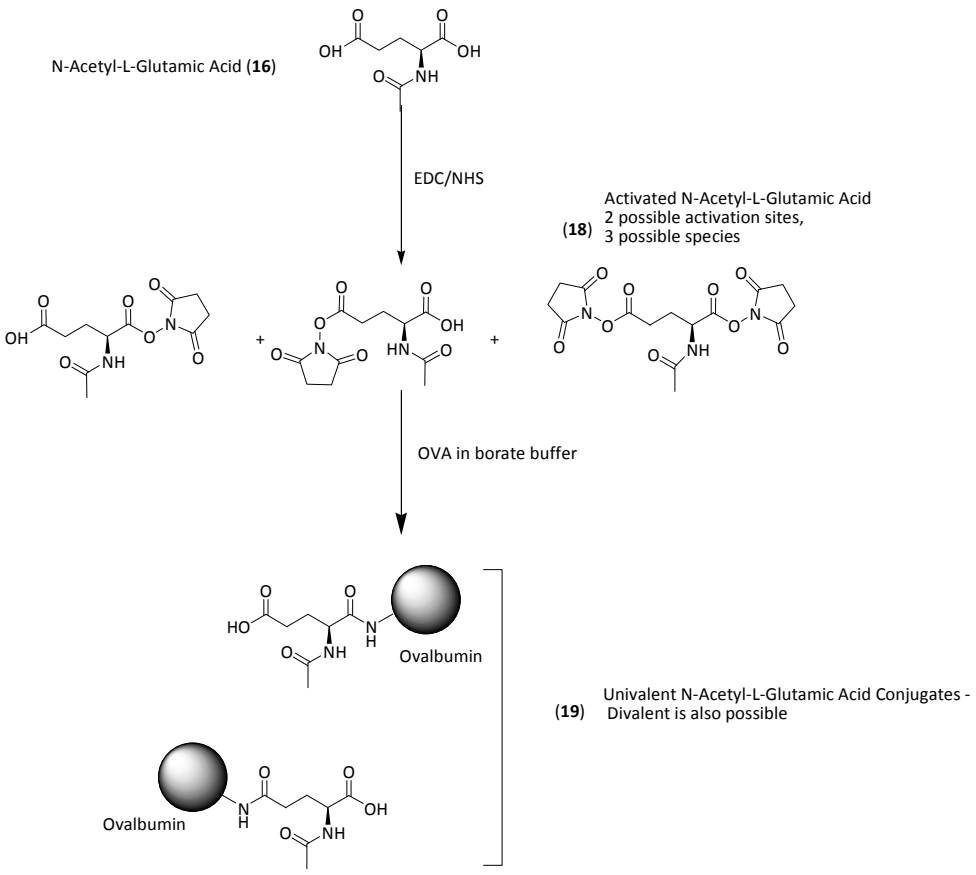

Scheme 2: Conjugation of *N*-acetyl glutamic acid to ovalbumin. The formation of more than one species of activated succinimide ester is possible and illustrated here, but only the 'single' conjugate is shown.

A domoic acid-ovalbumin conjugate (10:1) was prepared in a similar manner (Scheme 3) using domoic acid 1.11 mg (3.6 μmol), 11 μL of *N*-ethyl-*N*-(3-dimethylaminopropyl)-carbodiimide as the hydrochloride (EDC), 80 mg/mL in dimethylsulphoxide (4.2 μmol) and 5.5 μL *N*-hydroxysuccinimide (NHS) 95 mg/mL in dimethylsulphoxide (4.2 μmol) and 780 μL of ovalbumin (OVA) solution (20 mg/mL, 0.45 μmol/mL in 0.085M borate buffer containing 0.06M NaCl, pH 8.2).

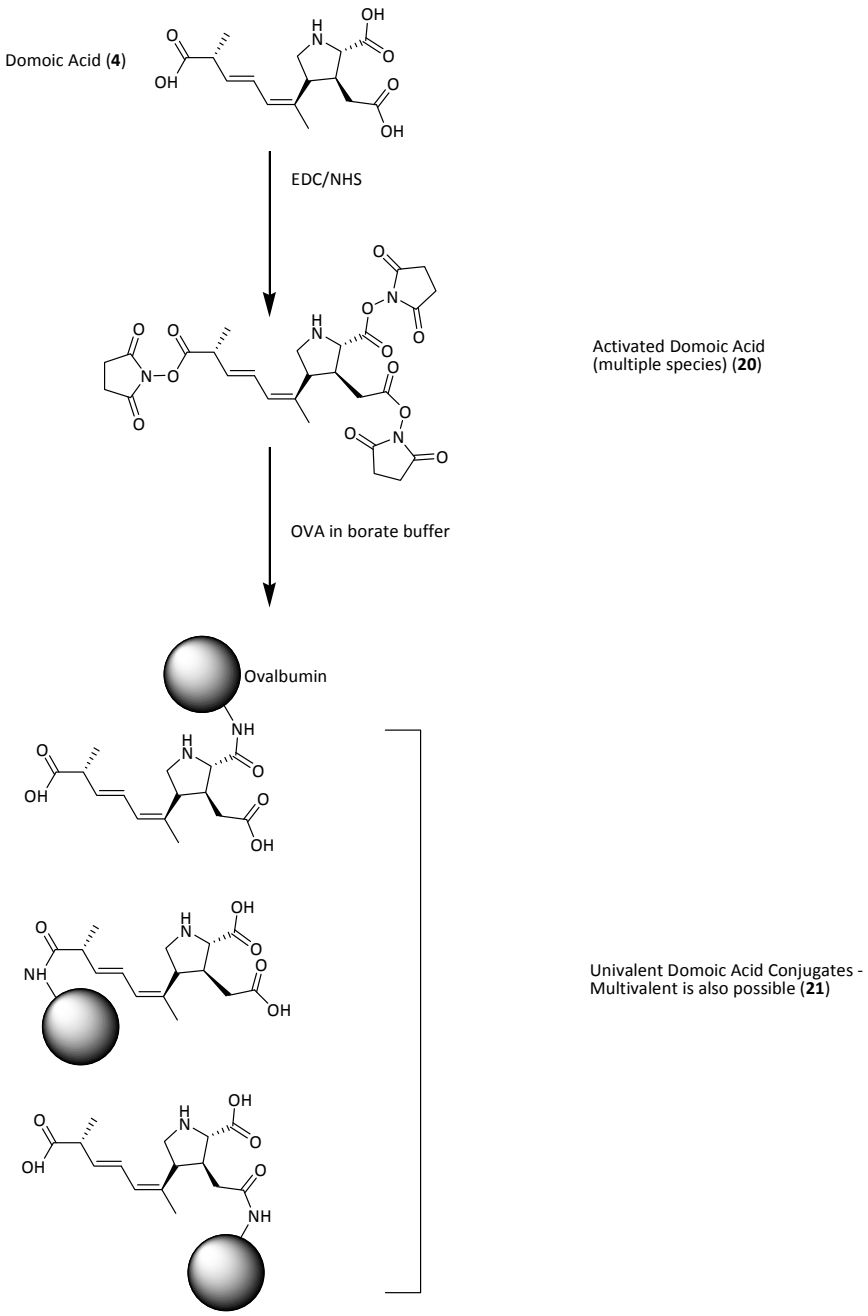

Scheme 3: Conjugation of domoic acid to ovalbumin.

All conjugates were dialysed at 4^{o}C against Milli-Q water for two days (3 changes/day), then passed through a pre-packed PD-10 desalting column (GE Healthcare, UK) using phosphate buffered saline pH 7.0 as eluent. The purified conjugate solution (3.5 mL) was collected and stored at -20^{o}C.

The ovalbumin conjugates were analysed by mass spectrometry at the University of Waikato, as for the estrone conjugates (Chapter 3).

4.4 Enzyme-Linked Immunosorbent Assay (ELISA)

The activity of the anti-domoic acid antibody supplied with the Biosense ASP ELISA kit was examined by an ELISA test, carried out in accordance with the manufacturer's instructions. Washing buffer (PBS-T: phosphate buffered saline with 0.05 % Tween 20) was prepared by dissolving the tablet supplied with the kit in 500 mL of Milli-Q water. Standard buffer (10 % methanol in 0.05 % Tween 20 in phosphate buffered saline) was prepared by mixing 5 mL of methanol with 45 mL of washing buffer. Antibody-horseradish peroxidase ovalbumin buffer (1 % w/v ovalbumin in 0.05 % Tween 20 in phosphate buffered saline) was prepared by dissolving 60 mg of ovalbumin in 6 mL of washing buffer. The peroxidase substrate solution of 3,3',5,5' tetramethyl benzidine (TMB) was used as supplied.

The ELISA kit's antibody, anti-domoic acid antibody-horseradish peroxidase conjugate was reconstituted in antibody-horseradish peroxidase ovalbumin buffer.

4.4.1 ELISA Procedure

300 μL of washing buffer was added to micro-titre wells coated with domoic acid-protein conjugate, and the wells pre-soaked for ten minutes, then the liquid removed by inverting strips over a sink and tapping over absorbent tissue. 50 μL of standard buffer was added to the A_{max} and blank wells. The A_{max} wells had the maximum absorbance because no domoic acid is added, and the blank wells give the background absorbance of the TMB peroxidase substrate. 50 μL of antibody-horseradish peroxidase ovalbumin buffer was added to the blank well only. For the calibration curve, 50 μL of each domoic acid standard solution was pipetted (in duplicate) to the standard wells. The ELISA antibody, anti-domoic acid antibody-horseradish peroxidase conjugate (50 μL) was added to all wells except the blank. The micro-titre plate was sealed and incubated in the dark at room temperature for one hour. Following incubation the micro-titre wells were emptied and washed four

times with 300 μL of washing buffer per well and dried over absorbent tissue as before.

The peroxidase substrate solution of 3,3',5,5' tetramethyl benzidine (TMB) was then added to each well (100 μL) and the plates incubated in the dark at room temperature for 15 minutes. The reaction was stopped by the addition of 100 μL of 0.3 M H_2SO_4 to all wells and the absorbance at 450 nm read after five minutes using a BioTek PowerWave XS plate reader. The calibration curve was generated using OriginPro software (OriginLab Corporation, MA, USA).

The ability of the ELISA antibody, anti-domoic acid antibody-horseradish peroxidase conjugate, to bind to the domoic acid-ovalbumin conjugate was checked by subjecting dilutions of the conjugate to the ELISA test. The dilutions used are shown in Table 6. An ELISA calibration curve was prepared as described above. Similarly, 50 μL of each of the diluted conjugate solutions was subjected to the ELISA, and the absorbances recorded.

Table 6: Dilution of domoic acid-ovalbumin conjugate used in ELISA assay.

Dilution	Volume of Conjugate (μL)	Volume of Buffer (μL)
A	5 μL of conjugate stock	385
B	50 μL of conjugate dilution A	450
C	50 μL of conjugate dilution B	450
D	100 μL of conjugate dilution C	100
E	50 μL of conjugate dilution C	450
F	50 μL of conjugate dilution E	450
G	100 μL of conjugate dilution F	100

4.5 Surface Plasmon Resonance (SPR)

4.5.1 SPR Scouting with ELISA Antibody

The ELISA antibody was diluted with HBS-EP+ running buffer before injecting separately over all the SPR chips (60 μL, 30 μL/min) and the surface regenerated with 50 mM NaOH (60 μL, 10 μL/min).

4.5.2 Domoic Acid-Ovalbumin SPR Chip – Binding Curve (Enhanced)

The binding curve investigated binding performance of the (primary) R866 rabbit polyclonal antibody supplied by Queen's University and the (secondary) goat anti-rabbit IgG/nanogold antibody conjugate. The results of the binding curve allowed the selection of a suitable antibody concentration for use in the inhibition assay.

A series of R866 antibody solutions were prepared in HBS-EP+ buffer in the concentration range 0 to 200 μg/mL, *i.e*. 0, 2.5, 5, 20, 100 and 200 μg/mL. A binding curve was prepared by injecting a fixed amount of antibody solution 60 μL (120 s, 30 μL/min) over the sensor surface of a domoic acid-ovalbumin conjugate-immobilised chip, followed by goat anti-rabbit IgG/nanogold 20 nm conjugate diluted 1:5 with PEG-400 (1 % v/v) (30 μL/ 10 μL/min). Regeneration of the surface was carried out using a pulse of 50 mM HCl (10 μL, 10 μL/min) followed by a second pulse of 50 mM NaOH (5 μL, 10 μL/min). Each antibody solution was injected in triplicate.

4.5.3 Domoic Acid-Ovalbumin SPR Chip – Standard Curve (Enhanced)

A competitive inhibition assay format was used (see 2.4.2), where a fixed, known amount of antibody was added to a concentration series of domoic acid standard solutions. Unbound antibody remaining in solution then bound to the sensor surface. Secondary antibody as a gold nanoparticle:antibody conjugate was injected over the sensor surface bound to the surface-bound primary antibody, enhancing the SPR signal.

A concentration series of domoic acid standard solutions were prepared in HBS-EP+ buffer in the range 0 to 100 μg domoic acid/mL, *i.e*. 0, 0.00001, 0.0001, 0.001, 0.01, 0.1, 1.0, 10 and 100 μg/mL. Each standard solution (125 μL) was incubated with an equal volume of R866 antibody solution (40 μg/mL) in HBS-EP+ buffer, and the resulting mixture passed over the chip surface (60 μL, 30 μL/min), followed by goat anti-rabbit IgG/nanogold 20 nm conjugate diluted 1:5 with PEG-400 (1 % v/v) (30 μL, 10 μL/min). The regeneration of the biosensor surfaces was performed as for the binding curve. Each standard solution was injected in triplicate.

4.6 Results and Discussion

Preparation of a domoic acid biosensor was initially focused on direct immobilisation of domoic acid on SPR chips without conjugation to the ovalbumin protein. The sensor surface (chip 1) was generated directly within the SPR instrument with activated domoic acid and incorporated a short ethylenediamine linker, based on the methods of Traynor [153] and Le Berre [154]. By preparing the chip surface in the instrument, a higher degree of control is possible, and the immobilisation sequence can be followed in real time by observing the change in surface plasmon resonance signal. It is also possible to prepare a reference cell by treating a second flow cell in the same manner, but omitting the binding partner. The reference cell can be used to correct for differences between the refractive indices of the analyte solution and the running buffer and to correct for 'non-specific' binding, *i.e.* the binding of non-analyte molecules to the surface of the chip.

However domoic acid, with a molecular mass of 311, is a relatively small molecule in surface plasmon resonance terms (the size of the SPR signal is proportional to the mass bound). It was likely therefore that signal changes would be very small, perhaps undetectable. It was found that this sensor surface gave no signal when an injection of diluted ELISA antibody (anti-domoic acid antibody-horseradish peroxidase conjugate) was made.

OEG Linker:

Replacing the relatively short ethylenediamine linker (Figure 25) with a longer oligo(ethyleneglycol) linker (in a 1:9 ratio with ethanolamine) (Figure 26) was intended to reduce steric crowding at the sensor surface and make the surface-bound domoic acid more accessible for antibody binding .

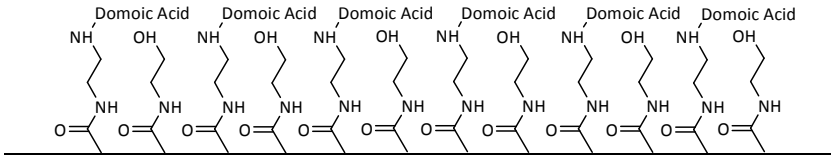

Figure 25: Schematic of sensor surface prepared with ethylenediamine linker, and with remaining activated sites capped using ethanolamine.

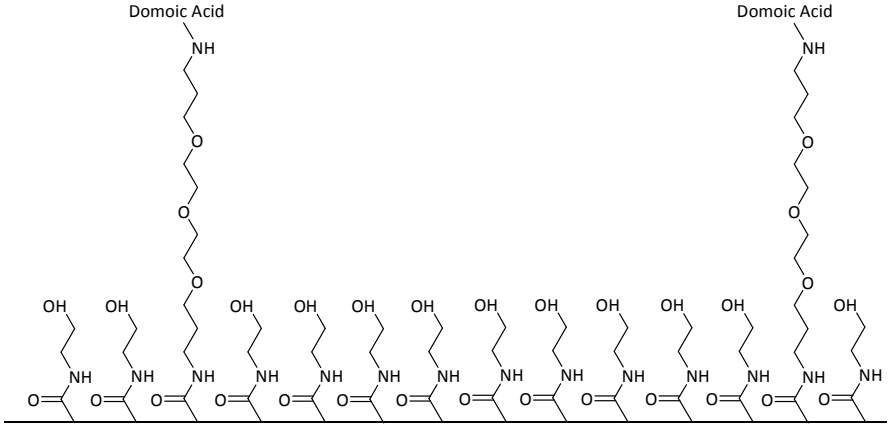

Figure 26: Schematic of sensor surface prepared using a mixture of OEG linker and ethanolamine.

This procedure was carried out in a step-wise fashion. The linker was deposited on the sensor surface, the linker's amine group de-protected and finally activated domoic acid was attached.

Dry Immobilisation:

The dry immobilisation method was applied to the method of Le Berre, using the ethylenediamine linker. The drying steps were intended to increase solution concentration, increasing the likelihood of the immobilisation reaction at the sensor

surface occurring. A disadvantage was that since this procedure was carried out 'off-line', it precluded the preparation of a reference cell. Also, the binding partner to be immobilised had to be sufficiently robust to withstand the drying steps.

Ovalbumin conjugate

The conjugation of domoic acid to a protein such as ovalbumin (44 kDa) reduced the difficulties inherent to the immobilisation of domoic acid. By attaching the domoic acid to the large ovalbumin molecule first, the course of the immobilisation could be followed in real time by observing the surface plasmon resonance signal. The ovalbumin conjugate generated an appreciable signal when binding to the sensor chip surface. The three-dimensional structure of the protein was expected to provide multiple attachment sites, potentially increasing the density of the domoic acid at the surface. The increase in signal over the immobilisation step was much larger for the domoic acid-ovalbumin conjugate (Figure 27) however, the immobilisation of activated domoic acid on to an ethylenediamine linker surface also produced an appreciable signal change (Figure 28).

The conjugation chemistry was very similar to that used to generate the steroid molecules discussed in 5.3.2, and the immobilisation of ovalbumin (as the domoic acid conjugate) to the matrix of the sensor surface is well established [62]. Since the domoic acid is expensive and not readily available, the conjugation procedure was optimised first with *N*-acetyl glutamic acid (*N*-Glu), using the method of Kawatsu [155]. Using the mass spectrometry results for the conjugates and for a pure ovalbumin sample, the degree of hapten conjugation of the *N*-acetylglutamic acid-ovalbumin conjugates were calculated (Table 7), and two selected to immobilise on a CM5 chip. These conjugates immobilised satisfactorily, as determined by observing the response when the conjugates were immobilised on the surface of a CM5 chip. This test immobilisation was only to observe the response change indicating satisfactory attachment, without testing the surface for antibody binding.

The conjugation procedure was then applied to domoic acid, using a ratio of ovalbumin to domoic acid, *i.e*. 1 OVA: 10 domoic acid, to ensure a number of lysine

residues on the ovalbumin remained available for covalent linkage to the sensor chip. Using the mass spectrometry results for the conjugates and for a pure ovalbumin sample (an average of two determinations), the ratios of hapten to ovalbumin were calculated and are shown in Table 7.

Table 7: Mass spectrometry results for the glutamic acid- and domoic acid conjugates. The hapten number per ovalbumin value is the molar ratio of the hapten (*N*-acetyl glutamic acid or domoic acid) to the ovalbumin.

Conjugate	Hapten Number/Ovalbumin
N-Acetyl Glutamic Acid: Ovalbumin (10:1)	3.5
N-Acetyl Glutamic Acid: Ovalbumin (20:1)	6.7
N-Acetyl Glutamic Acid: Ovalbumin (26.5:1)	8.4
Domoic Acid: Ovalbumin (10:1)	2.0

Table 8: Response of the two anti-domoic acid antibodies on different sensor surfaces. ND=Not Detected

CM5 Sensor Surface	ELISA pAb	R866 pAb
1 Domoic Acid +Ethylenediamine linker	ND (Dilution 0.5)	123 RU (0.2 mg pAb/mL)
2 Domoic Acid +OEG linker	ND (Dilution 0.5)	42 RU (0.2 mg pAb/mL)
3 Domoic Acid +Ethylenediamine linker ('dry' immobilisation	ND (Dilution 0.5)	95 RU (0.2 mg pAb/mL)
4 Domoic Acid-Ovalbumin Conjugate (6000 RU)	ND (Dilution 0.5)	88 RU (0.1 mg pAb/mL)
5 Domoic Acid-Ovalbumin Conjugate (8500 RU)	ND (Dilution 0.5)	265 RU (0.2 mg pAb/mL)

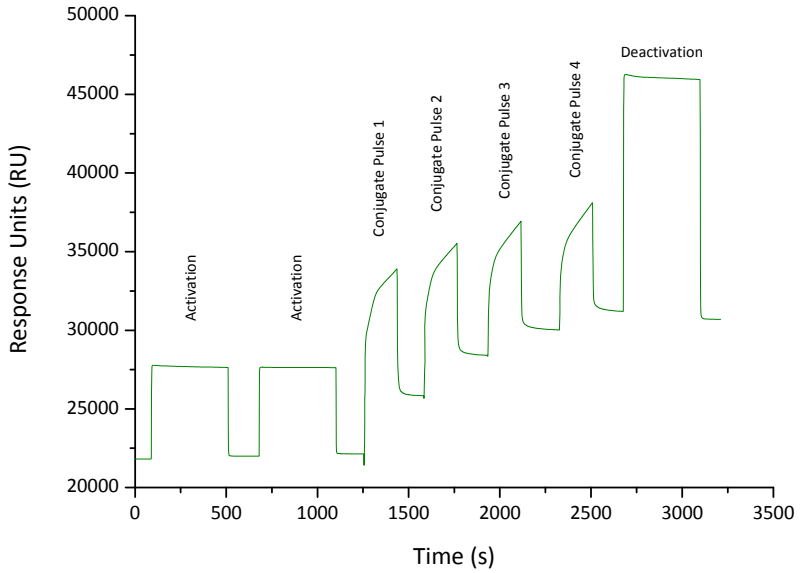

Figure 27: Sensorgram for the immobilisation of domoic acid-ovalbumin conjugate to the surface of a CM5 chip. Two pulses of EDC/NHS mixture activated the surface esters. Four pulses of the conjugate showed increasing levels of conjugate binding. The final pulse of ethanolamine 'capped' any remaining activated esters.

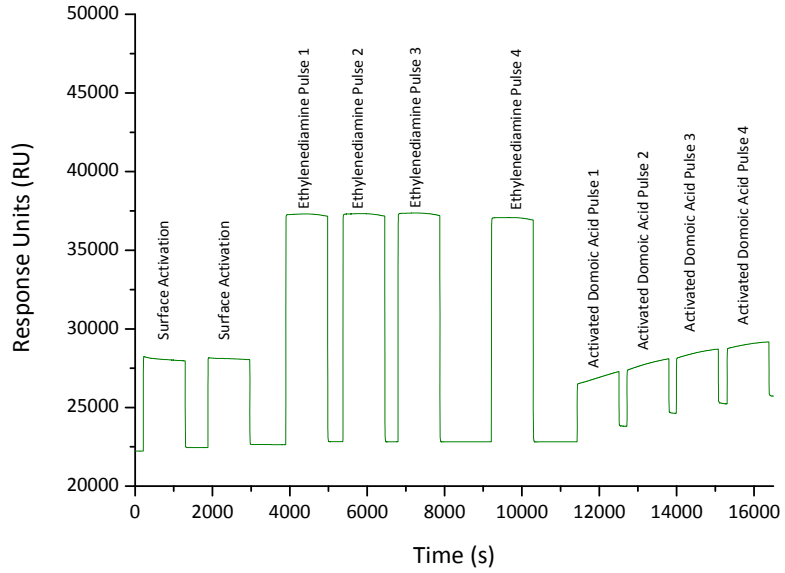

Figure 28: Sensorgram for the immobilisation of activated domoic acid to the surface of a CM5 chip. Two pulses of EDC/NHS mixture activated the surface esters. Four pulses of 1M ethylenediamine pH 8.5 formed the short linker on the sensor surface. Finally, four pulses of pre-activated domoic acid were injected. The difference between the initial response and the final response is smaller than in Figure 27 above, where the much larger domoic acid-ovalbumin conjugate was immobilised.

When domoic acid only (not the ovalbumin conjugate) was used to form the biosensor surface, no binding of the ELISA antibody to the sensor surface was observed (Table 8). The activity of the ELISA antibody was checked by running an ELISA calibration curve, and found to be performing satisfactorily (Figure 29).

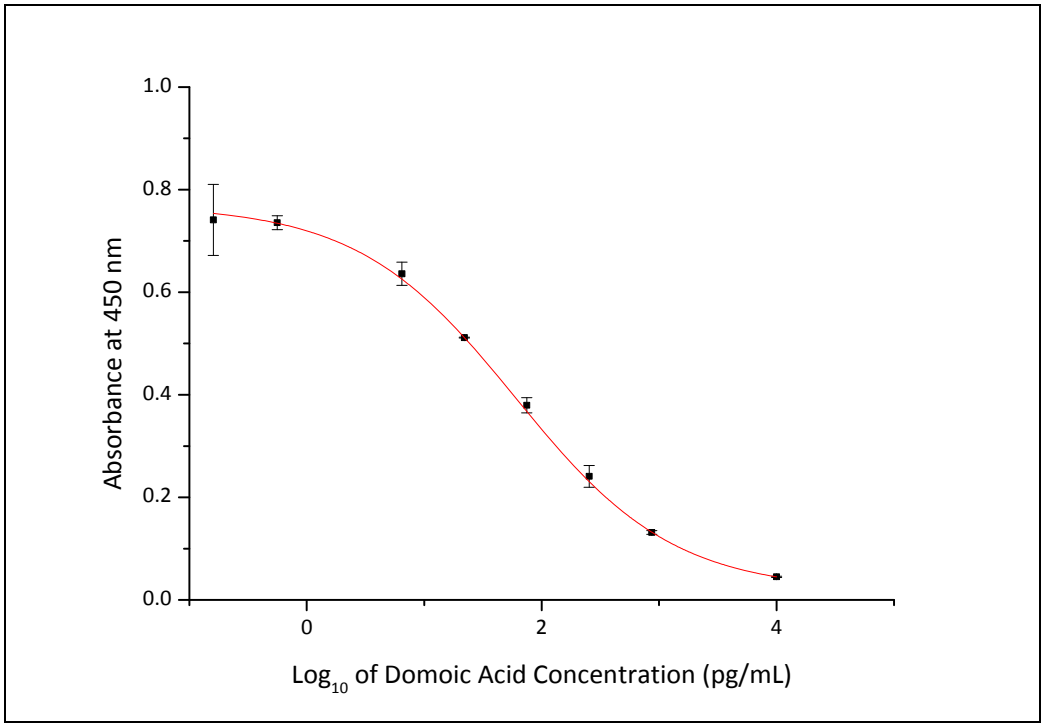

Figure 29: The calibration curve for the assay of domoic acid using the Biosense ELISA kit. Error bars shown on the graph represent one standard deviation (SD) of the mean.

Attaching the domoic acid to ovalbumin allowed the immobilisation step to be followed by observing the increase in response in the sensorgram. Domoic acid is expensive and not readily available. For this reason, the conjugation step was optimised first using a cheap, readily available model compound, *N*-acetyl glutamic acid (**16**). The *N*-acetylglutamic acid was considered a suitable model compound in part because it is a dicarboxylic acid, allowing experimentation with the ratio of activation agents in order to optimise the formation of the desired activated mono-ester. Accordingly, a slight excess (1.2) of EDC and NHS was added. Mass

spectrometry of the model compound (Table 7) indicated that the conjugation was satisfactory. Two of the *N*-acetyl glutamic acid conjugates (ratios 10:1 and 20:1) were immobilised on the surface of a CM5 chip, purely to ensure that the immobilisation step would occur without difficulty. No antibody binding was attempted. Both conjugates performed adequately, reaching 3900 RU and 2400 RU (10:1 and 20:1 respectively), and giving confidence that the procedure would be sufficiently reliable to proceed using the more valuable domoic acid material. Accordingly, the domoic acid-ovalbumin conjugate (10:1) was prepared using the same conditions, with a resulting hapten ratio of 2 moles of domoic acid per mole of ovalbumin.

To ensure that the ELISA antibody would bind to the ovalbumin conjugate (in the ELISA the antibody binds to 'free' or un-conjugated domoic acid), solutions of the diluted conjugate were treated as samples in the ELISA test. Three of the diluted conjugate solutions gave absorbance values within the range of the ELISA standard curve, indicating that binding of the antibody to the conjugate had occurred (data not shown).

A sensor surface was prepared using this conjugate in flow cell 2 and ovalbumin in the reference flow cell (flow cell 1), with immobilisation levels of 6000 RU, and the antibody supplied with the Biosense ASP ELISA kit (anti-domoic acid antibody-horseradish peroxidase conjugate) was passed over the sensor surface, but no signal was produced. The polyclonal anti-domoic acid rabbit antibody R866 was used to check all sensor surfaces, and all gave a satisfactory response (Table 8). It is likely that the ELISA antibody as supplied was too dilute for use in the surface plasmon resonance study. The R866 antibody was used for subsequent studies.

A second chip was prepared using a high loading of the domoic acid-ovalbumin conjugate (8500 RU), and a binding curve (Figure 30) and standard curve (Figure 31) generated.

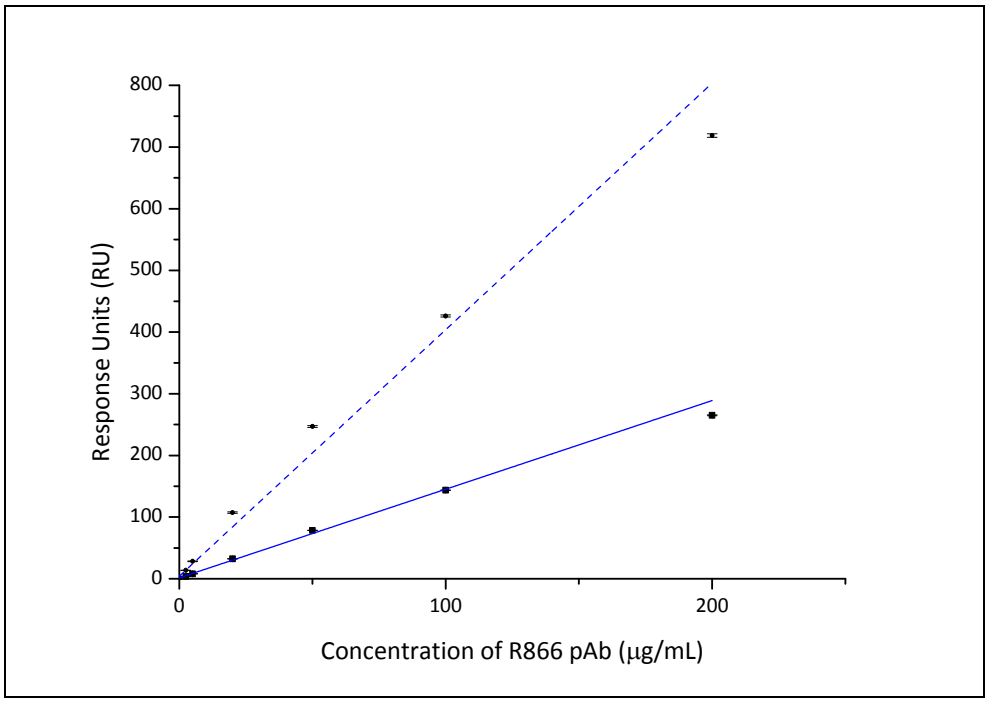

Figure 30: Domoic Acid Binding Curve, Plot of signal response (RU) vs R866 pAb concentration for pAb signal alone (solid line) and with IgG-nanogold 20nm enhancement (broken line). Error bars shown on the graph represent one standard deviation (SD) of the mean.

The domoic acid assay calibration curve results are given in Table 9. The limits of detection, the IC_{50} and the working range were determined as described in Chapter 2.

A three-fold signal enhancement was obtained by the use of a commercially available secondary antibody-20 nm gold conjugate (diluted five-fold) as shown in Figure 30. Unlike the secondary:gold nanoparticle conjugate prepared in Chapter 3, little signal variation was noted with the second binding event. The non-specific binding was negligible (less than 6 RU). The signal enhancement was sufficient to allow the use of a modest amount of primary antibody in the inhibition assay, allowing the development of a highly sensitive assay for domoic acid.

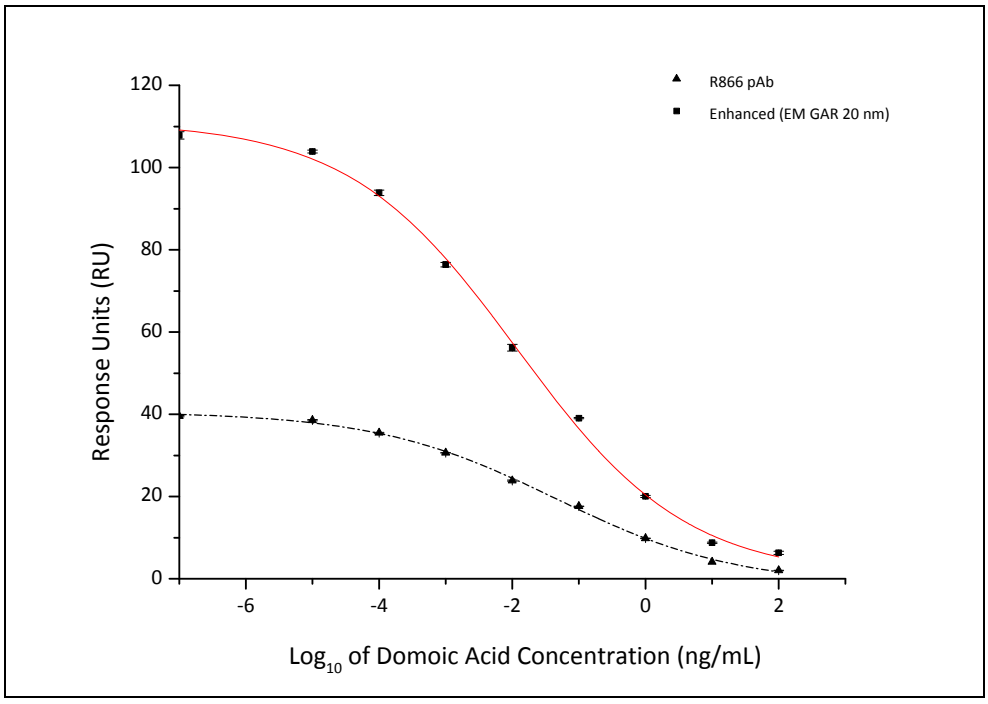

Figure 31: Surface plasmon resonance inhibition assay standard curve for domoic acid, using domoic acid-ovalbumin conjugate immobilised on a CM5 chip as the sensing surface, and polyclonal antibody R866 as the detecting element. The primary antibody (broken line) and secondary antibody:20 nm gold enhanced assay (solid line) curves are shown. Error bars shown on the graph represent one standard deviation (SD) of the mean.

Table 9: Limits of Detection, IC_{50} and working range for the enhanced and un-enhanced SPR assay of domoic acid. The domoic acid-ovalbumin conjugate immobilised on a CM5 chip was used as the sensing surface.

	R866 pAb (Unenhanced)	EM GAR 20 nm (Enhanced)
IC50	45 ng/mL	12 ng/mL
Working Range	0.5 to 3500 ng/mL	0.2 to 680 ng/mL
LOD	0.046 ng/mL (46 pg/mL)	0.019 ng/mL (19 pg/mL)

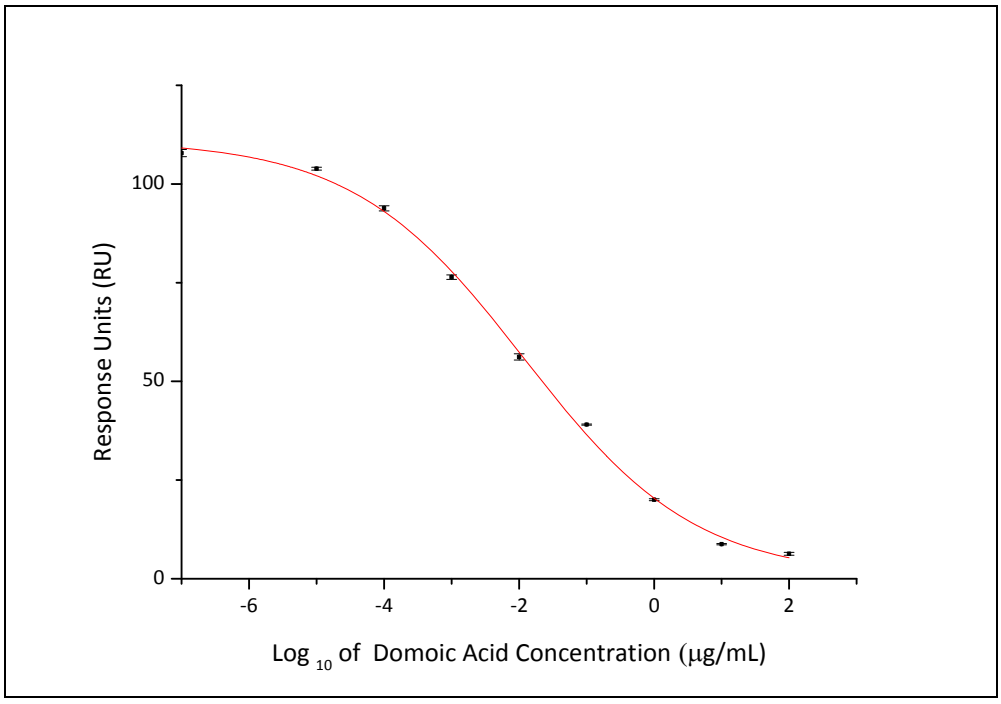

Figure 32: Assay standard curve for IgG-nanogold 20 nm enhanced SPR assay of domoic acid. Error bars shown on the graph represent one standard deviation (SD) of the mean.

The immobilisation of the domoic acid-ovalbumin conjugate to the CM5 sensor chip gave a high yield of immobilisation (8500 RU) and a high binding capacity (Figure 30). The covalent attachment method used here gives a stable surface. The three fold signal enhancement afforded by introducing a second binding event with a secondary antibody:gold conjugate was relatively modest, but still allowed a small amount of primary antibody to be used in assay. The application of the commercially available secondary antibody:gold conjugate was very successful, without the signal variation observed in the SPR assay for estrone glucuronide (see Chapter 3). Reducing the amount of primary antibody by using signal enhancement strategies generated a more cost-effective and sensitive assay, and was straight-forward to apply. The low limits of detection (Table 9) for both the un-enhanced and the enhanced assays would be capable of detecting levels of the shellfish toxin which exceeded regulatory limits, but the higher signals obtained in the enhanced assay make the latter more suitable for use with real-world samples, with the larger signals less likely to be swamped by a complex biological matrix. The limit of

detection for the enhanced assay (19 pg/mL) begins to approach that of the ELISA assay (10 pg/mL) [26].

4.7 Summary

A comparison was made among sensor surfaces prepared by covalently attaching domoic acid directly to surface-bound linkers of differing lengths. Here, the longer oligo(ethylene) glycol linker performed no better than the ethylenediamine linker. A domoic acid-ovalbumin conjugate sensor surface was investigated in developing an assay for the shellfish toxin, making use of a commercially available secondary antibody-gold conjugate for signal enhancement. The approach was successful in improving the sensitivity for domoic acid to the extent that the sensitivity of the assay (LOD 19 pg/mL) approached that of an ELISA assay (LOD 10 pg/mL). For the assay of the shellfish toxin, signal enhancement exploiting gold nanoparticles gave highly sensitive detection, while adding only a modest level of complexity to the assay.

For the method to be applied to real samples would require testing of shellfish extracts prepared with the extraction procedure used in the liquid chromatography methods accepted by regulatory bodies [157]. The SPR method would then be sufficiently sensitive to be useful for rapid screening of samples. A lateral flow immunoassay developed using the SPR binding system might provide a test method which would require minimal user expertise. The lateral flow immunoassay in particular would have advantages over the lengthier liquid chromatography methods which require transport of samples from remote locations, impacting upon the time from sampling to analysis.

Chapter 5

A Dextran-Free Terthiophene Scaffold

One limitation of surface plasmon resonance (SPR) sensing is that the plasmonic effect decays exponentially from the gold surface, typically falling to almost nothing at about 300 nm. Hence, the closer the sensing element is to the surface, the greater is the response to the binding of the binding partner. Attachment of the binding agent to a Biacore™ CM5 chip is realised by a 100 nm carboxylated-dextran scaffold, which effectively blocks the use of the most sensitive region.

The focus of this section is investigation of the effect of reducing the thickness of the scaffold layer to which the sensing element is attached. A functionalised terthiophene-OEG-COOH (**22**) (Figure 33) was synthesised (refer to the Appendix for details of the synthesis). A second goal was to investigate the effect of eliminating ovalbumin and instead immobilise the steroid-linker moiety directly by including terminal amine functionality on the linker.

The work proceeded in three stages. Firstly, a preliminary investigation was carried out by preparing a functionalised terthiophene scaffold by immersing a bare gold surface plasmon resonance chip in a solution of the functionalised terthiophene (**22**). Initial surface plasmon resonance studies used ovalbumin and an estrone glucuronide-ovalbumin conjugate (as used in Chapter 3) to determine whether the sensor surface produced was worthy of further study. Secondly, an un-conjugated progesterone-linker with amine functionality (**23**) and a progesterone-linker-ovalbumin conjugate (**24**) (Figure 33) were used to assess the performance of the scaffold produced in this manner. These progesterone capture elements were used for more detailed studies of the scaffold surface. The progesterone-linker moiety was available in the laboratory, and suitable for generation of a progesterone-linker-amine compound for covalent attachment to the scaffold without the use of

a protein conjugation step. Using an amine linker would allow the same chemistry of attachment to be used for both conjugated and un-conjugated progesterone.

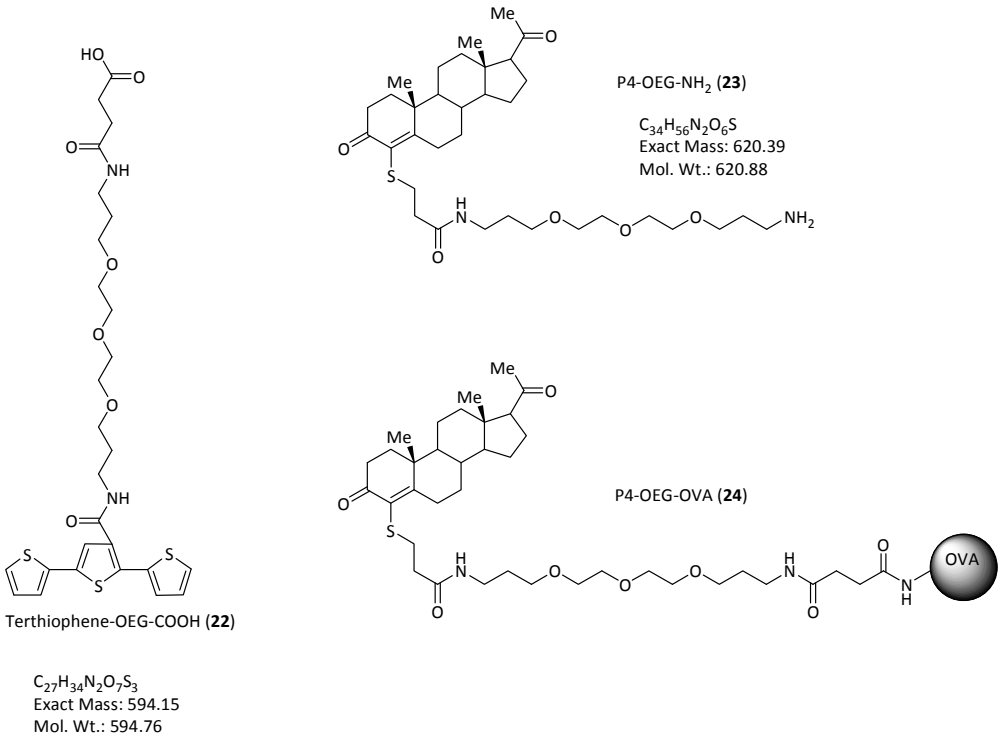

Figure 33: Progesterone-OEG-NH_2 (P4-OEG-NH_2) and the progesterone-OEG-ovalbumin conjugate (P4-OEG-OVA) used as the sensing elements, and the functionalised terthiophene, terthiophene-OEG-COOH used to form the scaffold on the gold SPR surface. An estrone glucuronide-ovalbumin conjugate (compound 8) as used in Chapter 3, was also used for preliminary studies.

Four sensor surfaces were investigated: the commercially prepared carboxymethylated dextran CM5 surfaces as used for earlier steroid study and the new functionalised terthiophene, each immobilised with both an (un-conjugated) progesterone-linker with a terminal amine (**23**) and with a progesterone-linker conjugated to ovalbumin (**24**)(Figure 34).

The aim was to determine the degree to which the sensitivity of an immunoassay might be affected, by the scaffold thickness, and by the use of protein-free (un-conjugated) compared to protein-conjugated sensing elements on the sensor surface. Finally, the use of electrochemical methods for coating of the functionalised terthiophene on to the gold surface was probed, with a view to improving the reproducibility and the stability of the resulting surface.

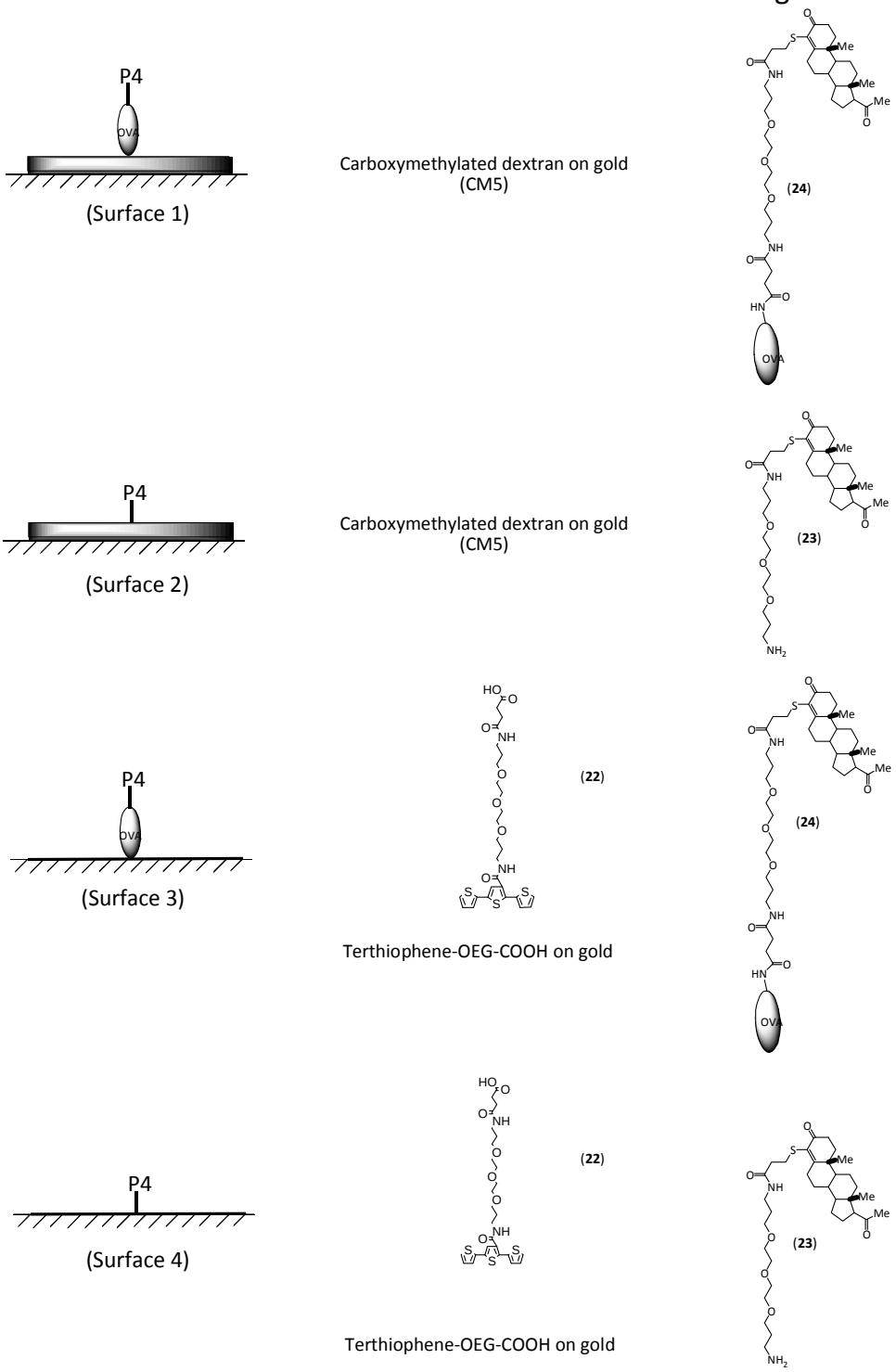

Figure 34: Schematic of sensors prepared with P4-OEG-ovalbumin conjugate on a CM5 scaffold (sensor surface 1), P4-OEG-NH_2 on a CM5 scaffold (sensor surface 2), P4-OEG-ovalbumin conjugate on a terthiophene-OEG-COOH scaffold (sensor surface 3) and P4-OEG-NH_2 on a terthiophene-OEG-COOH scaffold (sensor surface 4).

5.1 Materials and Methods

The Biacore™ X-100 SPR instrument, sensor chips including the CM5 and bare gold sensor surface chips, the amine coupling kit and HBS-EP+ running buffer were all supplied by GE Healthcare, Uppsala, Sweden as detailed in Chapter 3. *N,N*'-dicyclohexylcarbodiimide was supplied by Merck-Schuchardt, Munich, Germany and used without further purification. Phosphate buffered saline 0.01 M pH 7.4 was supplied by Sigma (P5368) and prepared according to the manufacturer's instructions. P1922 anti-progesterone rat monoclonal antibody was supplied by Sigma. Other reagents were used as supplied.

Matrix-assisted laser desorption/ionization mass spectrometry with time-of-flight (MALDI-TOF) were recorded on a Bruker Daltonics Autoflex spectrometer at the University of Waikato as described in Chapter 3.

An atomic force microscope (MFP-MDT Asylum research, Santa Barbara, CA) was used to study the thickness of the film at the edge of the electrochemically coated surface. Silicon cantilevers (Ultrasharp CSG-11 NT-MDT, Zelenograd, Moscow, Russia) were used to study the sample in contact mode. The tip, nominally 10 nm in radius, was located at the free end of a cantilever (350 μm long, 35 μm wide, and 0.7 – 1.3 μm thick) with a nominal force constant of 0.01 to 0.08 N/m. A tip speed of 250 μm/s was used to scan the sample.

5.2 Functionalised Terthiophene-on-Gold Surface (Immersion Method)

Bare gold substrate (BR-1004-05) was cleaned in freshly prepared piranha solution (hydrogen peroxide 30 vol: concentrated sulphuric acid in a 1:3 ratio) for thirty minutes, then rinsed in Milli-Q water and allowed to drain. A blast of oil-free compressed air was used to completely dry the surface. The cleaned gold chips were immersed in a solution of the functionalised terthiophene (5, 10 and 20 mM in 95 % ethanol) overnight. The resulting gold surface was rinsed with 95 % ethanol, then with Milli-Q water, and finally with 95 % ethanol. The surface was drained to

dry, then allowed to air-dry before assembling in accordance with the manufacturer's instructions. A blank chip was prepared by treating a cleaned chip in a similar manner, using 95 % ethanol in place of the functionalised terthiophene solution.

Ferric Chloride Treatment

A bare-gold chip surface was immersed in a 5 mM solution of functionalised terthiophene in 95 % ethanol as above, rinsed with 95 % ethanol, followed by Milli-Q water, and then a drop of 0.1M $FeCl_3$ solution was applied to the gold surface. The chip was allowed to stand (covered) for thirty minutes before rinsing with Milli-Q water and draining dry before assembling as before.

5.2.1 Immobilisation of Ovalbumin on Functionalised Terthiophene-on-Gold Surfaces

The surfaces produced with varying concentrations of functionalised terthiophene solution were examined by immobilising ovalbumin only on flow cell 1 of each chip, including the blank chip. In each case the immobilisation conditions were the same: activation using a single 70 μL injection of Biacore™ coupling solutions 390 mM EDC/100 mM NHS (mixed in 1:1 ratio) at 10 μL/min, followed by six injections of ovalbumin, *i.e.* 2.5 μL (30 s at 5 μL/min) and 2 x 25 μL (2 x 300 s at 5 μL/min) using 100 μg ovalbumin/mL, then 2.5 μL (30 s at 5 μL/min) and 25 μL (300 s at 5 μL/min) using 330 μg ovalbumin/mL. Two pulses of running buffer were then injected, 2.5 μL (30 s at 5 μL/min) and 25 μL (300 s at 5 μL/min) before capping any sites remaining activated using a 70 μL injection of 1 M ethanolamine hydrochloride pH 8.5. The surface was conditioned before further use by flushing with running buffer at 10 μL/min overnight.

5.2.2 Estrone Glucuronide Conjugate on Functionalised Terthiophene-on-Gold Surface

5.2.2.1 Immobilisation

The estrone glucuronide conjugate (**12**) used in Chapter 3 was immobilised on flow cell 2 of the gold surface plasmon resonance chip surface prepared with a 10 mM concentration of the functionalised terthiophene. The method of immobilisation was the same as described for the CM5 chip in Chapter 3, using one 70 μL injection of injection of Biacore™ coupling solutions 390 mM EDC/100 mM NHS (mixed in 1:1 ratio) at 10 μL/min and five pulses of estrone glucuronide conjugate diluted in 10 mM sodium acetate solution pH 4.0. The surface was then deactivated as before. Flow cell 1 was immobilised in a similar manner, using ovalbumin in place of the conjugate solution.

The surface was conditioned before further use by flushing with running buffer at 10 μL/min overnight.

5.2.2.2 Estrone Glucuronide Conjugate on Functionalised Terthiophene-on-Gold Surface - Ferric Chloride Treated

The estrone glucuronide conjugate used in Chapter 3 was immobilised on to flow cell 2 of the ferric chloride treated 5 mM functionalised terthiophene-on-gold surface. The method of immobilisation was similar to those chips not treated with ferric chloride (above), *i.e.*, two injections of Biacore™ coupling solutions 390 mM EDC/100 mM NHS (mixed in 1:1 ratio) (70 μL, 20 μL at 5 μL/min). Nine pulses of estrone glucuronide conjugate diluted in 10 mM sodium acetate solution pH 4.0 were injected (5 μL, 50 μL x 3, 86 μL x 5 at 5 μL/min), and then the surface was deactivated as before.

5.2.2.3 Injections of Antibody W mAb (scouting)

To test the sensitivity of a surface, 60 μL injections of 1 μg/mL antibody W mAb (120 s at 30 μL/min) were injected on to the surface, followed by a single 2 μL pulse of 50 mM NaOH (12 s at 10 μL/min) to regenerate.

5.3 Progesterone

5.3.1 Preparation of P4-OEG-COOH and P4-OEG-NH_2

The syntheses for the progesterone-linker-amine (P4-OEG-NH_2) (**23**) and the progesterone-linker-carboxyl group (P4-OEG-COOH) (**25**) used in the conjugation to ovalbumin are described in the Appendix.

5.3.2 Preparation of a Progesterone-OEG-Ovalbumin Conjugate (24)

The conjugate (**24**) was prepared using a method based on that of Wu *et al.* [68].

To a solution of P4-OEG-COOH (**25**) (23 mg, 32 μmol) in dimethylformamide (60 μL), *N,N*'-dicyclohexylcarbodiimide (30 μL of a 1M solution in dimethylformamide, 30 μmol) and *N*-hydroxysuccinimide (30 μL of a 1M solution in dimethylformamide, 30 μmol) were added. The solution was stirred at room temperature for two hours, then transferred to an ice-cold solution of ovalbumin (21 mg in 2 mL of 0.01M phosphate buffered saline pH 7.4, 0.48 μmol), using 40 μL of dimethylformamide. The solution was stirred overnight at 4^{o}C. The resulting conjugate was dialysed at 4^{o}C against Milli-Q water for two days (3 changes/day), 0.01 M phosphate buffered saline pH 7.4 for two days (3 changes per day), then passed through a pre-packed PD-10 desalting column (GE Healthcare, UK) using 0.01M phosphate buffered saline pH 7.4 as eluent. 3.5 mL of purified conjugate solution was collected, divided into aliquots and stored at -20^{o}C.

The ovalbumin conjugates were analysed by mass spectrometry at the University of Waikato, as for the estrone conjugates (Chapter 3).

5.3.3 Immobilisation of Progesterone

The immobilisation of the progesterone sensing elements on to CM5 and functionalised terthiophene-on-gold surfaces was carried out as follows:

5.3.3.1 P4-OEG-OVA Conjugate:

Flow Cell 2: The carboxyl groups on the surface of the CM5 chip were activated by 70 μL injections of Biacore™ coupling solutions 390 mM EDC/100 mM NHS (mixed in 1:1 ratio) at 10 μL/min. The conjugate was diluted in 10 mM sodium acetate solution pH 4.0 and filtered through a 0.45 μm Phenomenex PES syringe filter to remove any insoluble material. Repeated injections of the conjugate solution at 5 μl/min were made until a satisfactory immobilisation level was reached. Any remaining activated carboxyl groups were deactivated by injecting 70 μL of 1 M ethanolamine hydrochloride pH 8.5.

Reference Flow Cell 1: The reference flow cell was then immobilised in a similar manner to flow cell 2, with ovalbumin solution (500 μg/mL in 10 mM sodium acetate solution pH 4.0), using as a target the final immobilisation level (in RU) obtained for flow cell 2.

5.3.3.2 P4-OEG-NH_2:

Flow Cell 2: As for the P4-OEG-OVA Conjugate

Reference flow cell 1: The reference flow cell was treated as for flow cell 2, but the conjugate injections were omitted *i.e.*, the surface was activated with coupling solution and deactivated with 1M ethanolamine solution pH 8.5.

5.3.4 Antibody Binding Studies:

For all P4-OEG immobilised surfaces, a plot of response versus antibody concentration was prepared by diluting Sigma P1922 anti-progesterone antibody in HBS-EP+ running buffer to produce a concentration series, and injecting three 60 μL individual replicates of each concentration, as follows:

For P4-OEG-OVA conjugate on CM5 surface, the antibody concentrations were 0, 0.1, 0.20, 0.50, 1.0, 2.0, 2.5, 3, 4, 5, 6, 7, 8, 9 and 10 μg/mL.

For P4-OEG-NH_2 on CM5 surface, the antibody concentrations were 0, 0.025, 0.050, 0.075, 0.10, 0.125, 0.150, 0.175, 0.200, 0.225, and 0.25 μg/mL.

For P4-OEG-OVA conjugate on the functionalised terthiophene-on-gold surface, the antibody concentrations were in the 0, 0.5, 0.10, 0.15, 0.20, 0.25, 0.30, 0.35, 0.40, 0.45 and 5.0 μg/mL.

For P4-OEG-NH_2 on the terthiophene-on-gold surface, the antibody concentrations were 0, 0.025, 0.050, 0.075, 0.100, 0.125, 0.150, 0.175, 0.200, 0.225, and 0.25 μg/mL.

For the functionalised terthiophene-on-gold surfaces, regeneration was with 50 mM NaOH solution at 10 μl/min, and for the CM5 surfaces the flow rate was unchanged, but 5 % v/v acetonitrile was included in the 50 mM NaOH. The number and duration of regeneration pulses was increased for higher antibody concentrations, as regeneration was considered to be complete only when the baseline returned to pre-injection levels.

5.3.5 Inhibitive Immunoassays (Standard Curves) Using Surface Plasmon Resonance

A stock solution of progesterone was prepared in methanol (approximately 50 μg progesterone/mL of methanol), and standard solutions were prepared by diluting the stock solution in HBS-EP+ buffer, before mixing with an equal volume of P1922 anti-progesterone antibody solution to give final concentrations of 0.25 μg/mL for both P4-OEG-NH_2 surfaces, 2.5 μg/mL for P4-OEG-OVA on the functionalised terthiophene surface, and 10 μg/mL for P4-OEG-OVA on the CM5 surface. The concentration of antibody in the final solution was chosen to give a response in the range 50 to 150 RU for the free antibody in solution, *i.e.,* in the absence of progesterone standard material. A range of standard solutions were prepared with

final concentrations of progesterone of 0, 0.127, 0.253, 0.506, 0.759, 1.01, 1.27, 1.52, 1.77, 2.024, 5.06, 12.65, 12.65, 25.3, 101.2, 253 and 2530 ng/mL.

Regeneration was as for the binding curves, *i.e.,* the CM5 surfaces required the addition of 5 % v/v acetonitrile in the 50 mM NaOH to ensure removal of bound material, whereas 50 mM NaOH only was used for the terthiophene surfaces.

5.4 Electrochemistry

5.4.1 Materials and Methods

The electrochemistry of terthiophene and the functionalised terthiophene (terthiophene-OEG-COOH) (**22**) was performed with an Ecochemie Autolab system PGSTAT30 potentiostat/glavanostat, with General Purpose Electrochemical System (GPES) software. In all cases, silver wire (2.68 mm diameter) was used as a quasi-reference electrode. The counter electrode was either a platinum disc voltammetry electrode with a surface area of 1.8 mm^2 or stainless steel 1 cm^2 which was used as the counter electrode for the early work, prior to the fabrication of the purpose-built cell. The supporting electrolyte was 0.1M tetrabutylammonium perchlorate (TBAP) in acetonitrile. The TBAP (Acros Organics, N.J., U.S.A.) was dried in *vacuo* at 70^{o}C for at least 48 hours before use and was stored over silica gel. Acetonitrile was used as supplied, but maintained in a nitrogen atmosphere after use. All solutions were degassed by sonication and bubbling with oxygen-free nitrogen prior to electrochemistry. All experiments were carried out at room temperature.

Early experiments on electrochemical deposition were carried out using 3.5 mL of 5 mM terthiophene-OEG-COOH (**22**) in 0.1 M TBAP in acetonitrile, using a stainless steel counter electrode. Later, a purpose-built set-up was used for coating gold-on-glass and surface plasmon resonance chips, which ensured a more constant distance between electrodes, and allowed a smaller volume (450 μL) of solution to be used.

Sputter–coated gold-on-glass

Squares of microscope slides were cut into 12 x 10 mm squares and cleaned with hexane, methanol, detergent, and finally by soaking for thirty minutes in piranha solution. The piranha solution was rinsed with Milli-Q water and the slides allowed to air dry.

The glass was sputter-coated with gold using a Polaron Equipment SEM Coating Unit E5100 Series II 'Cool' Sputter Coater (Polaron Equipment Limited, Herts, England). The gold surface on the sputter coated gold-on-glass slides was less robust and more prone to scratching than the commercial SPR chips, but was suitable for preliminary studies.

Bare gold surface plasmon resonance chips were cleaned as for the glass used in sputter-coating.

5.4.2 Electrochemical Set up

The cell used for the electrochemical measurement was a three-electrode system comprised of a working electrode (WE), a counter electrode (CE) and a reference electrode (RE). The WE was either a glass slide sputter-coated with gold (gold-on-glass surface), which was used to determine the optimum conditions for attachment, or a bare gold Biacore^{TM} surface plasmon resonance chip. The potentiostat controlled the current flowing between the WE and the CE in order to maintain the required potential difference between the WE and the RE.

Characterisation of the terthiophene-OEG-COOH was carried out initially using a platinum voltammetry working electrode, and later with a gold voltammetry working electrode.

Terthiophene was used as a model to determine the parameters for the electrochemical coating on the gold WE. Polyterthiophene was deposited from a solution of 3.5 mL of 5 mM terthiophene in supporting electrolyte (0.1 M TBAP in

acetonitrile) on to a gold voltammetry electrode, using a platinum counter electrode and a silver wire as a quasi-reference electrode.

All solutions of functionalised terthiophene for electrochemistry were prepared with a concentration of 5 mM in a large excess (0.1 M) of supporting electrolyte. Acetonitrile was used for all electrochemistry in this study, offering as it does good solubility of the terthiophene and of the functionalised terthiophene used in this study.

Cyclic voltammetry was used for the electrochemical characterisation of the functionalised terthiophene on both gold and platinum working electrodes. In all other cases, cyclic voltammetry and potential-pulse methods were used to electrochemically deposit a film of terthiophene or functionalised terthiophene onto the gold surface. The deposited films were rinsed with acetonitrile to remove residual terthiophene or functionalised terthiophene which had not deposited on the surface, before carrying out post-coating cyclic voltammetry.

The coated surface plasmon resonance chips were assembled in accordance with the manufacturer's instructions (Figure 35) and stored at 4^{o}C over silica gel. The gold surface plasmon resonance chip was placed into a well in the assembly unit with the coated surface uppermost (A and B) and an adhesive-coated cassette lowered on to the chip. The mounted chip (C) was then inserted into a protective cover for use in the instrument.

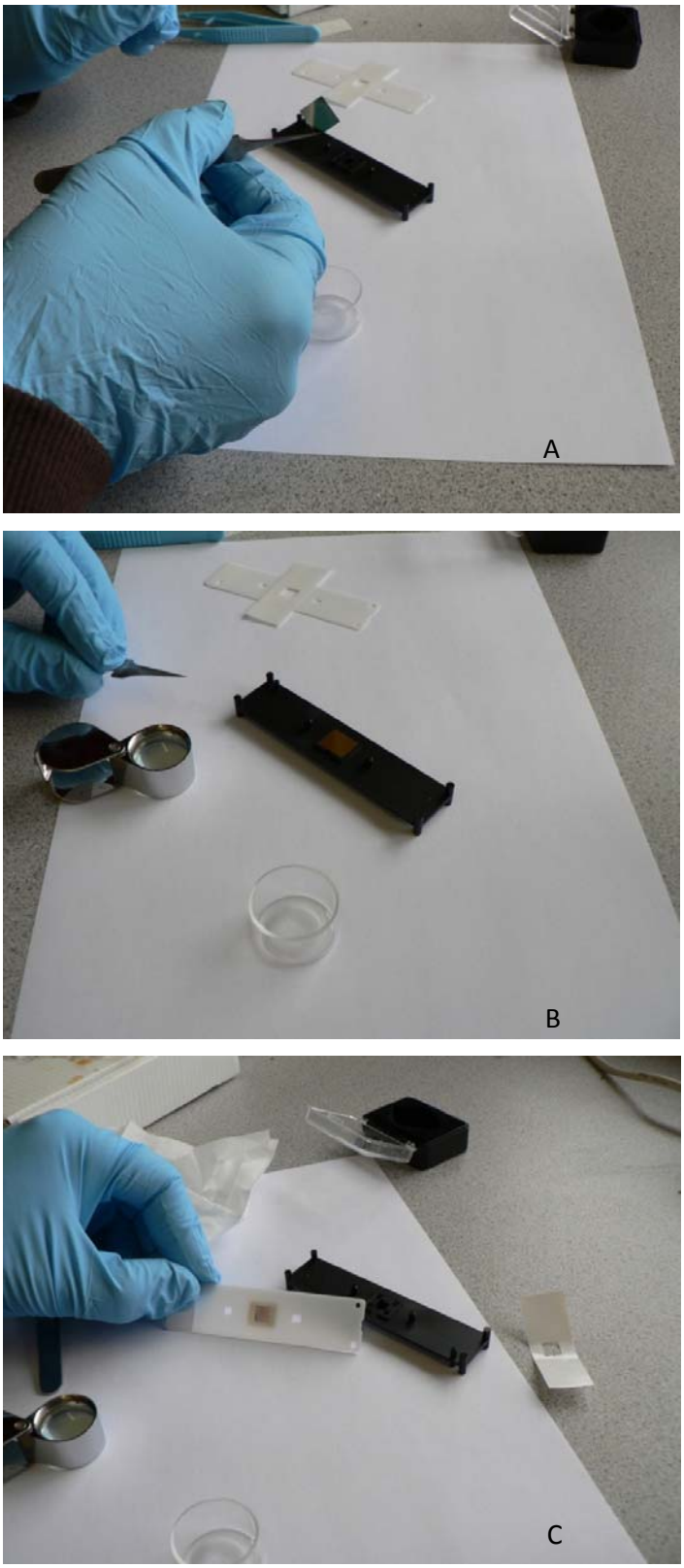

Figure 35: Assembly of the coated SPR chip in to the SPR cassette

5.4.3 Electrochemical Characterisation of Terthiophene-OEG-COOH:

A 5 mM solution of terthiophene-OEG-COOH in 0.1 M TBAP was used for electrochemical characterisation, with both a platinum voltammetry electrode, and a gold voltammetry working electrode. The scan rate for the coating scans and the post-coating cyclic voltammetry was 100 mV/s. The procedure was repeated using a sputter-coated gold-on-glass working electrode.

5.4.4 Electrochemical Coating Methods:

Both a potential-pulse and a potentiodynamic method were investigated as approaches to coating the functionalised terthiophene on gold surfaces. The aim was to find the most even surface and to determine which would give sufficient scope as regards the thickness of the resulting polymer.

Potential-Pulse Method

In the potential-pulse method used in this study, the potential was stepped from a point where no reaction occurred to the potential where oxidation occurred (1.2 – 1.25 V), and the potential then held constant at the latter value. The pulsing process was repeated to build up a coating of functionalised terthiophene scaffold on the sensor surface.

Two surface plasmon resonance chip surfaces were prepared using this method using 3.5 mL of 5 mM terthiophene-OEG-COOH in 0.1 M TBAP. One chip was coated for 50 ms at 1.25 V for 10 pulses, and the second under the same conditions, for 50 pulses. Every effort was made to ensure that the distance between the electrodes was the same for both experiments, but it is acknowledged that differences might have occurred which introduced variation in the coating.

The surfaces of the resulting two chips with films of different thicknesses were immobilised with estrone glucuronide-ovalbumin conjugate. The immobilisation method was as described for the estrone glucuronide conjugate immobilised on to a functionalised terthiophene-on-gold surface prepared using the immersion

method (see 5.2.2.1), with two activation injections (70 μL and 10 μL at 10 μL/min) and four pulses of estrone glucuronide-ovalbumin conjugate (**12**) diluted in 10 mM sodium acetate solution pH 4.5 (4 x 60 s, at 5 μL/min). The surface was deactivated as before.

The surface was conditioned by ten blanks runs, *i.e.* running buffer (60 μL, at 30 μL/min) followed by regeneration solution 50 mM NaOH (2 μL, at 5 μL/min). As a check on the signal size and reproducibility, fifteen injections of monoclonal antibody W (1 μg/mL) (60 μL, at 30 μL/min) were made, using two 60 μL pulses of 50 mM NaOH to regenerate the surface.

5.4.5 Purpose-Built Electrochemical Cell

An electrochemical cell was designed and constructed specifically for electrochemical coating of surface plasmon resonance sensor surfaces (see Figure 36). This special cell was also suitable for the sputter-coated gold-on-glass slides which were used for optimisation of the electrochemical conditions. The cell gave a surface with an uncoated border region which was useful when determining the thickness of the coated surface using AFM. The main aims were to make the coating process as uniform as possible, so that any variation in film thickness and uniformity was due to a change in the electrochemistry conditions, and to facilitate reproducible generation of surfaces. The cell was designed to be used with relatively modest amounts of the 5 mM terthiophene-OEG-COOH coating solution.

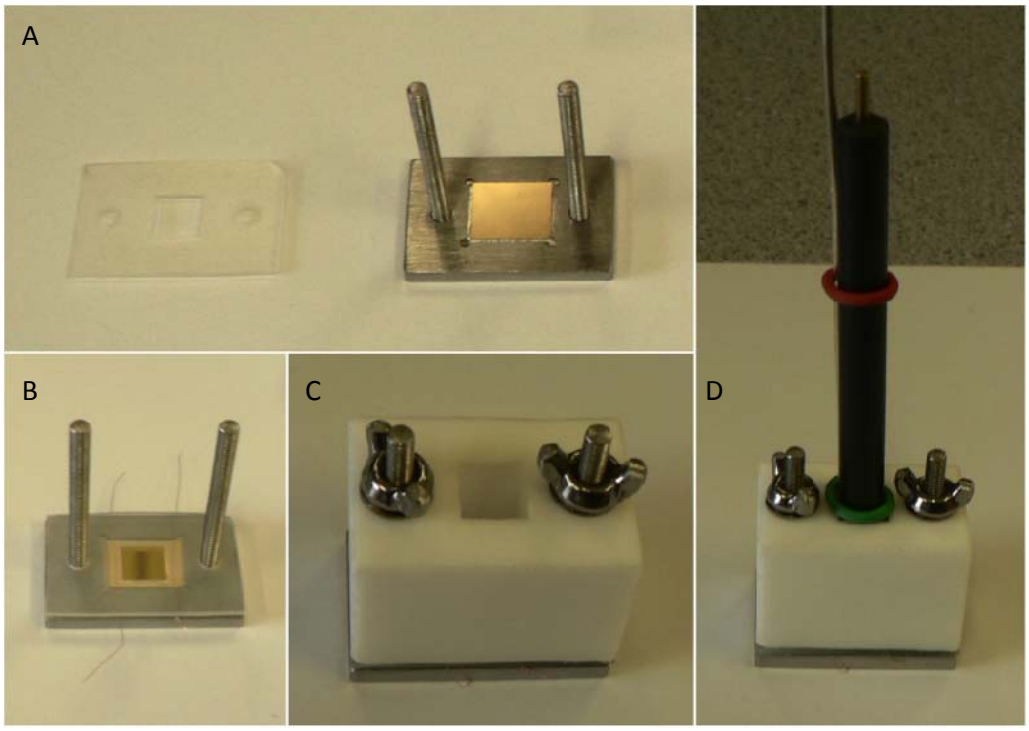

Figure 36: The electrochemical cell used for coating gold-on-glass slides and SPR sensor surfaces. Copper wire was placed over both ends of the chip to provide contact, a gasket fitted over the stainless steel rods and then the Teflon block was lowered into position. The platinum counter electrode and the silver wire reference electrode were lowered into position at a constant depth, after addition of 450 μL of coating solution.

The cell was assembled by using placing a glass slide to act as a spacer into a shallow chip cavity before inserting the surface plasmon resonance chip (or gold-on-glass slide) as illustrated in Figure 36 (A). Two strands of copper wire provided a contact for the gold surface, and a silicon gasket was inserted (B) before lowering the Teflon block and screwing the assembly together (C). Coating solution (450 μL) was dispensed into the cavity using an auto-pipettor, before inserting the counter electrode and reference electrode to a constant, pre-determined depth (D).

After electro-deposition and prior to post-coating cyclic voltammetry, the electrodes were removed and the cell cavity and electrodes were rinsed with acetonitrile to remove any remaining coating solution. The cell body was not disassembled during the rinsing step, so it is possible that traces of coating solution might have remained.

Coating Conditions:

Using the purpose-built cell, experiments were carried out to optimise the coating of the functionalised terthiophene. A coating which was just visible was considered to be the thickest coating desirable, and the intention was to investigate also the performance of thinner coatings.

5.4.6 Optimisation of Potential Pulse Coating conditions:

In all cases the potential was stepped to 1.2 V. Initially, 5000 pulses with a pulse time of 50 ms was trialed, then the time reduced to 25 ms. The pulse time and number of cycles was altered by trial-and-error until conditions for deposition could be generated, which would produce a chip surface with a faint brown colour. Accordingly, five sputter-coated gold-on-glass slides were pulsed at 1.2 V for 13 ms for 6000 cycles to produce a slightly brown coating on the surfaces. The first chip was left untreated following coating. For the second chip the coating solution was removed, the cell rinsed with acetonitrile then 0.1 M TBAP in acetonitrile, and 450 μL of 0.1 M TBAP in acetonitrile added to carry out cyclic voltammetry (0 to 1.2 V) at 100 mV/s for 5 scans. The third coated chip was rinsed and 450 μL of 0.1 M TBAP in acetonitrile added as for the second chip, but, instead of subjecting the resulting surface to cyclic voltammetry, the supporting electrolyte was pulsed using the coating conditions (1.2 V for 13 ms for 6000 cycles). The fourth and fifth chips were coated, rinsed and supporting electrolyte added as for the second chip, except that one (fourth chip) and five (fifth chip) 4 s pulses were applied respectively, following coating. The final colour and uniformity of the coated surfaces were examined visually.

5.4.7 Optimisation of Potentiodynamic Coating Conditions:

Using potentiodynamic (cyclic voltammetry) to deposit the functionalised terthiophene, it was possible to control thickness of the coating by varying both the number of cycles, and the speed of the scan. In this technique an increasing potential is applied to the working electrode with a fixed scan speed. When the

potential reaches a pre-determined maximum the potential is reversed. The cycling can be applied repeatedly. A typical post-coating cyclic voltammogram is carried out at 100 mV/s, and this was found to produce a highly coloured coating so to produce a thinner surface, a faster speed was considered to be necessary.

Two gold-on-glass surfaces were prepared using a scan speed of 2.5 V/s with 10 scans in one case and 20 scans in the other (0 to 1.2 V). A third chip was prepared similarly, but cycled for 50 scans at 5 V/s. Post-coating cyclic voltammetry was run at 100 mV/s, (0 to 1.2 V) using supporting electrolyte only.

5.4.8 Preparation of Surface Plasmon Resonance Scaffolds

Four surface plasmon resonance sensor surface scaffolds were prepared using the potentiodynamic coating method with a scan speed of 5 V/s, cycling between 0 and 1.2 V, with 50, 10, 5 and 1 cycles respectively to coat the surfaces.

Finally, four surface plasmon resonance surfaces were coated with a single cycle (chips A, B and C), using the potentiodynamic method with a 5 V/s setting as above, to determine the reproducibility of a surface prepared in this manner. Three of these single-cycle chips were subjected to surface plasmon resonance immobilisation and antibody-binding studies, and the fourth was examined by atomic force microscopy (AFM).

5.4.9 Surface Plasmon Resonance of Electrochemically Coated SPR chips:

5.4.9.1 Immobilisation:

Each of the four electrochemically coated surface plasmon resonance chips (50-cycle, 10-cycle, 5-cycle and 1-cycle) and three of the four single-cycle chips (Chip A, B and C) were immobilised with progesterone-OEG-OVA conjugate (**24**), using the conditions described above in 5.3.3.1. To compare the behaviour of each of the prepared surfaces, each was immobilised using the same conditions, *i.e.* two pulses of EDC/NHS (as described in 2.2.1 Immobilisation Chemistry) activation solution (2 x 70 μL, 10 μL/min), followed by seven pulses of progesterone-OEG-OVA conjugate

solution in 10 mM sodium acetate solution pH 4.0 (2 μL, 5 μL, 2 x 15 μL, 3 x 30 μL, 5 μL/min). A single pulse of 1 M ethanolamine hydrochloride pH 8.5 (70 μL, 10 μL/min) was made to deactivate any remaining activated carboxyl groups. The reference flow cells on each chip were then immobilised in a similar manner to flow cell 2, with ovalbumin solution (500 μg/mL in 10 mM sodium acetate solution pH 4.0) in place of the conjugate, using as a target the final immobilisation level (in RU) obtained for flow cell 2.

All chip surfaces were conditioned by making ten injections of running buffer (60 μL, 30 μL/min) followed by 50 mM NaOH regeneration solution (10 μL, 10 μL/min) through both flow cells of each chip.

5.4.9.2 Antibody Response and Stability Check: (1-, 5-, 10- and 50-Cycle Chips

To determine the antibody response of each of the four electrochemically coated chips, and the degree to which the antibody signal decayed over time, five injections of P1922 antibody 1 μg/mL (60 μL, 30 μL/min) followed by 50 mM NaOH regeneration solution (10 μL, 10 μL/min) were made over each chip surface. This was followed by ten 'blank' injections where running buffer was injected in place of the antibody, and finally a further five antibody injections, as before.

Before running the antibody response and stability check, three to five 'start-up' injections (*i.e.* running buffer followed by regeneration solution) were made on to each sensor surface. The system was considered to be suitable for running when the baseline values for each flow cell appeared stable, with little change between injections.

5.4.9.3 Antibody Binding Studies (Single-Cycle Chips A, B and C):

The antibody binding studies were carried out as for the terthiophene-on-gold surfaces for progesterone-OEG-OVA, using 0, 0.5, 1.0, 1.5, 2.0, 2.5, 3.0, 3.5, 4.0, 4.5 and 5.0 μg/mL P1922 antibody concentrations. For Chip A, regeneration was by 10

μL, then 2 x 5 μL (10 μL/min) injections of 50 mM NaOH. For Chips B and C, the number of regeneration pulses was increased to 3 x 10 μL to ensure complete regeneration.

5.4.9.4 Antibody Response and Stability Check: (Single-Cycle Chips A, B and C)

This was carried out as for the electrochemically coated chips of varying thickness (see Section 5.4.9.2 above).

5.4.9.5 Inhibitive Immunoassay (Standard Curve)

The inhibition assay was carried out on single-cycle Chip C as for the functionalised terthiophene-on-gold surfaces (see Section 5.3.5), with final concentrations of 2552, 255.2, 102.1, 25.5, 12.76, 5.10, 2.04, 1.276, 1.021, 0.510, and 0.128 ng progesterone/mL. The P1922 anti-progesterone antibody solution in the final solutions was 2.5 μg/mL. Regeneration was by 2 x 10 μL, 5 μL (10 μL/min) of 50 mM NaOH.

5.4.10 Functionalised Terthiophene Scaffold: Immersion Method vs Electrochemically Deposited Surface

To investigate the stability of the functionalised terthiophene layer deposited on the gold surface by immersion of the surface plasmon resonance chip in the coating solution, compared to that of the electrochemically deposited functionalised-terthiophene, a surface plasmon resonance chip surface prepared using the immersion method (see Section 5.2) was compared with an electrochemically deposited functionalised terthiophene surface (Chip C). The procedure was similar to that used to that described above (5.4.9.2), with five 'start-up' injections, five injections of P1922 antibody 1 μg/mL (60 μL, 30 μL/min) then 50 mM NaOH regeneration solution (2 x 10 μL, 10 μL/min) over each chip surface. This was followed as before by ten 'blank' injections where running buffer was injected in place of the antibody, and a further five antibody injections. Finally, two buffer

injections and two antibody injections were made to give a total of 12 antibody injections in the sequence.

5.5 Results and Discussion

The sensorgram of the immobilisation of the estrone glucuronide conjugate on the 5 mM functionalised terthiophene-on-gold surface indicated that an immobilisation protocol similar to that used for the CM5 carboxymethylated dextran would be suitable for this new scaffold. The blank chip, which was cleaned and immersed in 95 % ethanol overnight and subjected to the ovalbumin immobilisation procedure, gave minimal binding (just 77 RU), which was completely removed following overnight running of buffer, as would be expected for a clean gold surface. Of the three gold surfaces immersed in different concentrations of functionalised terthiophene solution, the 5 mM-coated chip had the highest level of immobilisation of ovalbumin and the lowest loss of signal after having been flushed with HBS-EP+ running buffer, indicating that the 5 mM concentration was adequate for coating and that there was no advantage in using a higher (10 or 20 mM) concentration.

Accordingly, a concentration of 5 mM coating solution was used for subsequent scaffold preparation.

Table 10: Anti-estrone glucuronide antibody (monoclonal antibody W) binding response for SPR chips immobilised with estrone glucuronide conjugate, on a terthiophene-OEG-COOH surface and on a terthiophene-OEG-COOH surface which had been treated with ferric chloride solution.

Sensor Surface	Immobilisation FC2 (RU)	Initial mAb Response (RU)	Final mAb Response (RU)	Response Change/Injection
Terthiophene-OEG-COOH Surface only	2162	350 RU	251 RU	6 RU
Terthiophene-OEG-COOH Surface: $FeCl_3$ Treated	999	262 RU	209 RU	3 RU

The results for the binding of monoclonal antibody W to the estrone glucuronide-ovalbumin conjugate immobilised on the functionalised terthiophene-on-gold surface showed a drop in response over time (Table 10), indicating that the surface stability was lower than that for a corresponding CM5 surface. Experiments with a similar chip surface treated with ferric chloride to induce polymerisation of the terthiophene surface before immobilising with estrone glucuronide conjugate, suggested that this treated surface was more stable, in that the drop in response was less. The decrease in the response was however, still much higher than that with a comparable CM5 chip. CM5 chips generally maintain their signal response over several hundred injections with less than 1 % loss of signal. The immobilisation of the ferric chloride-treated chip at a lower level than the untreated chip appeared to have little effect on the final antibody binding responses, which were relatively similar to each other (209 RU *vs* 251 RU) (Table 10).

These preliminary results indicated that the functionalised terthiophene material was suitable for use as a surface plasmon resonance scaffold and that its usefulness would be even greater if the stability of the surface could be enhanced to a point where it approached that of a CM5 surface. It is emphasised that the ferric chloride treatment method was carried out on only one occasion and that a more rigorous investigation would be worthwhile. Nonetheless, the improvement in the performance of the ferric chloride-treated chip surface (Table 10) indicated that investigating means of polymerising the terthiophene scaffold might provide the necessary enhanced stability of the sensor surface. Electrochemical coating was considered to have the potential to offer good control and reproducibility of the process, allowing the production of chips with consistent characteristics.

5.5.1 Progesterone:

The next step was to consider a steroid which could be directly covalently attached to both the functionalised terthiophene and the CM5 surfaces and which could be conjugated to ovalbumin and compared with the protein-free form. In this way the

impact of the protein and of the surface thickness could be investigated in terms of binding sensitivity.

Progesterone bound to a linker appended with an amino terminus (**23**) was synthesised (see Appendix). This compound could be attached to both the CM5 and to the carboxyl-functionalised terthiophene surface using the same immobilisation chemistry. Similarly, inserting the same linker prior to conjugating to a protein such as ovalbumin was well-established chemistry [54]. Accordingly, the progesterone-ovalbumin conjugate (**24**) was attached to a CM5 surface, and to a terthiophene-OEG-COOH coated surface prepared by immersing the gold in a 5 mM solution. The mass spectrometry results for the conjugate indicated a modest level of conjugation, approximately one molecule of progesterone per molecule of ovalbumin. The (un-conjugated) progesterone-OEG-NH_2 was attached to a CM5 surface, and to a terthiophene-OEG-COOH surface.

Immobilisation Results:

The results of the immobilisation of progesterone on to the sensor surfaces are given in Table 11. Where the progesterone-ovalbumin conjugate was used as the sensing element in flow cell 2, ovalbumin was immobilised in the reference flow cell 1. This was not necessary where the progesterone was used in its un-conjugated form; instead the flow cell 1 surface was treated by activation and deactivation only, and therefore gave only minimal changes in response after this treatment. Both conjugate surfaces had a relatively higher response level, as expected for a much higher-molecular-weight molecule in surface plasmon resonance.

Table 11: Immobilisation of the progesterone-OEG-ovalbumin conjugate and progesterone-OEG-NH_2 on the CM5 surface, and on the terthiophene-OEG-COOH surface. Flow cell 1 is the reference flow cell, and flow cell 2 contains the sensing element progesterone either as the ovalbumin conjugate or in the un-conjugated form where the amine moiety attaches to the surface.

	Scaffold	Flow Cell 2	Flow Cell 1
P4-OEG-OVA (1)	CM5	6371 RU	6235 RU
P4-OEG-NH_2 (2)	CM5	934 RU	69 RU
P4-OEG-OVA (3)	Terthiophene-OEG-COOH	2942 RU	2041 RU
P4-OEG-NH_2 (4)	Terthiophene-OEG-COOH	680 RU	-47 RU

Progesterone Antibody Binding Studies:

The terthiophene surfaces were regenerated sufficiently without the addition of acetonitrile to the regeneration cocktail. Several injections of 50 mM NaOH were used until the baseline returned to the initial value.

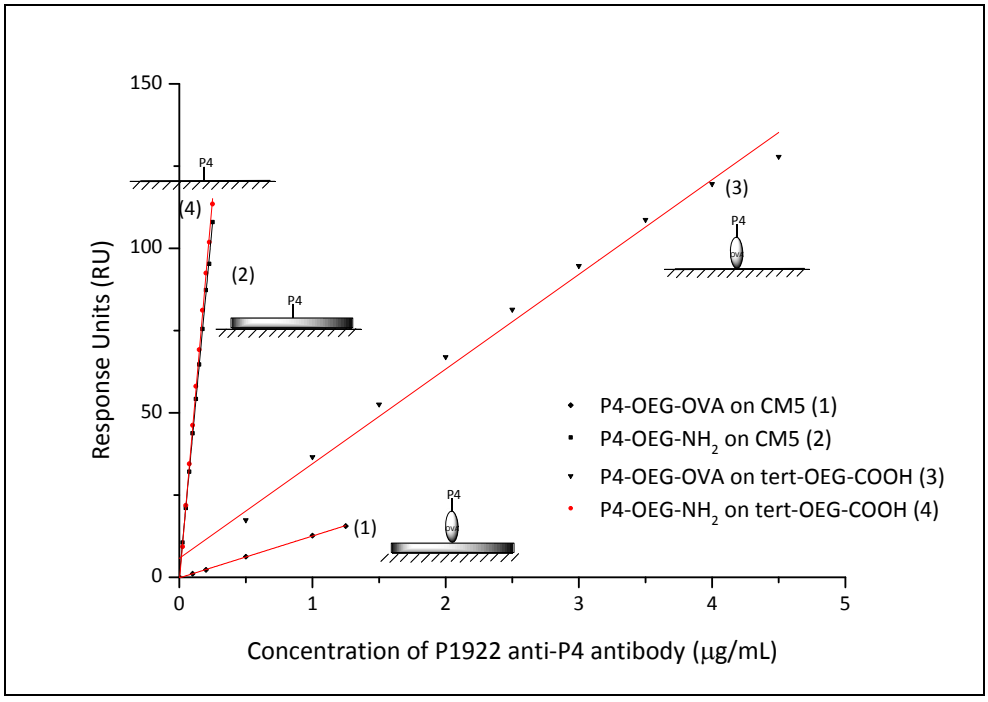

Figure 37: Antibody binding response curves for the anti-progesterone rat antibody P1922 on each of the four progesterone sensor surfaces.

The SPR antibody binding curves (Figure 37) suggest that a major factor in determining signal sensitivity is not only the thickness of the scaffold, but the use of the protein conjugate as the sensing element. The protein conjugate gave a lower antibody binding response whether immobilised on the CM5 chip or immobilised on the terthiophene-OEG-COOH (functionalised terthiophene) surface.

It was envisaged that the thinner functionalised terthiophene surface would give a more sensitive antibody response (a higher signal for the same concentration of antibody solution) than the CM5's 100 nm surface. However, only a modest antibody response was obtained for the progesterone-ovalbumin conjugate on the terthiophene (Surface 3). This may be due to low levels of scaffold on the surface, with correspondingly low amounts of the sensing element immobilised to the scaffold. The attachment of the conjugate on this surface was also relatively low compared with that on the CM5 (surface 1) (Table 11). If we consider that the immobilisation on terthiophene has occurred much closer to the surface and therefore in a more sensitive surface plasmon resonance region, the lower immobilisation signal might indicate a scaffold coverage which is much lower than on the CM5 chip, where the immobilisation occurs further away from the surface, and where the surface plasmon resonance response is comparatively lower. The functionalised terthiophene surface was expected to have the higher antibody binding response for both the conjugate (surface 3) and the protein-free progesterone sensing elements (surface 4) (refer to Table 17) but again the lower level of immobilisation on both the functionalised terthiophene surfaces might suggest that scaffold coverage is low.

The un-conjugated progesterone on CM5 (surface 2) and on terthiophene (surface 4) gave high antibody binding responses, *i.e.* the un-conjugated progesterone sensor surfaces give a considerably higher antibody binding response than their protein-conjugated counterparts, irrespective of which scaffold was used for attachment. The CM5 scaffold with un-conjugated progesterone (Surface 2) performed particularly well in the antibody binding study, comparable to the un-

conjugated progesterone on the terthiophene scaffold. The progesterone-OEG-ovalbumin conjugate had relatively low hapten ratio, may contain un-conjugated ovalbumin, and therefore have relatively fewer steroid molecules available for binding. While a conjugate with a higher ratio of progesterone to ovalbumin would give a higher response, it would be unlikely to approach the binding response obtained by either of the un-conjugated progesterone surfaces.

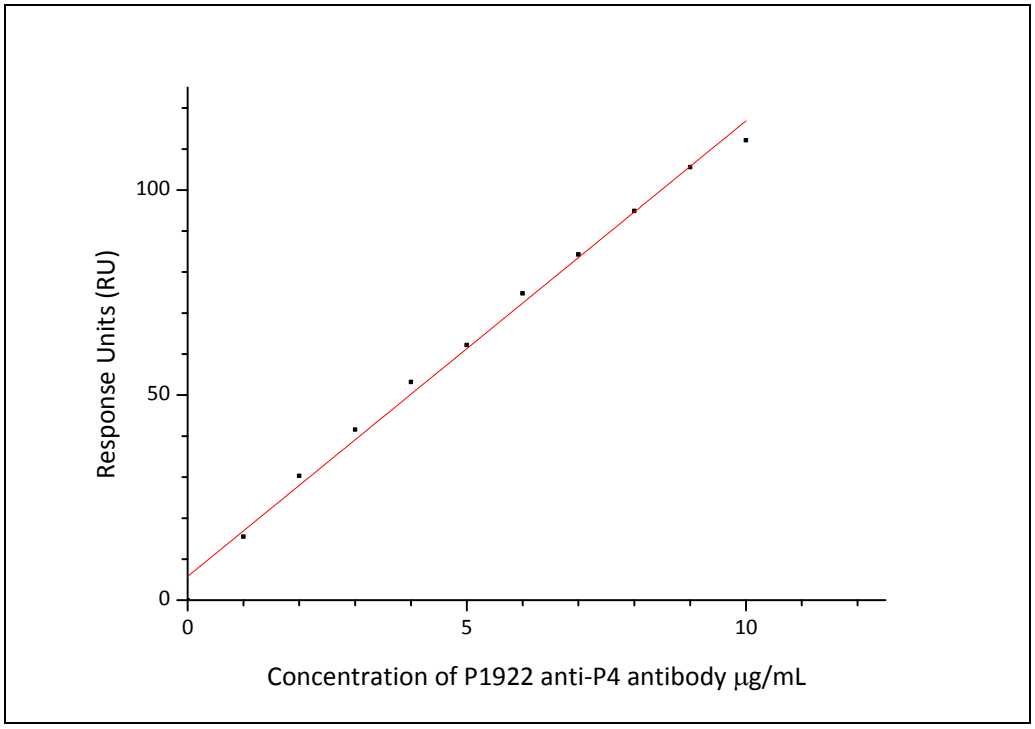

Figure 38: Binding curve for P4-OEG-OVA conjugate on the CM5 surface.

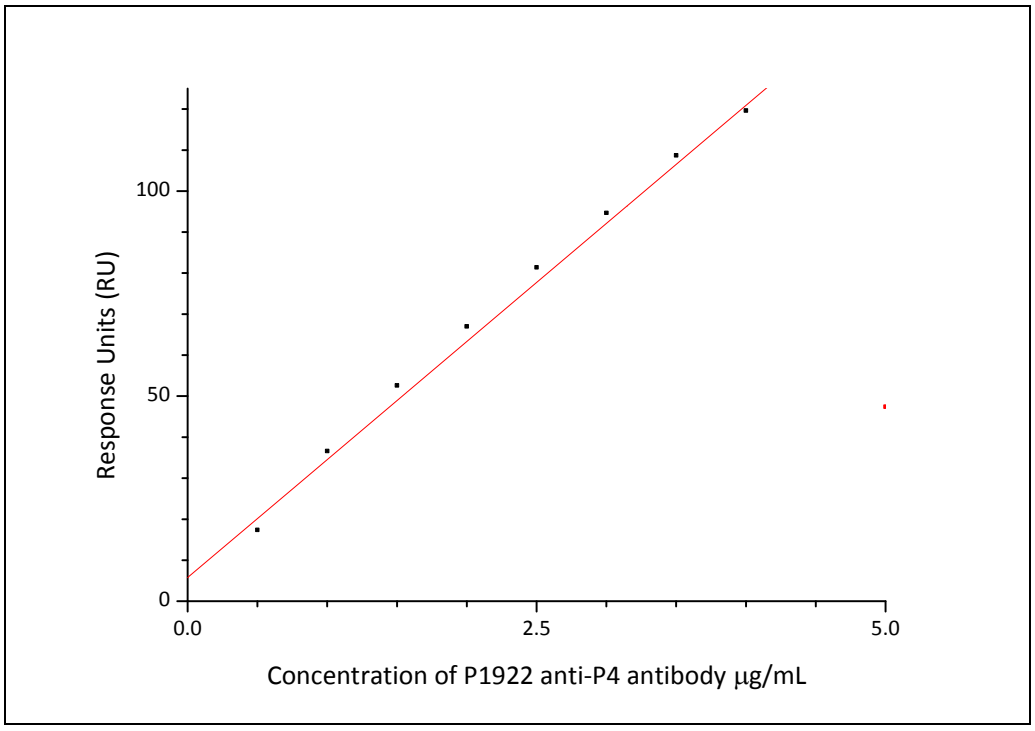

Figure 39: Binding curve for P4-OEG-OVA conjugate on the functionalised terthiophene surface.

For the same approximate response (up to 100 RU), the binding response curves of the ovalbumin conjugates exhibited a degree of curvature. This curvature occurred on both the CM5 (Figure 38) and the functionalised terthiophene surface (Figure 39). The surfaces without the conjugated protein did not exhibit curvature.

Scaffold Stability

The results with the estrone-ovalbumin sensor chips prepared using the immersion method suggested that the functionalised terthiophene surface would benefit by being more stable. The ferric chloride treatment was designed to effect polymerisation of the terthiophene surface [158], and this surface certainly appeared to suffer less from loss of signal response than the untreated chip. Polymerisation of the functionalised terthiophene by electrochemical methods was considered to be worthy of investigation, offering as it does the possibility of controlling the characteristics of the coated surface. The aim of replacing the 100 nm thick carboxymethylated dextran surface was to reduce the scaffold thickness,

so there was a requirement that the functionalised terthiophene surface be significantly thinner.

5.5.2 Terthiophene:

Initial studies used un-substituted terthiophene in place of the functionalised terthiophene which had been synthesised for use as a surface plasmon resonance scaffold. Cyclic voltammetry was carried out with a view to coating polyterthiophene on to a gold voltammetry electrode (Figure 40). The results for the cyclic voltammogram are not inconsistent with the formation of a conducting polymer.

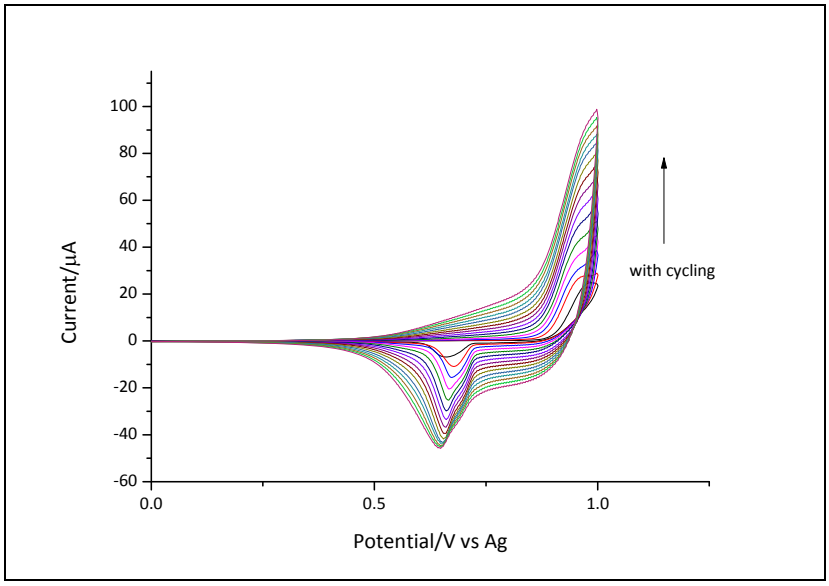

Figure 40: Cyclic voltammetry of terthiophene on a gold voltammetry electrode (surface area 1.8 mm^2). Supporting electrolyte 0.1 M TBAP in acetonitrile. Potential limits 0/+1.0 V. 15 cycles. Scan rate 100 mV/s. Stainless steel counter electrode.

The gold voltammetry electrode was coloured a deep red after this electrochemistry. Post-growth cycles of this coated electrode carried out in terthiophene-free electrolyte are shown in Figure 41.

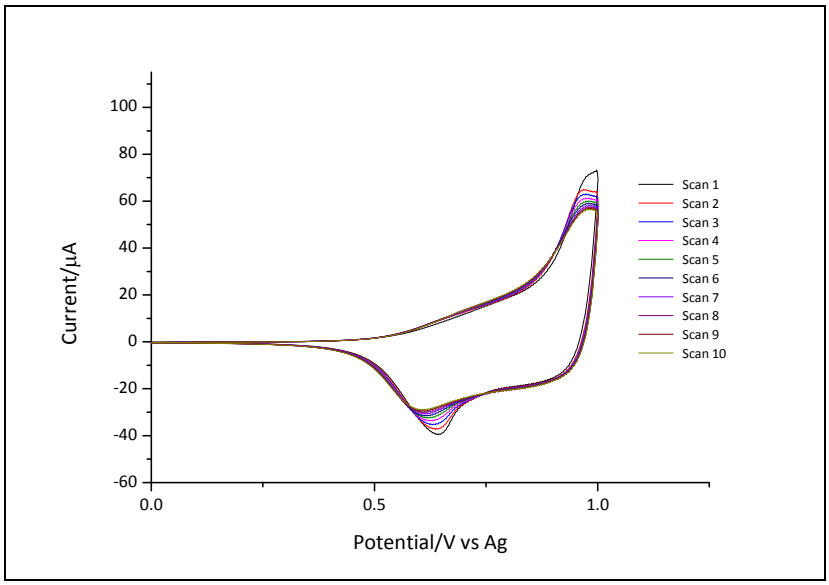

Figure 41: Post-coating cyclic voltammogram of terthiophene on a gold voltammetry electrode (surface area 1.8 mm^2) in supporting electrolyte (0.1 M TBAP in acetonitrile). Potential limits 0/+1.0 V. 10 cycles. Scan rate 100 mV/s. Stainless steel counter electrode.

5.5.3 Electrochemical Characterisation of Terthiophene-OEG-COOH

The functionalised terthiophene material was characterised by cyclic voltammetry using both platinum and gold voltammetry working electrodes. The results for the ferrocene couple in a solution of supporting electrolyte are given in Figure 42. The oxidation potential (E_{ox}) is 0.343 V, and the reduction potential (E_{red}) is 0.182V.

The cyclic voltammogram generated with a platinum WE is shown in Figure 43 and the post-coating cyclic voltammogram in Figure 44. The corresponding voltammograms for coating and post-coating cycling using a gold working electrode are shown in Figure 45 and 46 respectively.

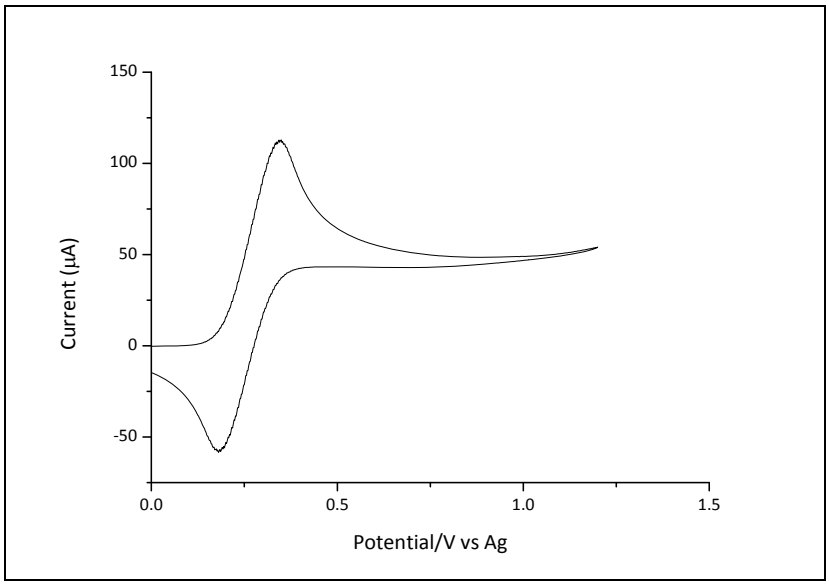

Figure 42: Cyclic voltammogram of ferrocene on a platinum disc electrode (surface area 1.8 mm^2) in supporting electrolyte (0.1M TBAP in acetonitrile). Potential limits 0/+1.2V. Scan rate 100 mV/s. Platinum voltammetry counter electrode.

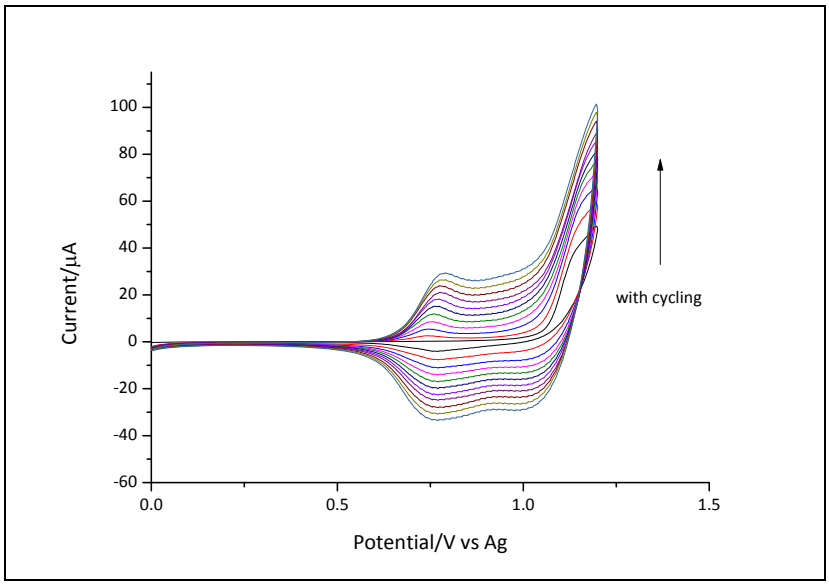

Figure 43: Cyclic voltammetry of terthiophene-OEG-COOH on a platinum voltammetry electrode (surface area 1.8 mm^2). Supporting electrolyte 0.1 M TBAP in acetonitrile. Potential limits 0/+1.2 V. 11 cycles. Scan rate 100 mV/s. Platinum voltammetry counter electrode.

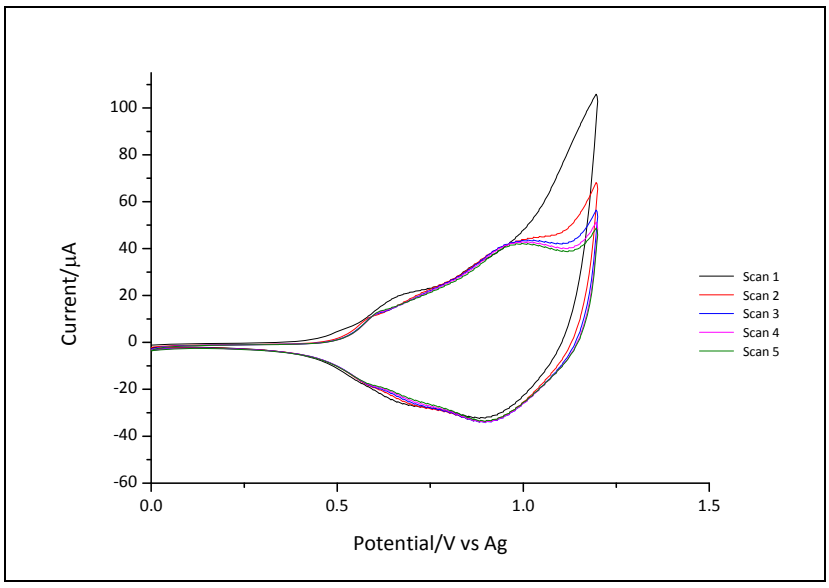

Figure 44: Post-coating cyclic voltammogram of terthiophene-OEG-COOH on a platinum voltammetry electrode (surface area 1.8 mm^2) in supporting electrolyte (0.1 M TBAP in acetonitrile). Potential limits 0/+1.2 V. 5 cycles. Scan rate 100 mV/s. Platinum voltammetry counter electrode.

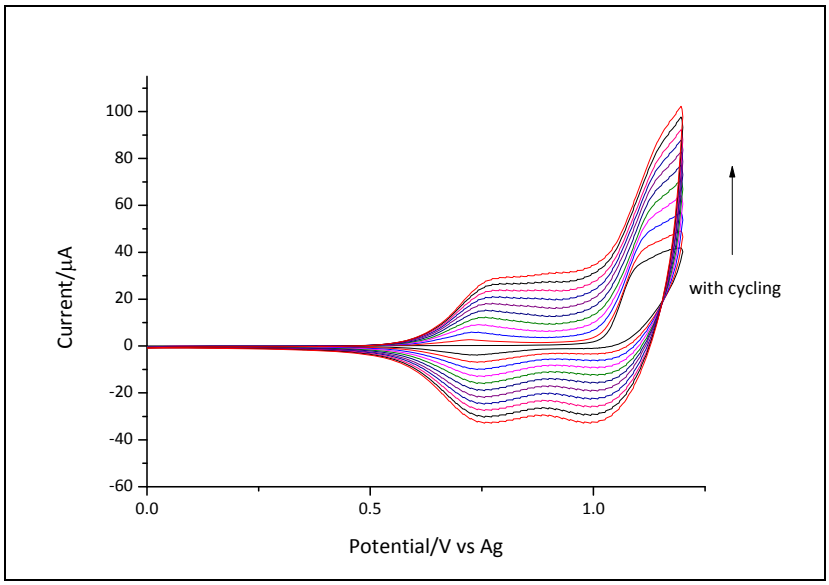

Figure 45: Cyclic voltammetry of terthiophene-OEG-COOH on a gold voltammetry electrode (surface area 1.8 mm2). Supporting electrolyte 0.1 M TBAP in acetonitrile. Potential limits 0/+1.2 V. 11 cycles. Scan rate 100 mV/s. Platinum voltammetry counter electrode.

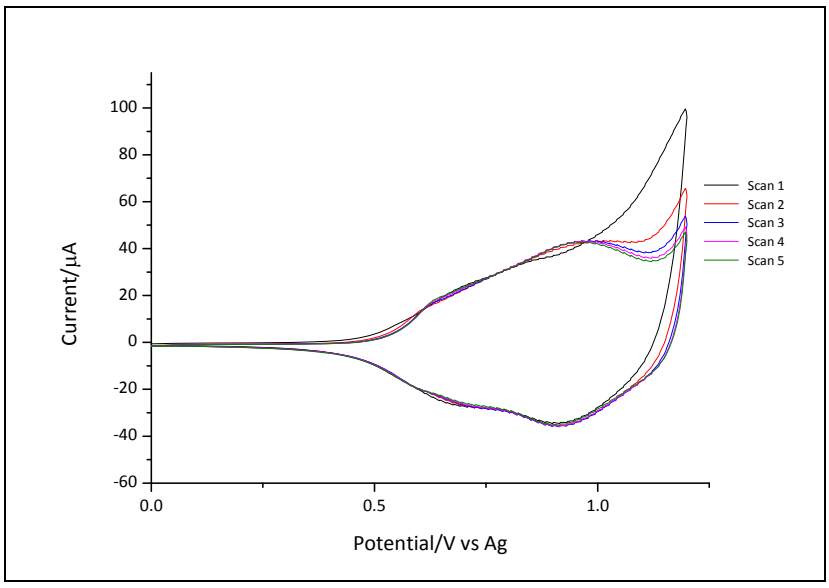

Figure 46: Post-coating cyclic voltammogram of terthiophene-OEG-COOH on a gold voltammetry electrode (surface area 1.8 mm^2) in supporting electrolyte (0.1 M TBAP in acetonitrile). Potential limits 0/+1.2 V. 5 cycles. Scan rate 100 mV/s. Platinum voltammetry counter electrode.

5.5.4 Potentiodynamic Coating of Gold-on-Glass Slides:

The gold voltammetry working electrode was replaced with a gold-on-glass surface, and the counter electrode with stainless steel bent to give a similar surface area to the working electrode. The gold-on-glass surface was coated potentiodynamically

using cyclic voltammetry, as below (Figure 47). The post-coating cyclic voltammogram of the coated electrode in supporting electrolyte is shown in Figure 48.

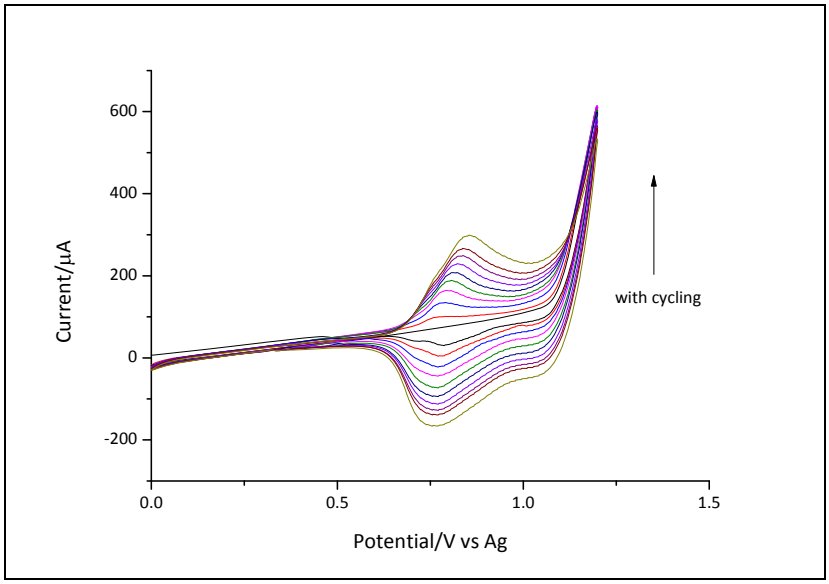

Figure 47: Cyclic voltammetry of terthiophene-OEG-COOH using a sputter-coated gold-on-glass working electrode. Supporting electrolyte 0.1 M TBAP in acetonitrile. Potential limits 0/+1.2 V. 11 cycles. Scan rate 100 mV/s. Stainless steel counter electrode.

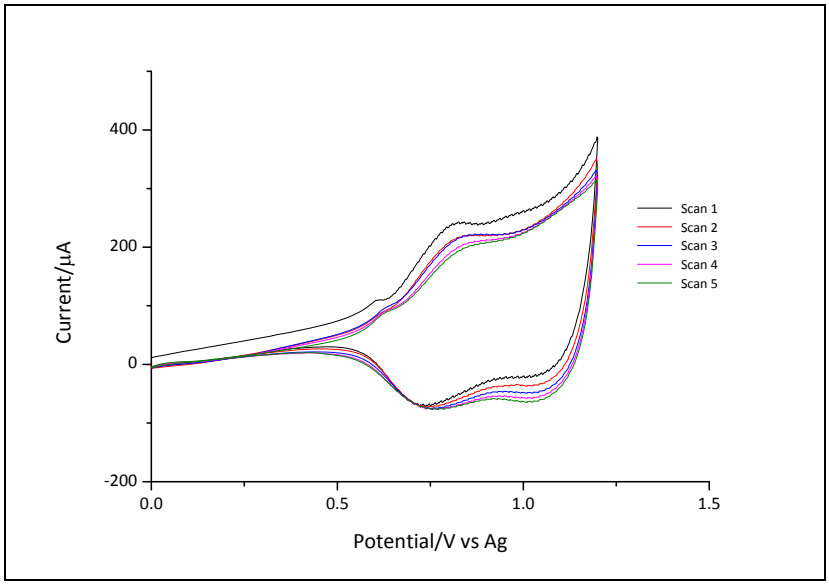

Figure 48: Post-coating cyclic voltammogram of terthiophene-OEG-COOH on a sputter-coated gold-on-glass working electrode in supporting electrolyte (0.1 M TBAP in acetonitrile). Potential limits 0/+1.2 V. 5 cycles. Scan rate 100 mV/s. Stainless steel counter electrode.

5.5.5 Potential-Pulse Coating of two SPR chips:

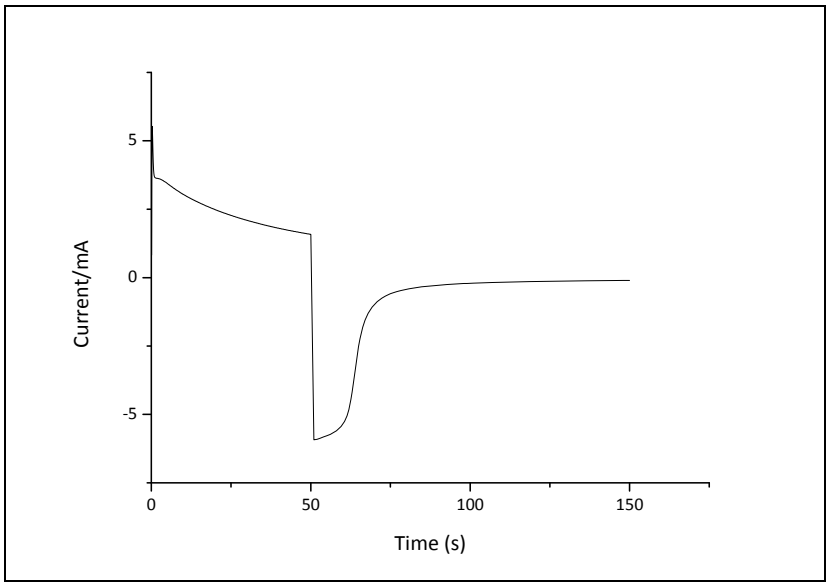

Figure 49: Chronoamperogram of the potential pulse coating of terthiophene-OEG-COOH on a gold SPR chip surface (single pulse only shown). Supporting electrolyte 0.1 M TBAP in acetonitrile. Pulsed at 1.25 V for 50 ms. Stainless steel counter electrode.

Two surface plasmon resonance chips were prepared using the potential pulse method with 10 and 50 pulses respectively for 50 ms used to coat the surface. The chronoamperogram for a single pulse is shown in Figure 49. The performance of the resulting surfaces was tested by immobilising estrone glucuronide-ovalbumin conjugate and observing the responses of repeated injections of monoclonal antibody W following conditioning injections (Table 12).

Table 12: Surface plasmon resonance immobilisation and antibody response data for sensor surfaces prepared by the potential-pulse coating of the gold surface with functionalised terthiophene.

Sensor Surface	Immobilisation FC2 (RU)	Initial Response (RU)	Final Response (RU)	Response Change/Injection
10 pulses	3409 RU	270 RU	213 RU	3.8 RU
50 pulses	4215 RU	277 RU	198 RU	5.3 RU

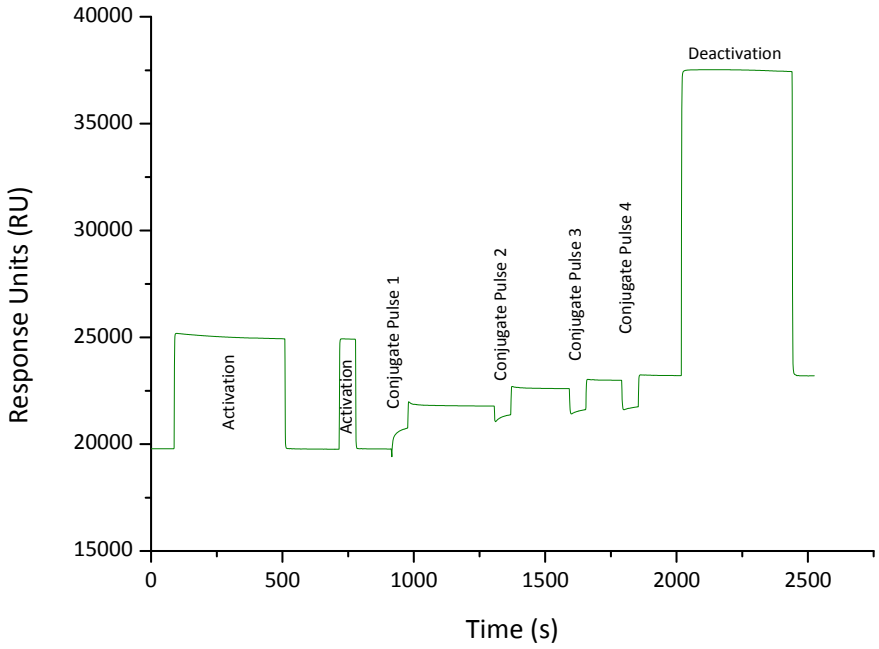

Figure 50: Immobilisation of estrone glucuronide conjugate on a terthiophene-OEG-COOH surface prepared using potential-pulse coating (50 ms at 1.25 V). 10 pulses.

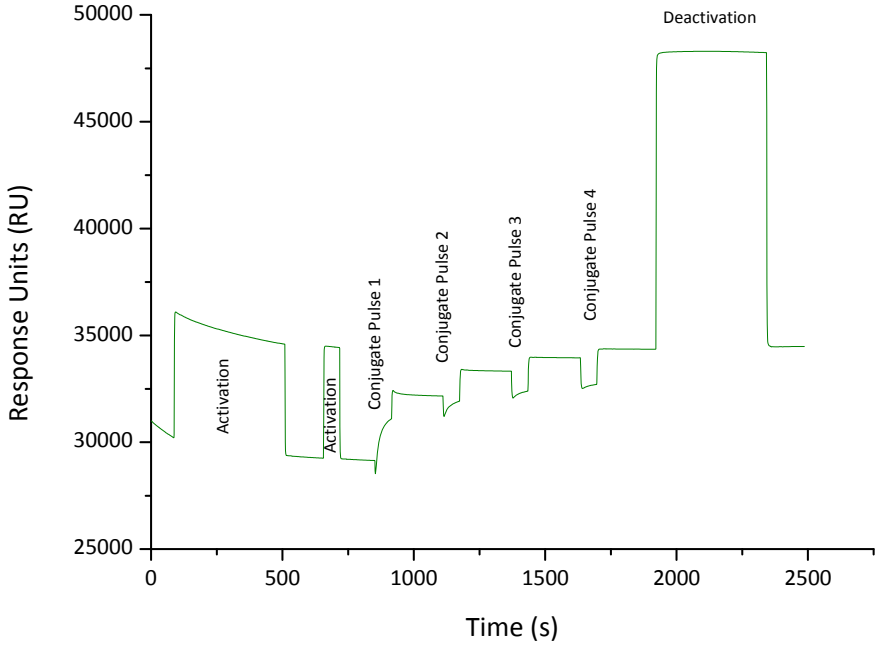

Figure 51: Immobilisation of estrone glucuronide conjugate on a terthiophene-OEG-COOH surface prepared using potential-pulse coating (50 ms at 1.25 V). 50 pulses.

The 10-pulse chip was a similar colour to a bare gold, uncoated chip surface, but the 50-pulse chip appeared to have a thicker coating, inasmuch as the surface was brown. The initial response was also different (see Table 12 and Figures 50 and 51). The initial response for a bare gold chip is typically around 20000 RU, similar to that obtained in the 10-pulse chip, 19800 RU. The 50-pulse chip response was initially approximately 31000 RU, and decayed rather than increased in the initial activation steps (Figure 51) suggesting some loss of the coating. Even after conditioning, the 50-pulse chip lost slightly more response than the 10-pulse chip. The 10-pulse chip was similar in stability to the ferric chloride treated surface prepared using the immersion method. In general, the coating which was visibly thinner performed better, and work proceeded to optimise the coating conditions.

5.5.6 Optimisation of Potential-Pulse Coating:

The length of the pulse 'step' time, and the number of pulses was varied. The aim was to find a set of conditions which would give sufficient flexibility in varying the coating colour, with a light brown coating as the thickest coating. Various thinner coatings would be generated by using a shorter pulse time and/or a lower number of pulses. Indications from the preliminary experiments using the potential-pulse coating method (10 pulses and 50 pulses) had indicated that the 50-pulse chip with visible brown colour did not perform better than the thinner 10-pulse chip. A thin coating was thought to be optimum for two reasons. A thinner coating could take advantage of the increased sensitivity obtained when the binding event in surface plasmon resonance occurs closer to the surface. From a practical standpoint, a thick coating might be more susceptible to decay in the flow of the surface plasmon resonance, potentially compromising the performance of the micro-fluidics.

With the purpose-built set-up, 5000 pulses from 0 to 1.2 V, with a pulse time of 50 ms gave a very brown coating, so the pulse time was reduced to 25 ms. 5000 pulses at this pulse time gave a lighter brown colour. By altering the pulse time and the number of pulses in this way, the optimised conditions for potential-pulse coating were selected as a 13 ms pulse time and around 6000 pulses and these conditions

gave a faint brown colour. The intention was to keep the pulse time constant at 13 ms, and produce a series of chips with varying levels of colour by reducing the number of cycles.

The five gold-on-glass surfaces coated using the potential-pulse coating method with a 13 ms pulse time (the chronoamperogram for the first pulse is shown in Figure 52) and treated with varying post-coating procedures had varying degrees of colour and uniformity. The coated surface subjected to cyclic voltammetry in monomer-free supporting electrolyte (Figure 53) was a much stronger colour than the relatively faint colour apparent directly after coating. The third coated gold-on-glass surface which was pulsed using the coating conditions (1.2 V for 13 ms for 6000 cycles) showed visible colour change. The post-coating treatment with slow (4 s) pulses gave more highly coloured chips than was obtained directly after coating, with the five 4 s pulsed chip more coloured than the single pulse, but the resulting coating for all chips was uneven. Even allowing for differences in the gold surface of the sputter-coated glass slides, it was apparent that the conditions applied during the post-coating cyclic voltammetry induced changes in the already-coated surface. Also, the surface of the coating produced using this method was uneven. It appeared that the potential-pulse method might not produce the desirable reproducible and uniform surface, so cyclic voltammetry (the potentiodynamic method) was investigated as a coating method.

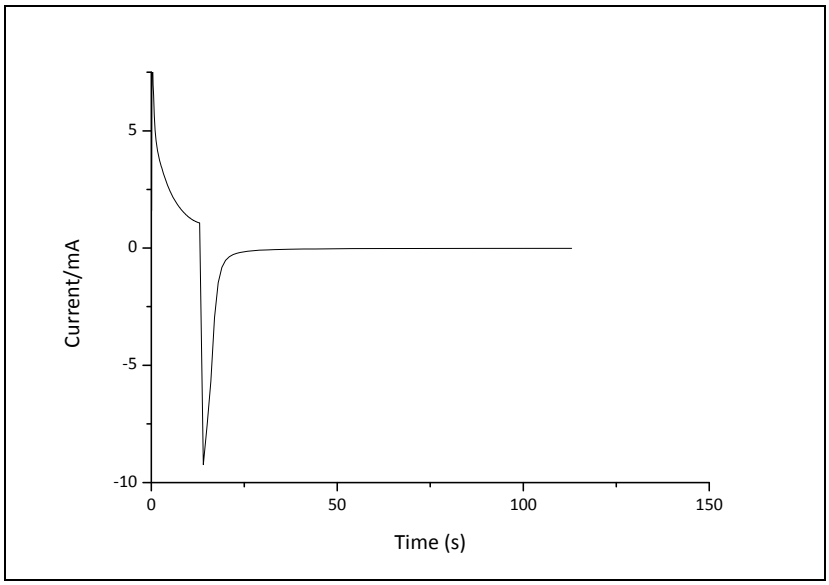

Figure 52: Chronoamperogram of the potential-pulse coating of terthiophene-OEG-COOH on a sputter-coated gold-on-glass surface. Supporting electrolyte 0.1 M TBAP in acetonitrile. Pulsed at 1.2 V for 13 ms. 6000 pulses. Stainless steel counter electrode.

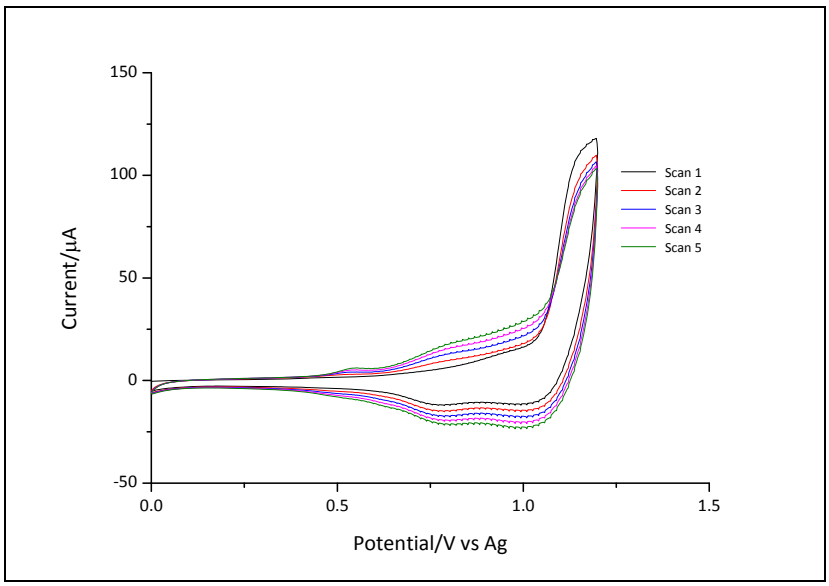

Figure 53: Post-coating cyclic voltammogram in supporting electrolyte (0.1 M TBAP in acetonitrile) of terthiophene-OEG-COOH deposited on a sputter-coated gold-on-glass surface using the potential-pulse method. Potential limits 0/+1.2 V. 5 cycles. Scan rate 100 mV/s. Stainless steel counter electrode.

5.5.7 Optimisation of Potentiodynamic Coating:

Since the potential-pulse method failed to produce a visually uniform coating, the focus returned to the potentiodynamic coating method, *i.e*. where an increasing potential is applied to the working electrode with a fixed scan speed. When the

potential reaches a pre-determined maximum the potential is reversed to complete the cycle (hence cyclic voltammetry).

The upper potential remained at 1.2 V and a scan speed of 2.5 V/s was trialed to determine the number of cycles necessary to produce a slight brown colour. A barely visible coating was noted after ten scans, and a 'slow' post-coating CV at 100 mV/s produced no further increase in colour. Twenty cycles produced the desirable light brown colour, and appeared even over the coated area. A faster scan speed (5 V/s) would require more cycles to produce the same degree of colour, and therefore allow more control over the coating thickness. Accordingly, 50 scans at 5 V/s produced a gold-on-glass surface with the desired light brown colour, and an apparently even coating. The cyclic voltammogram for coating the gold-on-glass slide is shown in Figure 54 and the post-coating cyclic voltammogram in Figure 55. The scan speed of 5 V/s was selected as a suitable scan speed, with 50 scans used to produce the thickest coating in the range to be examined.

Accordingly, four surface plasmon resonance chips prepared with 50, 10, 5 and 1 cycles respectively using a scan speed of 5 V/s. The cyclic voltammograms for the electrochemical coating of these 50, 10, 5 and 1-cycle surface plasmon resonance surfaces are shown in Figures 56, 58, 60 and 62. The corresponding post-coating cyclic voltammogram for each surface is given in Figures 57, 59, 61 and 63 respectively. The cyclic voltammogram of the background electrolyte (0.1M TBAP in acetonitrile) are shown in the Appendix.

The current increase during the oxidation scans suggests the growth of a conducting polymer. However, the subsequent post-coating cyclic voltammograms suggest that the coating prepared at higher speed may not stable be under the post-coating conditions, because the current decreases with each cycle. It is likely that the increase in scan speed has affected the quality of the film produced, because this was not observed where a slow scan speed was used to coat the surface (see Figures 47 and 48). However, using a slow scan speed to coat was thought to give films too thick to be useful in surface plasmon resonance, and so

four single-cycle surface plasmon resonance chips were prepared using the fast (5 V/s) potentiodynamic method to examine whether this coating method would still generate a thin scaffold sufficiently stable enough for use in surface plasmon resonance. The coating cyclic voltammograms for the thinner coatings (less than 50 cycles) are not inconsistent with the growth of a conducting polymer, but little information can be drawn from their corresponding post-coating cyclic voltammograms, most likely because the resulting films are very thin. They are included here for completion only.

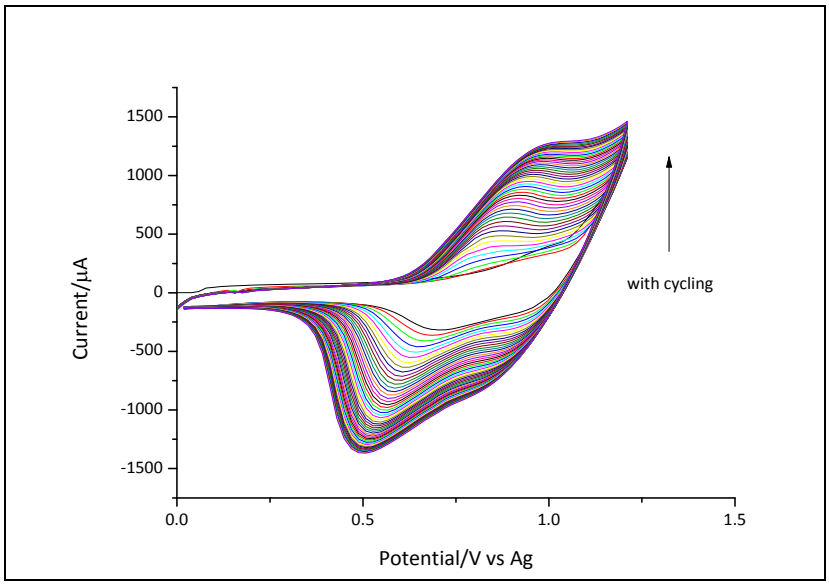

Figure 54: Cyclic voltammetric coating of terthiophene-OEG-COOH on a sputter-coated gold-on-glass surface. Supporting electrolyte 0.1 M TBAP in acetonitrile. Potential limits 0/+1.2 V. 50 cycles. Scan rate 5 V/s. Stainless steel counter electrode.

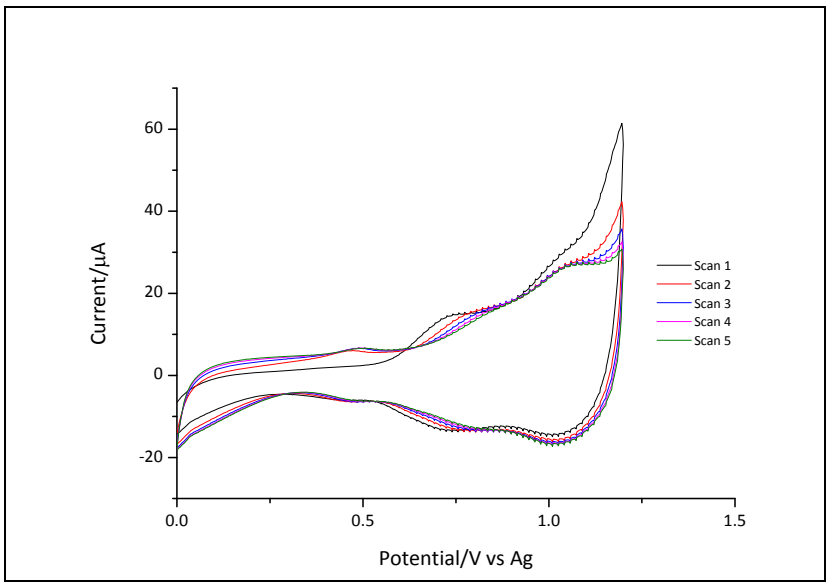

Figure 55: Post-coating cyclic voltammogram in supporting electrolyte (0.1 M TBAP in acetonitrile) of terthiophene-OEG-COOH coated on a sputter-coated gold-on-glass surface. Potential limits 0/+1.2 V. 5 cycles. Scan rate 100 mV/s. Stainless steel counter electrode.

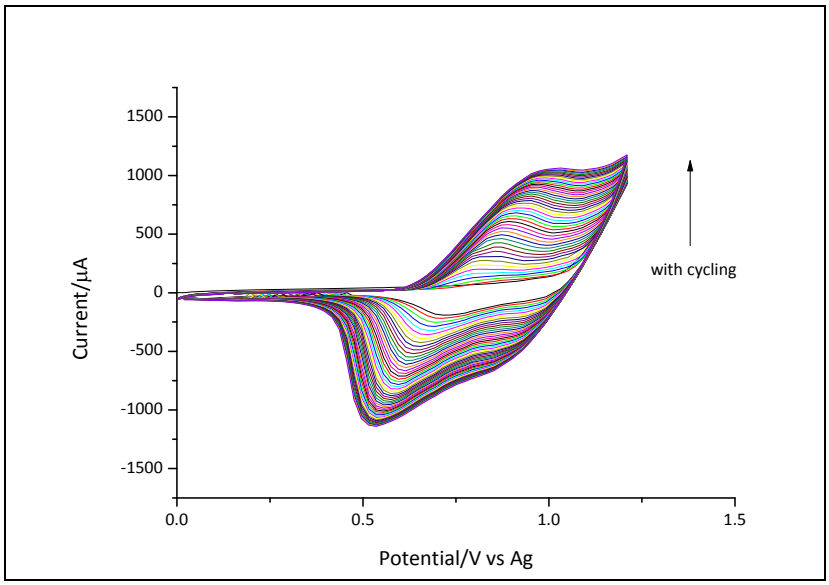

Figure 56: Cyclic voltammetric coating of terthiophene-OEG-COOH on a gold SPR chip surface. Supporting electrolyte 0.1 M TBAP in acetonitrile. Potential limits 0/+1.2 V. 50 cycles. Scan rate 5 V/s. Stainless steel counter electrode.

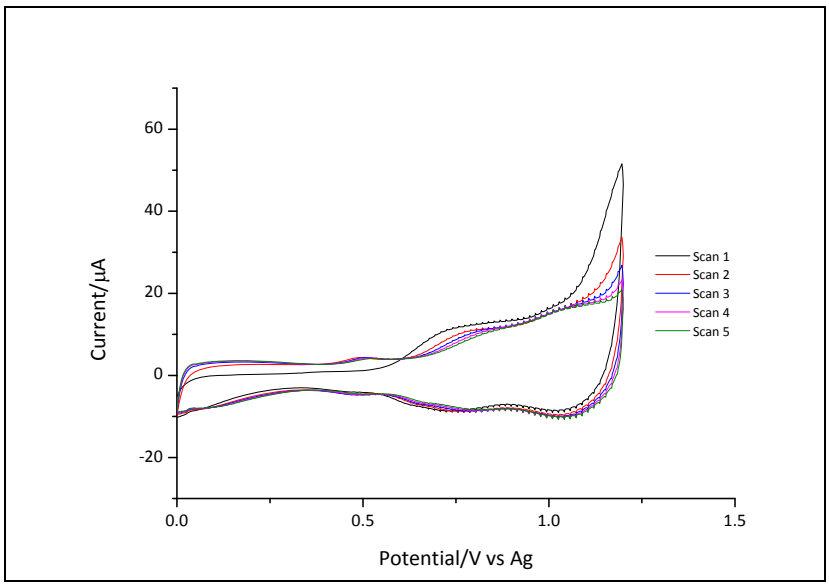

Figure 57: Post-coating cyclic voltammogram in supporting electrolyte (0.1 M TBAP in acetonitrile) of terthiophene-OEG-COOH coated on a gold SPR chip surface (50 cycles to coat). Potential limits 0/+1.2 V. 5 cycles. Scan rate 100 mV/s. Stainless steel counter electrode.

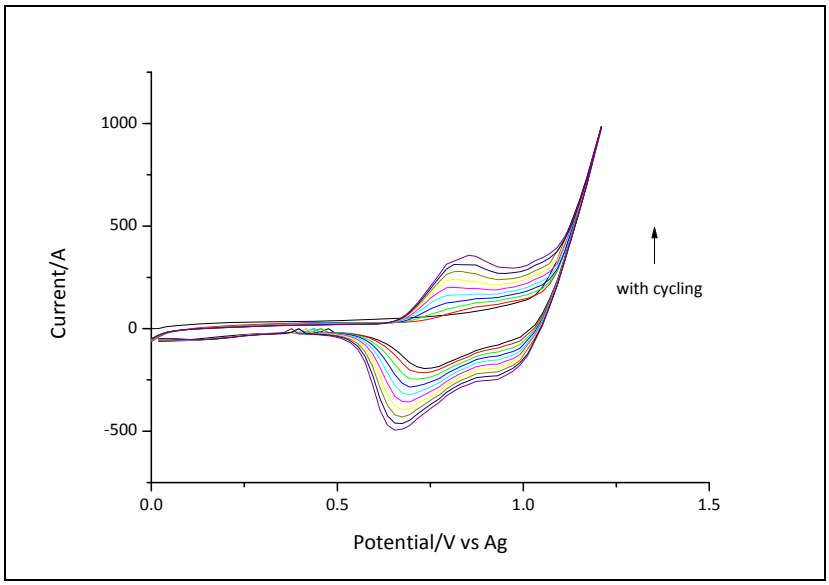

Figure 58: Cyclic voltammetric coating of terthiophene-OEG-COOH on a gold SPR chip surface. Supporting electrolyte 0.1 M TBAP in acetonitrile. Potential limits 0/+1.2 V. 10 cycles. Scan rate 5 V/s. Stainless steel counter electrode.

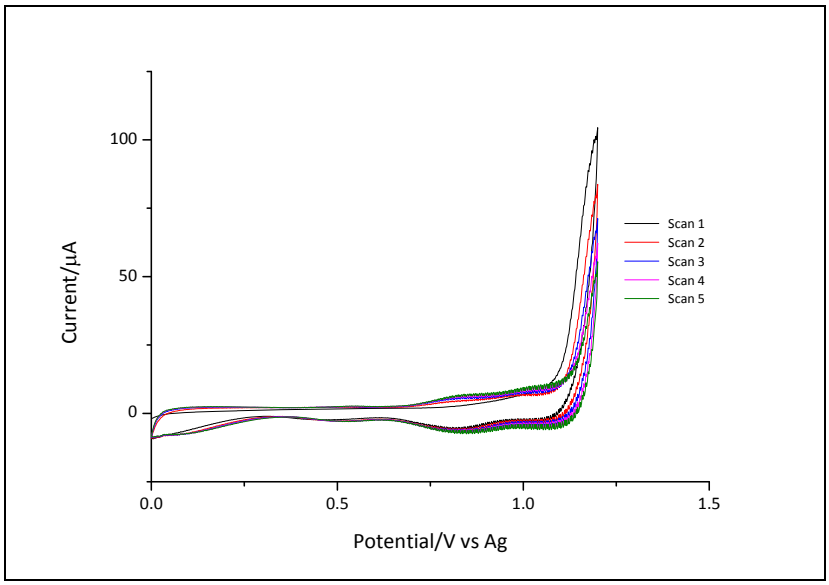

Figure 59: Post-coating cyclic voltammogram in supporting electrolyte (0.1 M TBAP in acetonitrile) of terthiophene-OEG-COOH coated on a gold SPR chip surface (10 cycles to coat). Potential limits 0/+1.2 V. 5 cycles. Scan rate 100 mV/s. Stainless steel counter electrode.

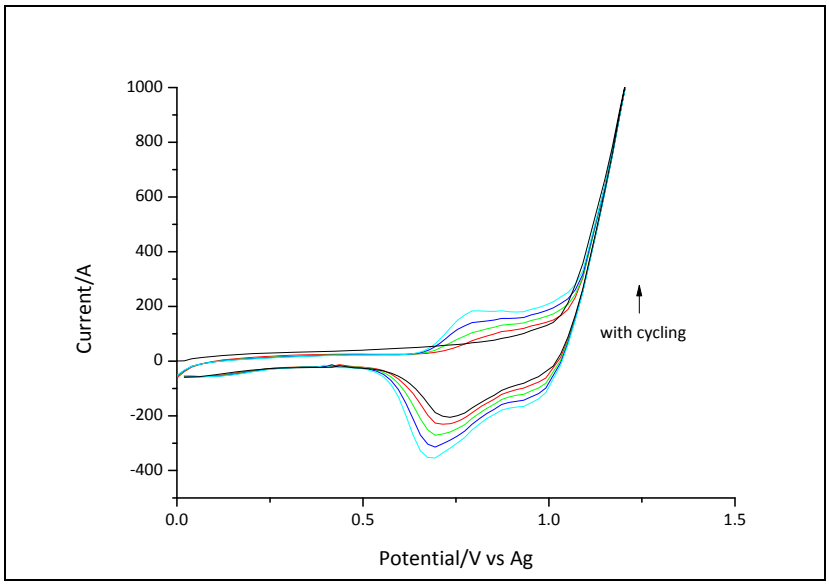

Figure 60: Cyclic voltammetric coating of terthiophene-OEG-COOH on a gold SPR chip surface. Supporting electrolyte 0.1 M TBAP in acetonitrile. Potential limits 0/+1.2 V. 5 cycles. Scan rate 5 V/s. Stainless steel counter electrode.

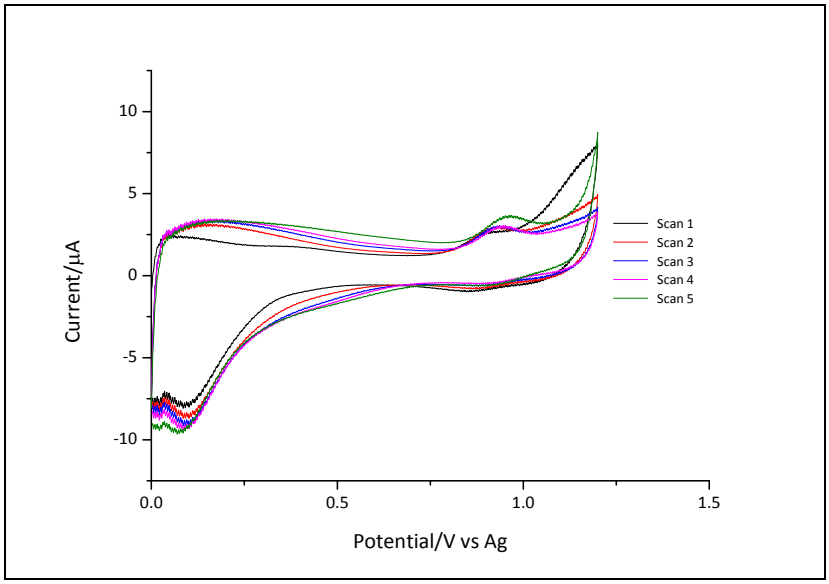

Figure 61: Post-coating cyclic voltammogram in supporting electrolyte (0.1 M TBAP in acetonitrile) of terthiophene-OEG-COOH coated on a gold SPR chip surface (5 cycles to coat). Potential limits 0/+1.2 V. 5 cycles. Scan rate 100 mV/s. Stainless steel counter electrode.

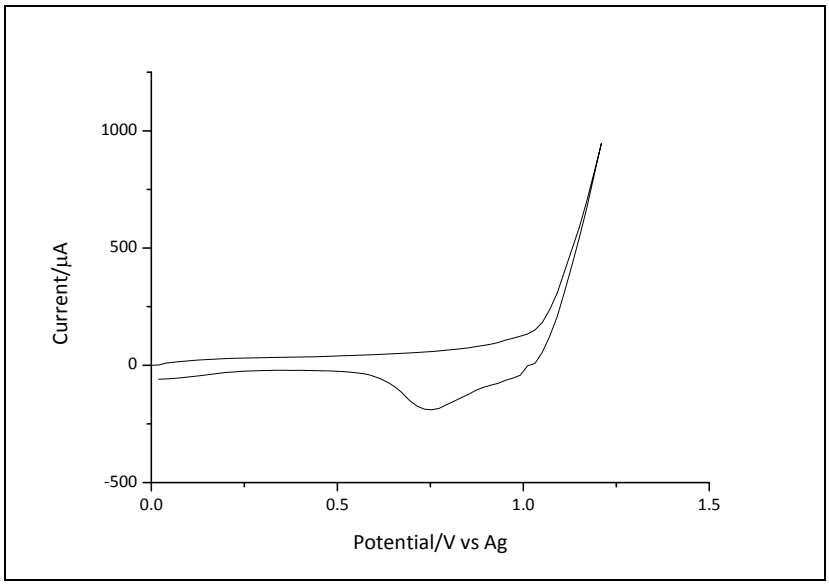

Figure 62: Cyclic voltammetric coating of terthiophene-OEG-COOH on a gold SPR chip surface. Supporting electrolyte 0.1 M TBAP in acetonitrile. Potential limits 0/+1.2 V. 1 cycle. Scan rate 5 V/s. Stainless steel counter electrode.

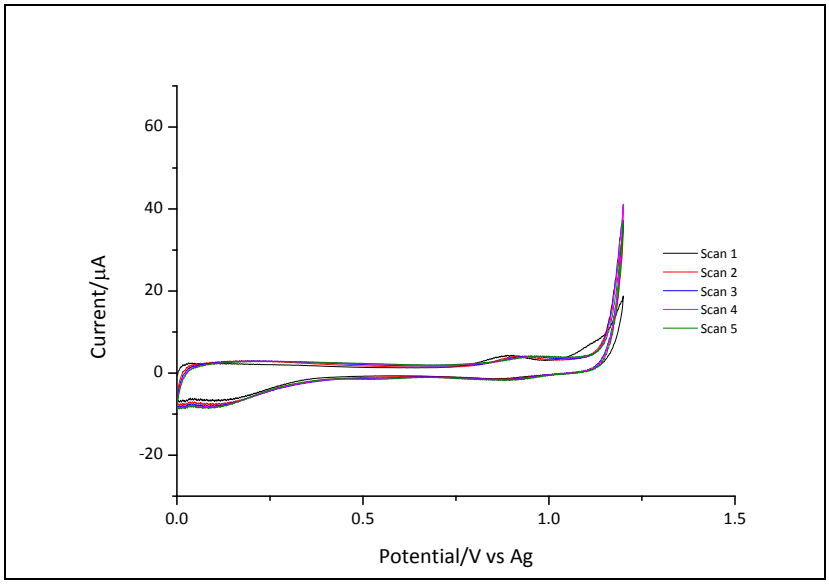

Figure 63: Post-coating cyclic voltammogram in supporting electrolyte (0.1 M TBAP in acetonitrile) of terthiophene-OEG-COOH coating on a gold SPR chip surface (1 cycle to coat). Potential limits 0/+1.2 V. 5 cycles. Scan rate 100 mV/s. Stainless steel counter electrode.

5.5.8 Surface Plasmon Resonance:

For the electrochemically coated SPR surfaces, the immobilisation of progesterone-OEG-OVA on to the flow cell of the sensor chips proceeded smoothly, but ovalbumin attachment to the reference flow cells was more difficult for the 10, 5 and 1-cycle chips, with all three unable to reach the level of the conjugate in the flow cell 2 (Table 13). The initial value (after coating) is the value in RU obtained on first docking the chip into the surface plasmon resonance instrument and immediately before immobilisation. The activation is the response obtained following the injection of the EDC/NHS coupling solution (see 2.2.1), and the final immobilisation response is that obtained following injection of progesterone-OEG-ovalbumin conjugate (flow cell 2) or ovalbumin (flow cell 1) and deactivation of remaining activated carboxyl groups on the surface. The immobilisation level is the difference between this final response, and the initial response immediately before the immobilisation step. The conditioning 'start' and 'finish' (RU) are the responses obtained before and after the ten conditioning injections made prior to antibody injections.

Table 13: Immobilisation and conditioning results for four sensor surfaces prepared by electrochemically coating 5 mM terthiophene-OEG-COOH at 5 V/s for 50, 10, 5, and 1 cycle respectively. A potentiodynamic method was used here.

	Initial (RU)	After Activation (RU)	Immobilisation Final (RU)	Immobilisation Level (RU)	Conditioning Start (RU)	Conditioning Finish (RU)	Start-Finish
EC 50 cycles							
P4-OEG-OVA (FC2)	47625	45471	52641	7283	52338	52018	-320
OVA (FC1)	47473	45643	52588	7076	52692	52953	260
EC 10 cycles							
P4-OEG-OVA (FC2)	30454	29198	35635	6501	35969	35250	-720
OVA (FC1)	26226	25754	29951	4255	29962	30026	60
EC 5 cycles							
P4-OEG-OVA (FC2)	21016	21068	25362	4359	25741	24936	-800
OVA (FC1)	20369	20570	23366	2845	23449	23227	-220
EC 1 cycles							
P4-OEG-OVA (FC2)	23847	23228	28836	5658	29304	28614	-690
OVA (FC1)	21666	21696	25328	3695	25330	25188	-140

Table 14: Antibody response and stability check results for four sensor surfaces prepared by electrochemically coating 5 mM terthiophene-OEG-COOH at 5 V/s for 50, 10, 5, and 1 cycle respectively. A potentiodynamic method was used here. Note that the difference is calculated over 7 injections, because the last three injections of ten were not collected for the 50 cycle chip.

P4-OEG-OVA (FC2) mAb (RU)						**Beg-End (RU)**	**Over 7 injections (%)**	**Over 10 injections (%)**
EC 50 cycles	77	67	69	62	59			
	58	52				**26**	**34**	
EC 10 cycles	57	57	55	51	52			
	50	49	46	45	45	**13**	**14**	**22**
EC 5 cycles	63	59	56	54	53			
	54	52	50	49	47	**16**	**17**	**25**
EC 1 cycles	61	58	52	50	50			
	50	47	45	45	42	**19**	**22**	**31**
OVA (FC1) mAb (RU)								
EC 50 cycles	26	18	22	18	17			
	17	15				**11**	**43**	
EC 10 cycles	20	20	20	17	19			
	18	18	17	17	17	**3.1**	**12**	**16**
EC 5 cycles	17	16	15	14	14			
	14	15	14	14	14	**1.9**	**11**	**16**
EC 1 cycles	12	11	10	10	10			
	11	11	11	11	9.4	**3.0**	**15**	**24**
FC(2-1) mAb (RU)								
EC 50 cycles	51	49	47	44	42			
	41	37				**15**	**29**	
EC 10 cycles	37	37	35	34	33			
	31	32	29	28	28	**9.5**	**15**	**25**
EC 5 cycles	46	43	41	40	39			
	40	37	36	35	33	**13**	**19**	**28**
EC 1 cycles	49	46	42	40	39			
	39	37	35	34	33	**16**	**24**	**32**

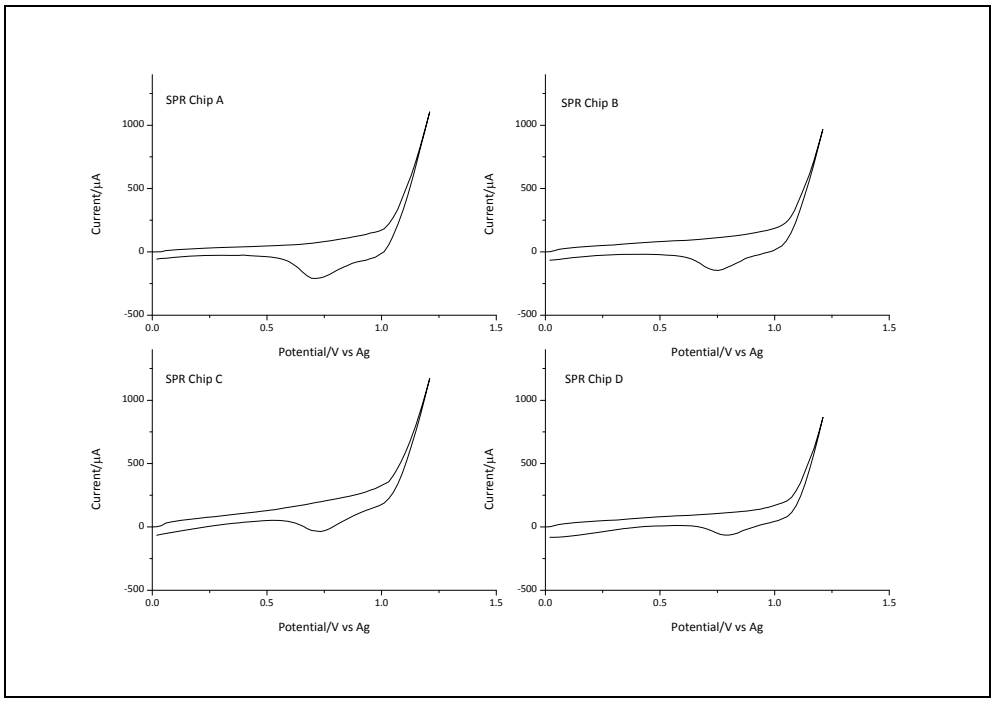

Figure 64: Cyclic voltammetric coating of terthiophene-OEG-COOH on gold SPR chip surface (Chips A-D). Supporting electrolyte 0.1 M TBAP in acetonitrile. Potential limits 0/+1.2 V. 1 cycle. Scan rate 5 V/s. Stainless steel counter electrode.

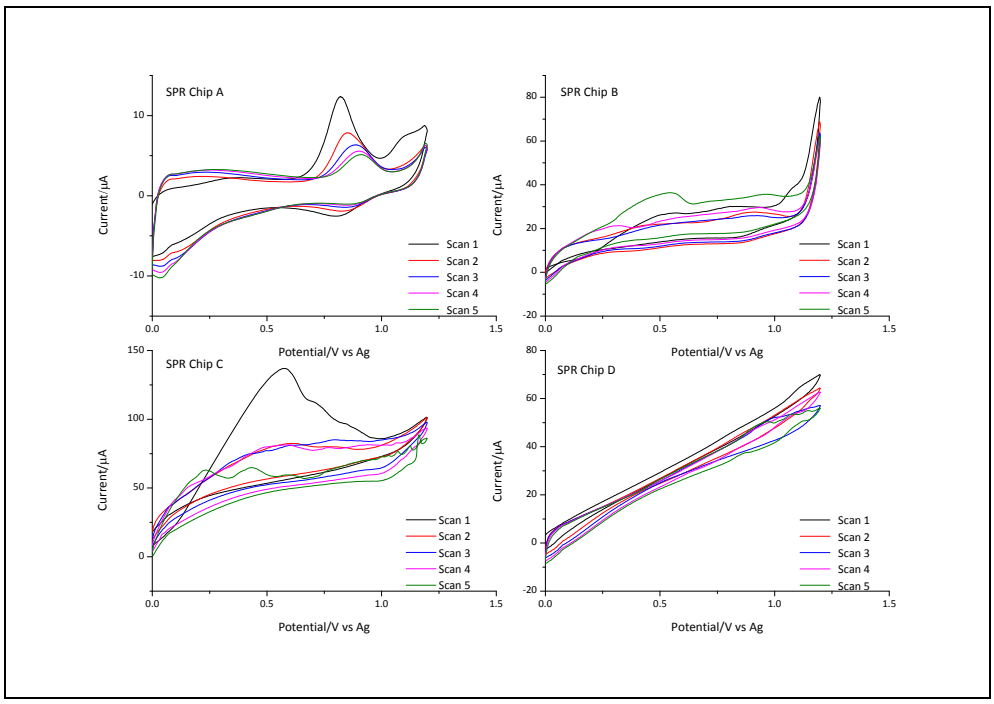

Figure 65: Post-coating cyclic voltammogram in supporting electrolyte (0.1 M TBAP in acetonitrile) of terthiophene-OEG-COOH coated on gold SPR chip surface (Chips A-D) (1 cycle to coat). Potential limits 0/+1.2 V. 5 cycles. Scan rate 100 mV/s. Stainless steel counter electrode.

Table 15: Immobilisation and conditioning results for three sensor surfaces prepared by electrochemically coating 5 mM terthiophene-OEG-COOH (1 cycle at 5 V/s) and immobilisation with progesterone-OEG-OVA conjugate in flow cell 2, and with ovalbumin in the reference flow cell 1. The cyclic voltammetry (potentiodynamic) method for coating was used here.

	After Coating (RU)	After Activation (RU)	Immobilisation Final (RU)	Immobilisation Level (RU)	Conditioning: Start (RU)	Conditioning: Finish (RU)	Start-Finish (RU)	Immobilisation level after Conditioning (RU)
EC 1 cycle								
Chip A								
P4-OEG-OVA (FC2)	20906	21084	25143	4074	25055	24518	-540	3536
OVA (FC1)	19784	20150	22744	2598	22843	22700	-140	2455
EC 1 cycle								
Chip B								
P4-OEG-OVA (FC2)	28847	28069	33822	5769	33995	33259	-740	5033
OVA (FC1)	26338	25722	29950	4240	30148	30130	-17	4223
EC 1 cycle								
Chip C								
P4-OEG-OVA (FC2)	21731	21907	26206	4311	26342	25859	-480	3828
OVA (FC1)	21071	21354	24326	2986	24642	24460	-180	2804

Table 16: Antibody response and stability check results for three SPR sensor surfaces prepared with electrochemically coated terthiophene-PEG-COOH (1 cycle at 5 V/s) and immobilised with progesterone-PEG-OVA conjugate in flow cell 2, and with ovalbumin in the reference flow cell 1. The cyclic voltammetry (potentiodynamic) method for coating was used here. The difference between first and last antibody injection is presented as absolute value (Beg-End RU), and as a percentage of the initial response.

P4-OEG-OVA (FC2) mAb RU	Response (RU)					Beg-End (RU)	%
EC 1 cycle Chip A							
	60	61	59	59	58		
	57	55	54	53	52	8	13
EC 1 cycle Chip B							
	59	57	55	54	53		
	52	50	49	48	47	13	21
EC 1 cycle Chip C							
	79	67	66	64	64		
	63	61	60	59	57	18	27
OVA (FC1) mAb RU							
EC 1 cycle Chip A							
	17	19	20	19	19		
	19	18	18	17	17	-0.2	-1
EC 1 cycle Chip B							
	12	12	11	11	11		
	10	9.7	9.7	9.6	9.3	3	24
EC 1 cycle Chip C							
	34	21	20	19	19		
	18	17	17	16	16	17	53
FC2-1 mAb RU							
EC 1 cycle Chip A							
	43	41	40	40	39		
	38	37	36	36	35	8	19
EC 1 cycle Chip B							
	47	46	44	43	42		
	41	40	39	38	38	10	20
EC 1 cycle Chip C							
	45	47	46	45	45		
	46	44	43	42	41	4	9

Three of the four 1-cycle chips were immobilised with progesterone-OEG-ovalbumin and ovalbumin, as for the 50-cycle, 10-cycle, 5-cycle and 1-cycle chips prepared earlier, using identical pulse length and flow rates, to allow a direct comparison to be made between the prepared surfaces (see Table 15). Note that there is some variation between the three surfaces; chip B in particular appears to have a heavier coating (note the higher initial RU value, immediately after deposition). This chip also has a higher final immobilisation level for both the progesterone-OEG-OVA conjugate and ovalbumin flow cells, but the values for all three chips are in line with the 1-cycle chip prepared earlier.

Table 16 gives the results of the stability check carried out using two series of five antibody injections with blank injections between each series. Again, little can be concluded in that none of the three performed better than the other. The antibody binding response (binding curves) (Figure 66) for chips B and C were similar, despite Chip B's relatively higher immobilisation). (The binding curve results for Chip A are not discussed here because the surface was incompletely regenerated between injections).

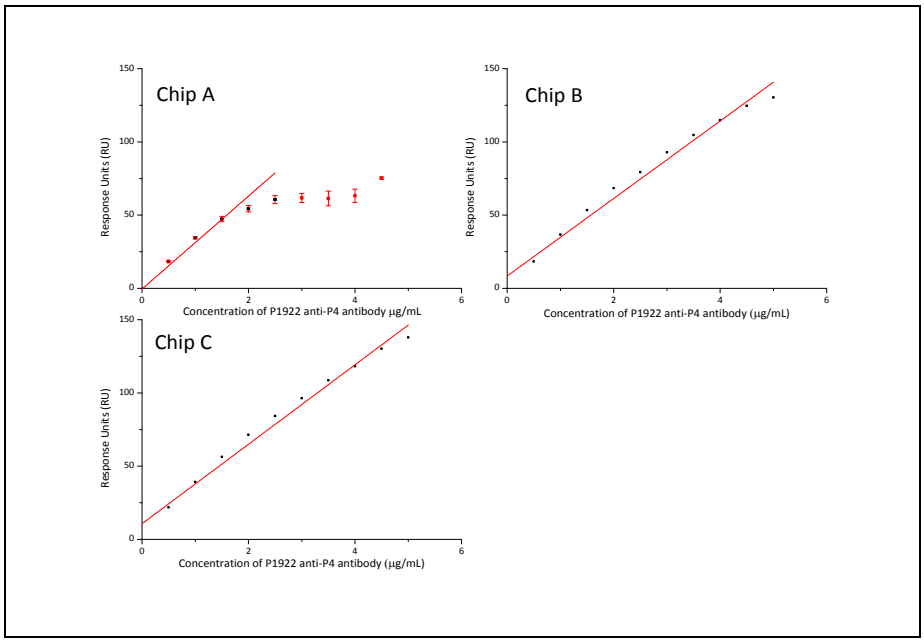

Figure 66: Antibody response (binding curves) for three electrochemically coated terthiophene-OEG-COOH SPR sensor surfaces immobilised with progesterone-OEG-OVA. All three chips A, B, and C were electrochemically coated (1 cycle at 5 V/s). Note that for Chip A, surface regeneration was incomplete before subsequent injections of antibody, resulting in curvature at higher antibody concentrations.

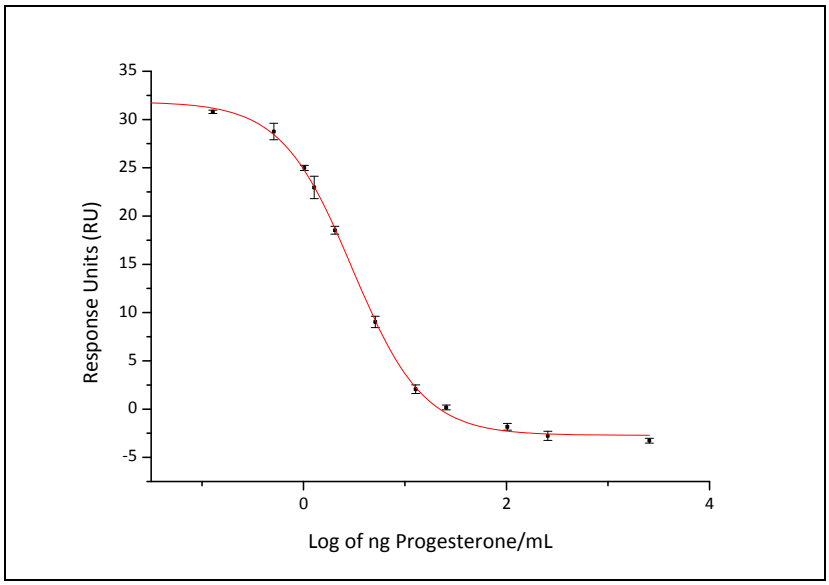

Figure 67: Inhibition assay standard curve for progesterone on an electrochemically coated terthiophene-OEG-COOH sensor surface immobilised with progesterone-OEG-OVA. Chip C (1 cycle at 5V/S) was used for this assay. Error bars shown on the graph represent one standard deviation (SD) of the mean.

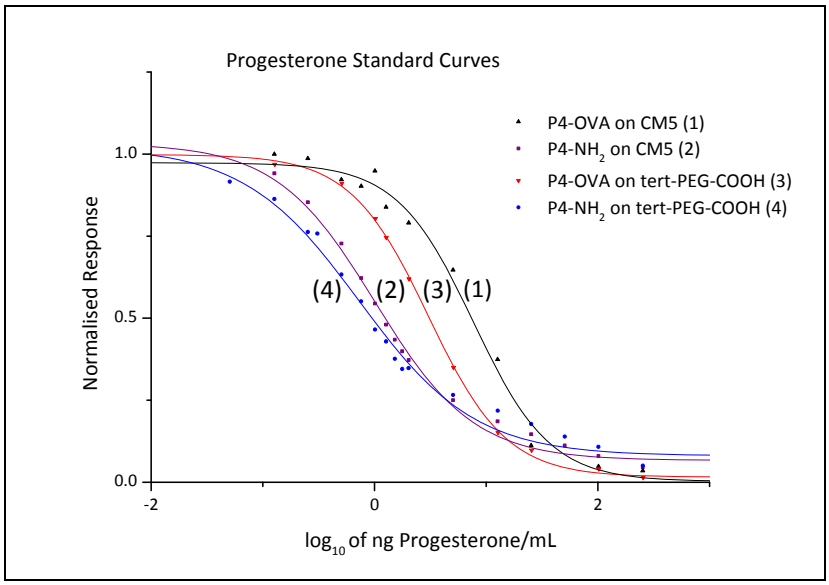

Figure 68: Inhibition assay standard curves for progesterone on CM5 and terthiophene-OEG-COOH sensor surfaces immobilised with progesterone-OEG-NH_2 and progesterone-OEG-OVA.

Table 17: Limits of detection (LOD), IC_{50} values and antibody response values (in RU.mL/μg) for CM5 and terthiophene-OEG-COOH sensor surfaces immobilised with progesterone-OEG-NH_2 and progesterone-OEG-OVA. [a] denotes that the functionalised terthiophene scaffold was prepared using the immersion method, [b] the scaffold was an electrochemically deposited layer of functionalised terthiophene.

Surface	Primary antibody concentration (μg/mL)	LOD (pg/mL)	IC_{50}(pg/mL)	RU.mL/μg
P4-OEG-OVA on CM5 (1)	10.0	1400 ± 280	7700 ± 800	11 ± 0.3
P4-OEG-NH_2 on CM5 (2)	0.25	100 ± 20	1000 ± 90	430 ± 3
P4-OEG-OVA on tert[a] (3)				29 ± 1
P4-OEG-OVA on tert[b] (3) Chip A				Incomplete regeneration
P4-OEG-OVA on tert[b] (3) Chip B				27 ± 1
P4-OEG-OVA on tert[b] (3) Chip C	2.5	520 ± 30	3000 ± 80	27 ± 1
P4-OEG-NH_2 on tert[a] (4)	0.25	60 ± 20	750 ± 100	470 ± 5

Table 18: Antibody response and stability check results for SPR sensor surfaces prepared by the immersion method and by electrochemically depositing terthiophene-OEG-COOH (1 cycle at 5 V/s). Both surfaces were immobilised with progesterone-OEG-OVA conjugate in flow cell 2, and with ovalbumin in the reference flow cell 1. The difference between the first and last antibody injection is presented as absolute value (Beg-End RU), and as a percentage of the initial response.

[#]Denotes that the first antibody injection was omitted in each case.

	Response (RU)					Beg-End (RU)	%	Beg-End (RU)[#]	%[#]
P4-OEG-OVA (FC2)									
Immersion Method	47	46	46	46	46				
	46	44	44	43	43				
	43	42				5	11	4	9
Electrochemical Method	51	49	49	49	48				
	48	47	46	46	46				
	45	44				7	13	5	10
OVA (FC1)									
Immersion Method	18	18	18	18	18				
	18	17	17	17	17	2	12	2	10
	17	16							
Electrochemical Method	23	17	16	16	16				
	16	15	15	15	13				
	14	14				9	40	3	17
FC(2-1)									
Immersion Method	28	28	28	28	28				
	28	27	27	26	26				
	26	26				3	10	3	9
Electrochemical Method	28	32	33	32	32				
	33	32	32	31	32				
	31	30				-2	-8	2	6

Atomic Force Microscopy (AFM): (Single-Cycle Chip D)

The surface of the fourth electrochemically polymerised surface plasmon resonance chip was examined using atomic force microscopy at the border between bare gold and the coated surface (Figure 69). The thickness of the surface taken at a cross section was estimated to be 10 to 12 nm. The area of coated surface and bare gold were also examined and found to be uniform (data not shown).

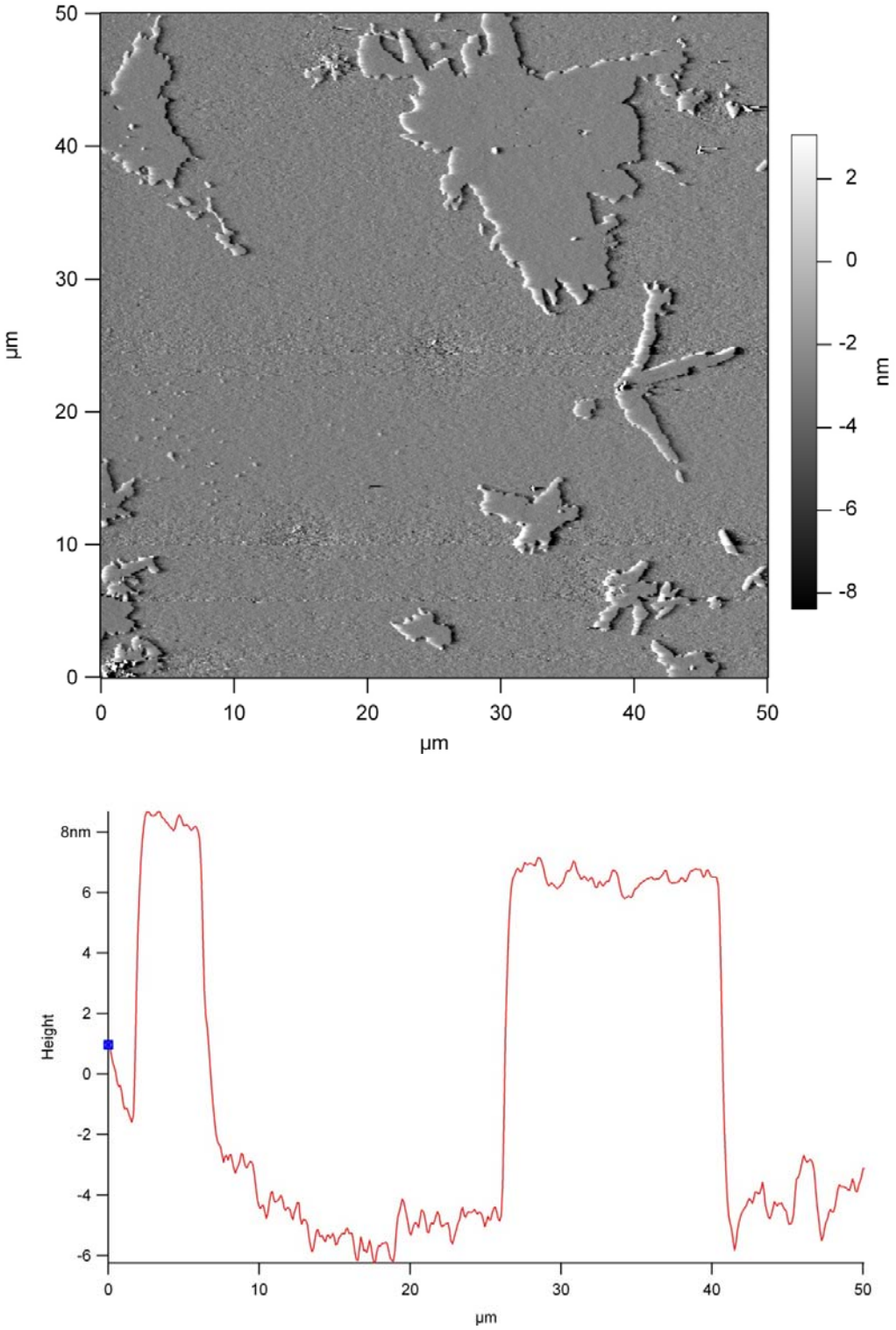

Figure 69: AFM (top) and the height image of a cross section (below) of an area of gold SPR chip surface taken at the border between bare gold and the electrochemically coated surface.

The results of the comparison between the immersion method and electrochemical deposition method for coating the surface plasmon resonance chip are given in Table 18.

The first injection for the electrochemical coating was omitted as an outlier, and the two columns on the far right were considered. Little difference between the two surfaces was apparent in terms of stability, when the responses in each flow cell were examined. While the electrochemical method might at first glance appear to produce a slightly more stable surface when the relative response (flow cell 2 – flow cell 1) is considered, the difference is too small to be conclusive. The results of the antibody binding curves for the electrochemically coated functionalised terthiophene surfaces compared to those prepared using the immersion method are very similar *i.e*. slopes of 27 for electrochemically coated single-cycle surfaces B and C compared to 29 for a surface prepared using the immersion method (see Table 17). Since the antibody signal determines the amount of antibody used in the inhibition assay, the chips prepared using either the immersion method or the electrochemical coating method would likely give similar sensitivities.

The immersion method appears to produce a scaffold with adequate stability for use in surface plasmon resonance. Electrochemistry or treatment with an oxidant such as ferric chloride may provide an improvement in stability of the surface, but the conditions used here suggest that it may not be necessary.

The standard curve of the inhibition assay for progesterone as the OEG-ovalbumin conjugate on the functionalised terthiophene surface is shown in Figure 67. The inhibition assay results carried out on the four surfaces are given in Table 17 with the calibration curves shown in Figure 68. The antibody binding response (given as the slope of the binding curve) determines the amount of antibody used in the inhibition assay, so for those surfaces with a higher antibody binding response (surfaces 2 and 4) a much lower concentration of antibody can be used. For both un-conjugated progesterone surfaces, a relatively low concentration of antibody was used (0.25 μg/mL) in the inhibition assay. This provides the potential of a highly

sensitive assay which uses much less expensive antibody, with a limit of detection in the pg/mL range.

The effect of removing the ovalbumin from the sensing element gave a considerable improvement in the antibody binding signal. If we consider only the behaviour on the CM5 scaffold, (surfaces 1 and 2), the improvement in antibody binding is marked, 11 for the conjugate compared to 430 for the protein-free progesterone, a forty-fold increase. Even allowing for the modest hapten to ovalbumin ratio for the conjugate used here, the increase in signal is very high. Ovalbumin is a globular protein with a radius of approximately 3 nm in an aqueous medium [159], which is not large in surface plasmon resonance terms. However, it is known to partially denature and aggregate under certain conditions [160], resulting in an increase in size. It may be that factors other than the protein's size can affect the behaviour of a protein-conjugated steroid such as progesterone in surface plasmon resonance.

The advantages of immobilising a protein conjugate rather than a small molecule analyte relate to the ease of observing the covalent attachment step in the instrument, given the huge molecular weight increase obtained following conjugation and the reducing the effect of steric crowding by spacing out the immobilised binding partner, but this work suggests that there may be a cost in loss of sensitivity.

5.6 Summary

The functionalised terthiophene surface appeared to offer a viable alternative to dextran scaffolds. The surface could be generated quickly, in a matter of seconds using the electrochemical method, and could be stripped and re-used without difficulty [161] providing a more cost-effective sensor surface. The synthesis of the amino analogue of the carboxyl-functionalised terthiophene was straight-forward, offering the versatility of other coupling chemistries.

The use of ovalbumin in the progesterone system appeared to offer no advantage in sensitivity terms. It is difficult to make exact quantitative comparisons between the progesterone-oligo(ethylene glycol)-NH_2 and its ovalbumin conjugate counterpart due to variations introduced during the conjugation and immobilisation steps, nevertheless the size of the antibody-binding response for the protein-free non-conjugated progesterone sensor surface was higher, (430 *vs* 11), and the limit of detection was lower (1000 pg/mL) (Table 17). The hapten ratio of progesterone to ovalbumin, *i.e.*, the progesterone bound to ovalbumin in the conjugate used for the sensing element was modest, and it is likely that some non-conjugated ovalbumin remained. This ovalbumin would bind to the surface, without providing a binding partner for the antibody. The modest hapten ratio would not, however, account for the remarkable difference in binding response between the conjugated and non-conjugated surfaces. The reasons for this may lie with the behaviour of the protein on the functionalised terthiophene surface. If the scaffold covered the sensor surface incompletely and bare gold patches remained, the ovalbumin might have denatured to some degree.

The results of the functionalised terthiophene surface compared to the commercially available carboxymethylated dextran (CM5) surface were unexpected. The surface with progesterone-oligo(ethylene glycol)-amine on the functionalised terthiophene scaffold and the surface with progesterone-oligo(ethylene glycol)-amine on the commercial dextran surface showed binding curve with similar slopes, (430 on commercial dextran CM5, 470 on functionalised terthiophene), with little difference in the limits of detection. The dextran scaffold is known to be around 100 nm thick, and the terthiophene scaffold was approximately 10 nm thick at the border region. The expectation was that a significant improvement in the sensitivity would be seen with the terthiophene surface. The removal of the ovalbumin from the sensing element provided the most striking enhancement in sensitivity. This is an interesting result, which suggests that elements other than scaffold thickness impact markedly on sensitivity in surface plasmon resonance assays. It should also be noted that the thinner functionalised

terthiophene layer would have a more limited binding capacity than a matrix such as the carboxymethylated dextran in a CM5 surface. This would be expected to offset at least some of the increased signal strength from a binding event occurring close to the sensor surface. The performance of the water-swollen hydrated dextran surface relies on the binding interaction occurring within a more native environment than would occur on a metal surface, and on the increase in binding capacity provided by a larger number of coupling sites than would be available on a bare surface [162, 163]. The results of the progesterone-OEG-ovalbumin conjugate on the commercial dextran CM5 sensor surface compared with the functionalised terthiophene would indicate that the carboxymethyldextran's environment compensates to a large degree for the loss in sensitivity due to binding interactions occurring further away from the surface.

Given the promising results for the progesterone assay where the un-conjugated sensing element produced a more sensitive method, it would be valuable to consider the behaviour of the estrone derivatives without protein conjugation. An improvement on the already low sensitivity might be possible, allowing even lower limits of detection to be obtained. This would also allow the effects of the linkers on binding response to be investigated without the complication of protein conjugation.

The use of a protein-conjugated binding partner on the sensor surface was found to offer inferior sensitivity in the progesterone system, suggesting that it may be possible to improve the sensitivity of other small-molecule surface plasmon resonance assays by attaching the binding partner to the sensor surface without first conjugating it to a protein. The foundation has been laid for the development of a generic surface plasmon resonance scaffold to which a binding partner can be attached, forming a biosensor. The scaffold can be easily generated and removed after use.

Chapter 6

Conclusions

Two highly sensitive surface plasmon resonance methods for the detection of toxins have been developed, which could potentially be applied to toxin detection in the field by using portable instruments. Both assays are sufficiently sensitive that pre-concentration of the samples is unnecessary. The strategies used in the detection of the estrone glucuronide and domoic acid could be readily exploited for the measurement of other micro-pollutants in the aquatic environment.

The use of a linker between the sensing surface and the surface bound binding partner did not improve the sensitivity of the estrone glucuronide assay because introduction of the linker made formation of the sensing surface more difficult. For the determination of domoic acid, the linker did not afford any sensitivity improvement. The sensitivity of both assays was enhanced however, by signal amplification using secondary antibodies and gold nanoparticles.

The success of the assays developed here is dependent upon their application to a portable format to allow use in the field. A portable SPR instrument would be suitable, or alternatively a lateral flow immunoassay developed with the binding system used in the SPR assay would provide a low-cost alternative.

Analysis of complex mixtures of compounds which have the same mode of action, but varying degrees of activity is challenging with antibody binding assays, because antibodies do not respond to the analytes in a manner which reflects the overall potency of the analyte. In this case, the use of an analyte and its receptor as the binding pair can offer a better predictor of activity *in vivo*, and would appear to be desirable *e.g*. toxin analysis, using surface plasmon resonance detection. This was not explored in the studies discussed here, but would be valuable future work. The monitoring of analyte and receptor binding could allow SPR to compete with

chromatographic methods which have superior sensitivity, but can be cumbersome when predicting total toxic potency of a toxin mixture.

SPR techniques which employ a sensing element other than an antibody show much promise. Aptamers (as discussed in Chapter 2) are more stable than antibodies, allowing for the production of a robust sensor surface. Their smaller size relative to antibodies does provide challenges in SPR where their smaller mass is a disadvantage, but they retain the high affinity and specificity of antibodies, with a higher degree of stability. SPR sensing surfaces produced by creating molecularly imprinted polymers which use the analyte as a template and form a tailor-made cavity have been described as an alternative to antibodies [123] and as 'artificial receptors' [124]. These surfaces can offer improved stability when compared to a sensor generated by attaching an antibody to the surface, and could potentially be more versatile and cost-effective than assay which relies on an antibody-antigen binding pair. The challenges for these techniques when applied to the analysis of small molecules remain.

The functionalised terthiophene surface developed here appears to offer a viable alternative to dextran scaffolds, and the capacity for re-using the surfaces is appealing in its cost-effectiveness. The surface could be generated quickly, in a matter of seconds using the electrochemical method, and could be stripped and re-used without difficulty.

The challenge for surface plasmon resonance in the future relies on the development of low cost portable units capable of high sample throughput. Widening the scope of SPR scaffolds which are commercially available would exploit the technique more fully, by allowing application to a wider range of analytes.

Appendix

The syntheses and characterisation of the compounds described were carried out at Massey University by Dr Krishanthi Jayasundera. Compound (**25**) was also used in the work of Yu Ting Hsu.

All reactions were conducted under a dry nitrogen atmosphere unless otherwise stated. Reagents were obtained from commercial suppliers and used directly, with the exception of toluene which was dried over sodium and distilled prior to use. Flash column chromatography was performed using Scharlau 60 silica gel (230-400 mesh) with the indicated solvents. Thin layer chromatography was carried out on pre-coated silica plates (Merck Kieselgel 60 F_{254}) and compounds were visualised by UV fluorescence or by staining with 10 % v/v concentrated sulphuric acid in methanol and heating. ^{1}H and ^{13}C NMR spectra were obtained using either Bruker Avance 400 or 500 MHz spectrometer. Chemical shifts for spectra in $CDCl_3$ are given in parts per million (ppm) down-field from tetramethylsilane as internal standard (^{1}H) or relative to residual solvent (^{13}C). High resolution mass spectra were recorded using VG7070 mass spectrometer operating at normal accelerating voltage of 70 eV (University of Auckland).

Synthesis of Estrone Derivatives

Synthesis of the estrone derivative E1C3, C5 (**9**) was carried out from commercially available estrone (**1**) according to Scheme 4. The short linker 7-aminoheptanoic acid (**26**) was used to prepare this material. The same conditions were used to generate compounds E1G, OEG (**10**) and E1C3, OEG (**11**) using the longer linker 1-amino-15-oxo- 4,7,10-trioxa-14-azaoctadecan-18-oic acid (**27**) in place of 7-aminoheptanoic acid (**26**) (Scheme 5).

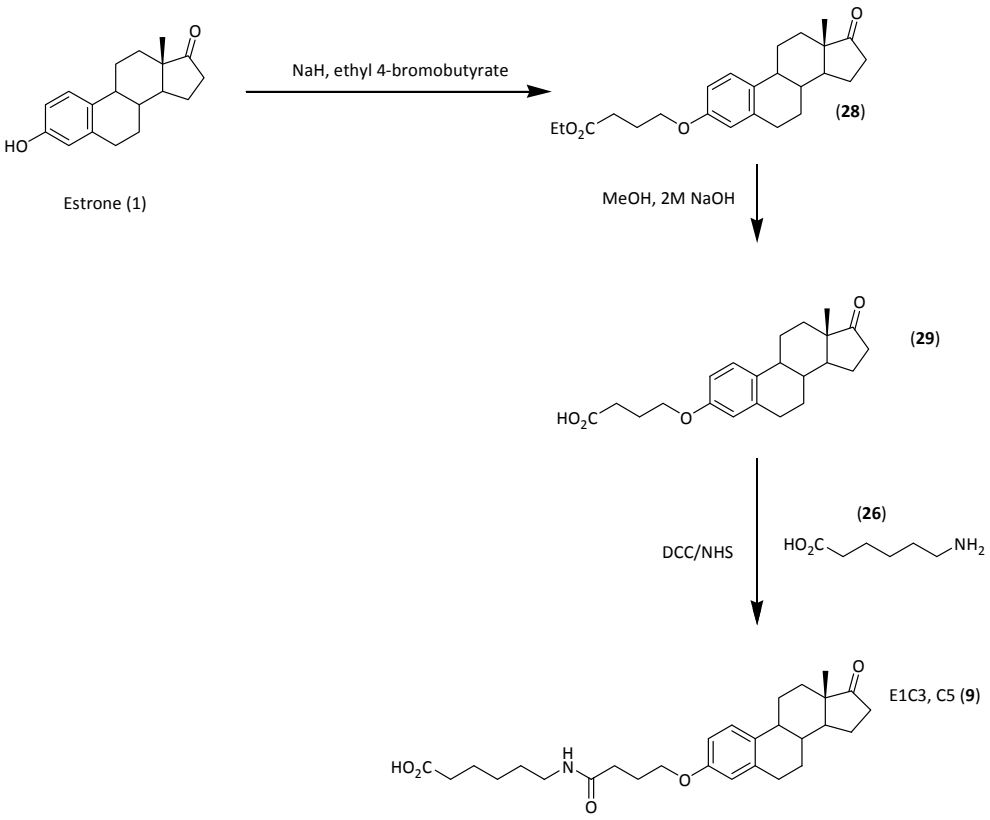

Scheme 4: Synthesis of estrone derivative E1C3, C5 from estrone.

1,3,5(10)-Estratrien-3-(hydroxyl propianoic acid ethyl ester)-17 one (28)

To a solution of estrone (**1**) (270 mg, 1.0 mmol, 1.0 equiv.) dissolved in DMF (3 mL) sodium hydride (40 mg, 1.0 mmol, 1.0 equiv.) was added and the resulting solution stirred for rt for 5 min under an atmosphere of nitrogen. A solution of ethyl 4-bromobutyrate (215 mg, 1.07 mmol, 1.07 equiv.) was added to the reaction mixture. The reaction mixture was stirred at rt for 3 h. The reaction mixture was diluted with ethyl acetate (20 mL) and layers were separated. The organic phase was washed with water (20 mL) and dried over $MgSO_4$, filtered and concentrated. The residue was purified by flash chromatography, eluting with Hex/EtOAc (4/1) to give the ester derivative (**28**) as a colourless solid (286 mg, 74 %).

^{1}H NMR (500 MHz, $CDCl_3$) δ 0.91 (s, 3H), 1.26 (t, *J* = 7.2 Hz, 3H), 1.24-1.38 (m, 6H), 1.92-2.55 (m, 11H), 2.85-2.95 (m, 2H), 3.98 (t, *J* = 5.9 Hz, 2H), 4.15 (q, *J* = 6.7 Hz, 2H), 6.64 (m, 1H), 6.70 (d, *J* = 9.2 Hz, 1H), (7.20 (d, *J* = 8.8 Hz, 1H).

^{13}C NMR (125 MHz, $CDCl_3$): δ 14.01, 14.4, 21.8, 24.9, 26.1, 26.8, 30.0, 31.0, 31.8, 36.1, 38.6, 44.2, 48.2, 50.6, 60.6, 66.9, 112.4, 114.7, 126.6, 132.3, 138.0, 157.1, 173.5.

HRMS (EI): MH+, found 384.23006. $C_{24}H_{32}O_4$ requires 384.22938.

1,3,5(10)-Estratrien-3-(hydroxyl propianoic acid)-17 one (29)

A solution of the above ester derivative (**28**) (250 mg, 0.65 mmol, 1.0 equiv.) in methanol (5 mL) and 2 M NaOH (2 mL) was stirred at rt for 3h. The mixture was concentrated to remove the methanol, diluted with water (10 mL) neutralized with dil. HCl, and extracted with ethyl acetate (2 x 20 mL). The combined organic extracts were washed with water (20 mL), dried over $MgSO_4$, filtered, and concentrated to give acid derivative (**29**) as a colorless solid (208 mg, 90 %). This crude product was used without further purification.

^{1}H NMR (500 MHz, $CDCl_3$) δ 0.93 (s, 3H), 1.42-1.69 (m, 6H), 1.94-2.20 (m, 6H), 2.24-2.31 (m, 1H), 2.39-2.44 (m, 1H), 2.53 (dd, *J* = 8.6, 18.9 Hz, 1H), 2.61 (t, *J* = 7.2 Hz, 2H), 2.89-2.91 (m, 2H), 4.02 (t, *J* = 6.1 Hz, 2H), 6.66 (d, *J* = 2.9 Hz, 1H), 6.73 (dd, *J* = 2.9, 8.5 Hz, 1H), 7.21 (d, *J* = 8.5 Hz, 1H).

^{13}C NMR (125 MHz, $CDCl_3$): δ 13.9, 21.6, 24.4, 25.9, 26.5, 29.6, 30.4, 31.6, 35.9, 38.4, 44.0, 48.0, 50.4, 66.5, 112.1, 114.6, 126.4, 132.3, 137.8, 156.8, 178.

E1C3, C5 (9)

A solution of DCC (137 mg, 0.66 mmol, 1.3 equiv.), followed by NHS (321 mg, 1.5 mmol, 3.0 equiv.) in DMF (1.5 mL) was added drop-wise to a stirred solution of 1,3,5(10)-estratrien-3-(hydroxyl propianoic acid)-17 one (**29**) (0.5 mmol, 1.0 equiv.) in DMF (3 mL) at rt under an atmosphere of nitrogen. The mixture was stirred for 3 h. The temperature was decreased to 0^{o}C and an aqueous solution of 7-aminoheptanoic acid (**26**) (2.5 mmol, 5 equiv.) was added followed by triethylamine (50 mL). The temperature was gradually warmed to rt and stirred for 12 h. After the addition of water (50 mL) the reaction mixture extracted with DCM (3 x 20 mL).

After removing DCM from aqueous phase, it was passed through Amberlite™ adsorbant resin XAD-2 ™ and eluted with MeOH/water 1/1. Following evaporation of the solvent, the residue was purified by column chromatography to afford the desired product (**9**) as a colourless solid.

^{1}H NMR (500 MHz, $CDCl_3$) δ 0.93 (s, 3H), 1.25-1.68 (m, 12 H), 1.93-1.2.42 (m, 12 H), 2.52 (dd, *J* = 2.5, 8.8 Hz, 1H), 2.87-2.93 (m, 2H), 3.25 (t, *J* = 6.5 Hz, 2H), 3.98 (t, *J* = 5.8 Hz, 1H), 4.50 (br s, 1H), 5.80 (br s, 1H), 6.65 (d, *J* = 3.5 Hz, 1H), 6.70 (dd, *J* = 2.4, 8.8 Hz, 1H), 7.20 (d, *J* = 8.8 Hz, 1H).

^{13}C NMR (125 MHz, $CDCl_3$): δ 13.9, 21.7, 25.4, 26.0, 26.3, 26.6, 29.2, 29.7, 31.6, 33.1, 35.9, 38.4, 39.3, 44.0, 48.0, 50.4, 66.9, 112.2, 114.5, 126.4, 137.9, 156.7, 161.4.

HRMS (EI): MH+, found 470.29032. $C_{28}H_{40}NO_5$ requires 470.29065.

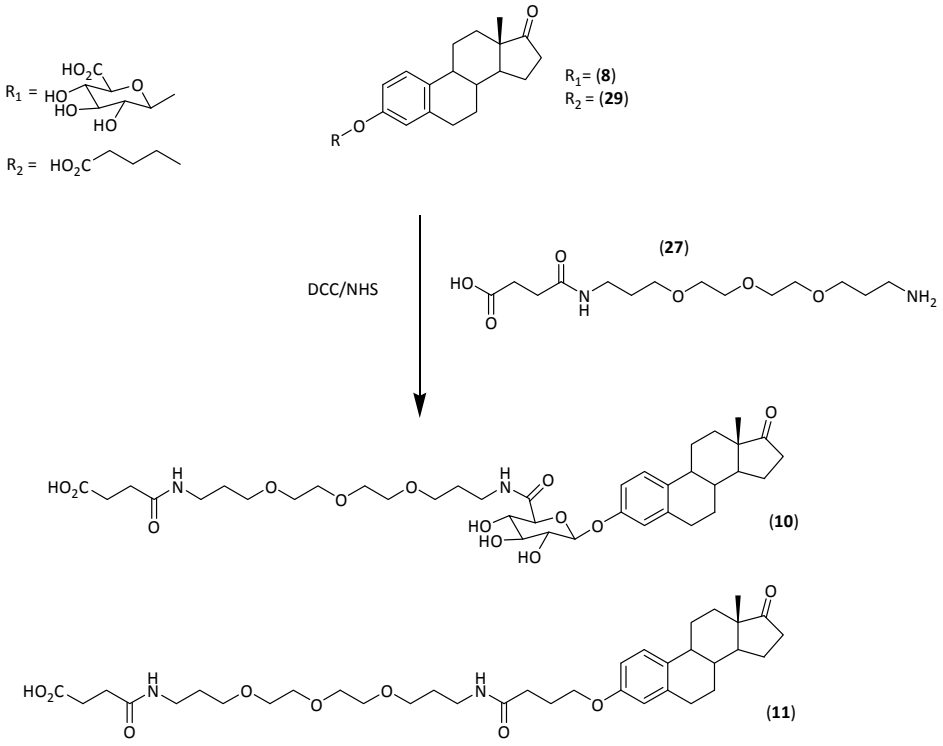

Scheme 5: General procedure for linker insertion to E1 esters

E1G, OEG (10) and E1C3, OEG (11) (Scheme 5)

The insertion of the long linker was carried out according to Scheme 5, using estrone glucuronide (**8**) (for E1G, OEG) and 1,3,5(10)-estratrien-3-(hydroxyl propianoic acid)-17 one (**29**) (for E1C3, OEG) as starting materials, and the long linker 1-amino-15-oxo- 4,7,10-trioxa-14-azaoctadecan-18-oic acid (**27**) in place of 7-aminoheptanoic acid (**26**).

The yields for E1G, OEG (**10**) and E1C3, OEG (**11**) were 40 to 50 %.

E1G, OEG: ^{1}H NMR (500 MHz, CDCl3) δ 0.94 (s, 3H), 1.41-1.82 (m, 8H), 1.89- 1.94 (m, 1H), 2.02-2.20 (m, 3H), 2.24-2.31 (m, 1H), 2.42-2.60 (m, 5H), 2.87-2.92 (m, 2H), 3.26 (t, *J* = 6.9 Hz, 2H), 3.30-3.37 (m, 8H), 3.49-3.52 (m, 14H), 3.88 (d, *J* = 9.3 Hz, 1H), 4.96 (d, *J* = 3.8 Hz, 1H), 6.82 (d, *J* = 2.5 Hz, 1H), 6.82 (dd, *J* = 2.5, 8.8 Hz, 1H), 7.23 (d, *J* = 8.4 Hz, 1H).

^{13}C NMR (125 MHz, CDCl3): δ 12.9, 21.1, 25.7, 26.2, 28.6, 29.0, 29.2, 30.5, 31.4, 35.3, 36.4, 36.6, 38.5, 44.0, 44.0, 50.2, 68.5, 68.7, 69.8, 69.8, 70.1, 72.0, 73.0, 74.9, 76.1, 101.1, 114.0, 116.6, 126.0, 134.1, 137.7, 155.5, 170.0.

HRMS (EI): MH+, found 749.38594. $C_{38}H_{57}N_2O_{13}$ requires 749.38607.

E1C3, OEG: ^{1}H NMR (500 MHz, CDCl3) δ 0.91 (s, 3H), 1.38-1.67 (m, 6H), 1.73-1.80 (m, 4H), 1.92-2.18 (m, 6H), 2.21-2.27 (m, 1H), 2.38 (t, *J* = 7.4 Hz, 2H), 2.45-2.54 (m, 3H), 2.65 (t, *J* = 6.5 Hz, 2H), 2.86-2.91 (m, 2H), 3.33-3.38 (m, 2H), 3.52-3.66 (m, 12H), 3.97 (t, *J* = 6.1 Hz, 2H), 6.45 (br t, *J* = 5.4 Hz, 1H), 6.62 (d, *J* = 2.9 Hz, 1H) 6.89 (dd, *J* = 2.9, 8.5 Hz, 1H), 6.87 (br t, *J* = 5.4 Hz, 1H), 7.18 (d, *J* = 8.5 Hz, 1H).

^{13}C NMR (125MHz,CDCl3) δ 13.9, 21.6, 25.9, 26.5, 28.7, 29.1, 29.7, 31.0, 31.6, 33.0, 35.0, 37.7, 38.2, 38.4, 44.0, 48.0, 50.4, 67.0, 69.7, 69.9, 70.0, 70.1, 70.3, 70.4, 112.2, 114.5, 126.4, 132.2, 137.8, 156.8, 172.7, 173.1.

HRMS (EI): MH+, found 659.39076. $C_{36}H_{55}N_2O_9$ requires 659.39122.

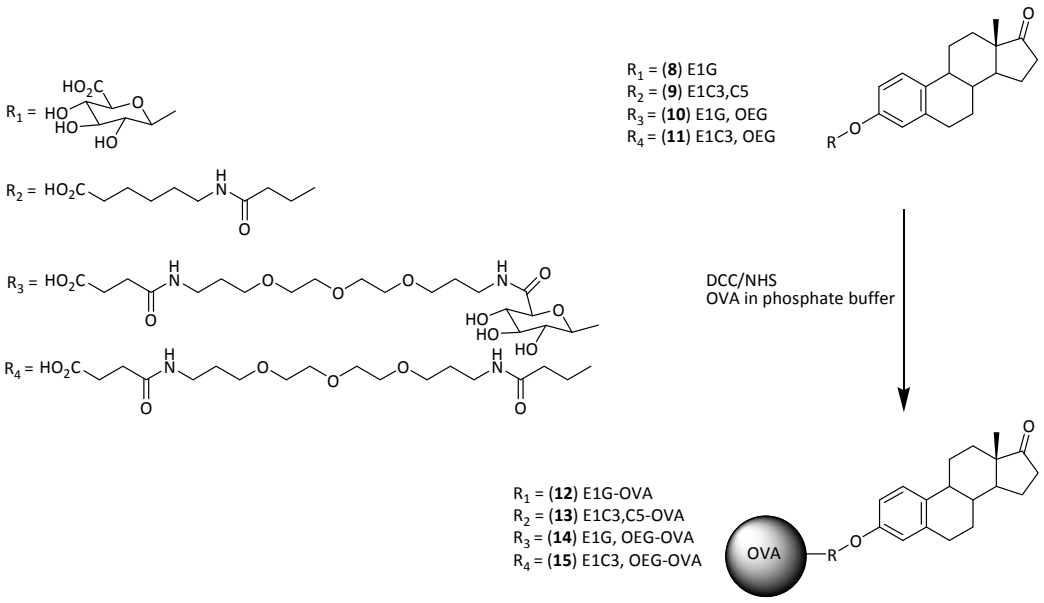

Scheme 6: Conjugation of E1 derivatives to ovalbumin.

Preparation of Estrone Linker-Ovalbumin conjugates (Scheme 6)

Estrone linker derivatives (**8** – **11**) (0.013 mmol, 1.0 equiv.) were dissolved in a mixture of DCC (0.04 mmol, 3.0 equiv.) and NHS (0.04 mmol, 3.0 equiv.) in DMF (0.20 mL), and the reaction was stirred at room temperature for 3 h until a white precipitate was formed. The solution was then added to OVA (0.65 mmol) in phosphate buffer (2.0 mL, 0.2 M, pH 7.4) and stirred at 4^{o}C overnight. After dialysis against deionised water for 2 days (3 changes per day) and PBS/T for one day (2 changes) at 4^{o}C, the conjugate (2.5 mL) was further purified by passing it through a PD-10 column using PBS/T as the eluent, and the purified conjugate **(12 – 15)** (3.5 mL) was collected.

Synthesis of Progesterone derivatives (Scheme 7)

Synthesis of the progesterone derivatives P4-OEG-NH_2 (**23**) and P4-OEG-COOH (**25**) was carried out according to Scheme 7. Commercially available progesterone (**30**) was used as the starting material. P4-COOH (**31**) was synthesized in high yield *via* epoxide method following the procedures for similar derivatives [164-166].

P4-OEG-NHBOC (33)

A solution of DCC (134 mg, 0.65 mmol, 1.3 equiv.), followed by NHS (74 mg, 0.65 mmol, 1.3 equiv.) in DMF (1.0 mL) was added drop wise to a stirred solution of P4-COOH (**31**) (209 mg, 0.5 mmol, 1.0 equiv.) in DMF (2 mL) at rt under an atmosphere of nitrogen. The mixture was stirred for 12 h in the dark. The resulting white precipitate was filtered off and the solvent was removed under reduced pressure and allowed to dry. To the solution of resulting active ester derivative in DMF an aqueous solution of OEG linker with a BOC-protected amine terminus (**17**) (240 mg, 0.75 mmol, 1.5 equiv.) was added followed by triethylamine (250 μL). The resulting solution was stirred for 12 h in the dark. After the addition of water (50 mL) the reaction mixture was extracted with DCM (20 mL x 3), washed with cold saturated $NaHCO_3$ (2 x 20 mL) and water (2 x 20 mL) and dried over $MgSO_4$. Following evaporation of the solvent, the residue was purified on column chromatography eluting with DCM/MeOH 15/1 to afford the desired product (**33**) as a yellow oil. (234 mg, 63 %).

^{1}H NMR (500 MHz, $CDCl_3$): δ 0.62 (s, 3H), 0.93-1.43 (m, 4H), 1.18 (s, 3H), 1.19-1.34 (m, 5H), 1.38 (s, 9H), 1.50-1.79 (m, 9H), 1.84-1.91 (m, 1H), 1.94-2.04 (m, 2H), 2.07 (s, 3H), 2.09-2.18 (m, 2H), 2.31 (t, *J* = 6.9 Hz, 2H), 2.43-2.50 (m, 3H), 2.80 (t, *J* = 6.9 Hz, 2H), 3.15- 3.18 (m, 2H), 3.33 (q, *J* = 6.4 Hz, 2H), 3.45-3.62 (m, 12H), 3.65 (dt, *J* = 3.2, 15.0 Hz, 1H), 5.02 (brs, 1H), 6.83 (brs, 1H) ppm.

^{13}C NMR (100 MHz, CDCl3): δ 13.4, 18.1, 21.1, 22.9, 24.3, 25.0, 25.6, 28.5, 29.1, 30.0, 30.6, 30.7, 31,5, 32.1, 33.9, 34.3, 34.6, 35.3, 36.7, 37.6, 38.6, 41.0, 41.4, 43.9,

54.1, 55.9, 63.9, 69.5, 69.7, 10.1, 70.2, 70.5, 128.7, 156.1, 171.1, 176.0, 195.4, 209.3.

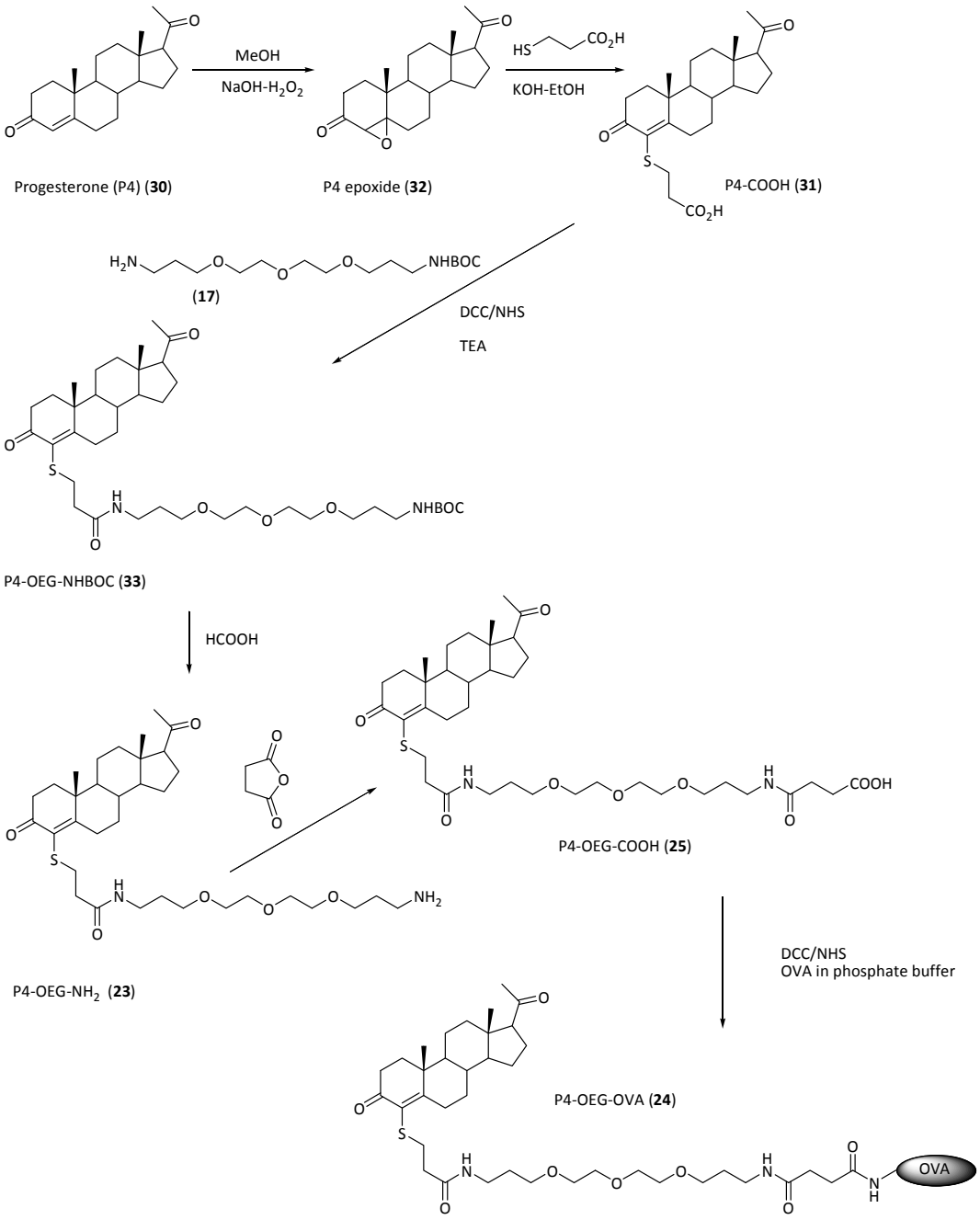

Scheme 7: Synthesis of progesterone-OEG linker-NH_2 and progesterone-OEG linker-ovalbumin conjugate used as sensing elements in the SPR sensor chip surface.

P4-OEG-NH_2 (23)

A solution of progesterone BOC derivative (**33**) (102 mg, 0.14 mmol) in formic acid (2 mL) was stirred for 3 h at rt. The solvent was removed and dried under vacuum

to give the desired product (**23**) as yellow-orange oil. This compound was used for the next reaction without further purification.

Compound (**23**) was also used for attachment to a CM5 sensor surface, and to a terthiophene-OEG-COOH sensor surface, again without further purification.

MS (ES+) m/z calculated $C_{34}H_{56}N_2O_6S$ 521.39: observed 621.83.

P4-OEG-COOH (25)

To a solution of progesterone derivative P4-OEG-NH_2 (**23**) (87 mg, 0.14 mmol, 1 eq.) in toluene/methanol: 4/1 (5 mL) was added succinic anhydride (17 mg, 0.16 mmol, 1.16 eq.) and the mixture was refluxed under an atmosphere of nitrogen for 1h. The solvent was removed in *vacuo* and purified by silica gel chromatography eluting DCM/MeOH/HCOOH 10/1/0.1, to afford the desired product (**25**) (40 mg, 40 %) as a yellow orange oil.

MS (ES-) m/z calculated $C_{38}H_{60}N_2O9S$ 719.39: observed 720.02.

This material was used in the preparation of its ovalbumin conjugate P4-OEG-OVA (**24**) for attachment to a CM5 sensor surface, and to a terthiophene-OEG-COOH sensor surface. (The details of the conjugation are included in the body of Chapter 5).

Synthesis of Functionalised Terthiophene (Scheme 8)

The linker used to project the carboxyl group away from the terthiophene backbone is the same as that used in the estrone work (**27**). Here the terminal amine group is BOC protected first to generate compound (**34**), before introduction of the linker to 2, 5-dibromothiophene-3-carbonyl chloride (**35**).

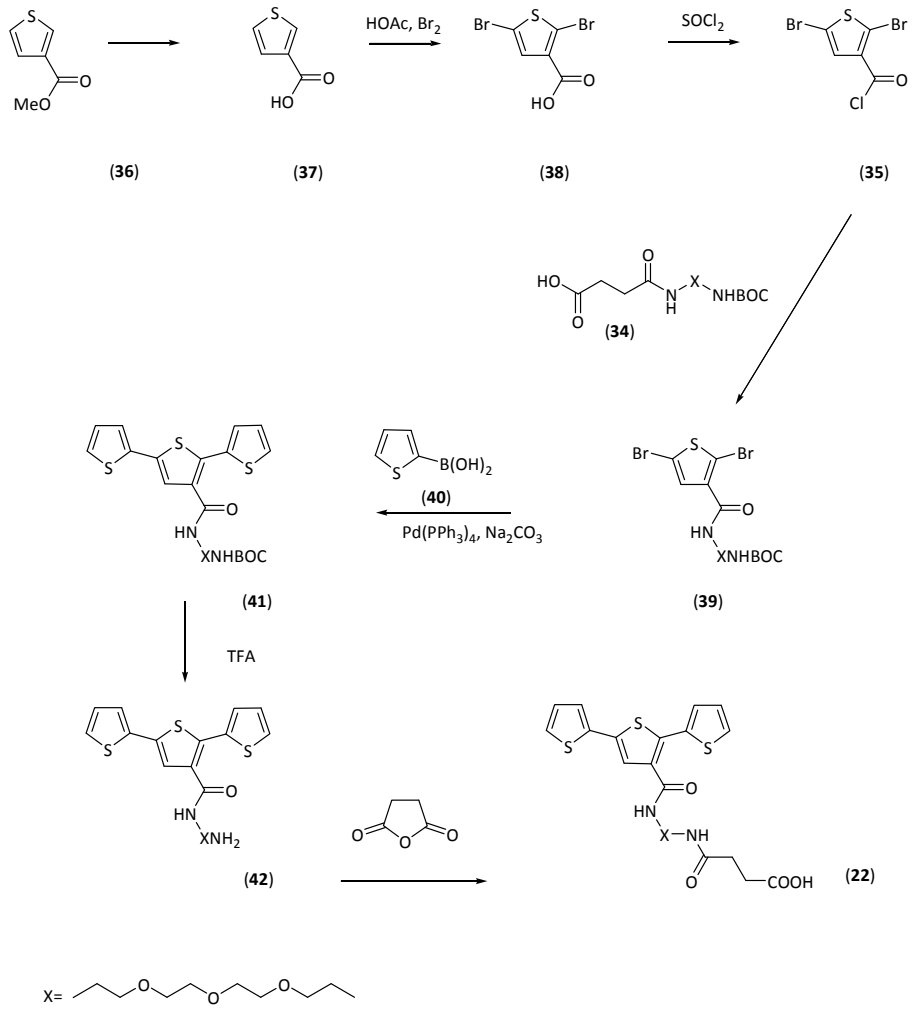

Scheme 8: Synthesis of a functionalised terthiophene for use as a scaffold on an SPR sensor surface.

2, 5-Dibromothiophene-3-carboxylic acid (38)

Thiophene-3-carboxylic acid (**37**)(1.28 g, 10 mmol) and glacial acetic acid (25 mL) were put into a three necked flask fitted with a condenser and pressure-equalising dropping funnel. Bromine (2.65 mL) was added drop-wise at rt, and the resulting

mixture was warmed to 60°C and stirred overnight. The mixture was poured into ice-water (100 mL) and treated with Na_2SO_3 (to remove excess bromine). The reaction mixture was filtered to give a light yellow/brown solid. The solid was recrystallised from ethanol/acetone to give the desired product (**38**) as a pale yellow solid (2.1 g, approximately 80 % yield).

^{13}C NMR (125 MHz, $CDCl_3$, MeOH): δ 111.1, 119.2, 132.0, 132.3, 162.6.

2, 5-Dibromothiophene-3-carbonyl chloride (35)

2, 5-Dibromothiophene-3-carboxylic acid (**38**) (1.71 g, 6 mmol) was dissolved in dry CH_2Cl_2 (20 mL) and thionyl chloride (3 mL) was added and the resulting mixture was refluxed for 6 h under an atmosphere of Ar. The solvent was removed under reduced pressure, and the resulting 2,5-dibromothiophene-3-carbonyl chloride (**35**) was dried for a few hours before the next reaction.

Dibromothiophene-OEG-BOC (39)

To a solution of the 2, 5-dibromothiophene-3-carbonyl chloride (**35**) prepared above in dry DMF was added an equimolar amount of the BOC-protected linker (**34**) in DMF followed by triethylamine under an argon atmosphere. The resulting solution was allowed to stir for 12 h. The reaction mixture was diluted with water and DCM. The organic layer was separated and washed with water, brine and dried over $MgSO_4$ and concentrated under reduced pressure to give the crude product, which was purified by FCC (DCM/MeOH = 10/1) to afford the desired product (**39**) as a pale yellow oil.

2-Thienylboronic acid (40)

A solution of thiophene (9.51 mL, 10.0g, 119 mol) in dry THF (120 mL) at -78 °C. *n*BuLi (95 mL, 1.24 M, 0.118 mol) was added drop-wise under an atmosphere of argon. The reaction mixture was stirred for 30 min at that temperature, and then allowed to warm to -20° C. This 2-thienyllithium was again cooled to -78° C and transferred by cannula into a solution of triisopropylborate (38.0 mL, 32.0 g, 0.165

mol) in dry THF (80 mL) at -78^{o} C. The mixture was then treated with 1 M aqueous HCl (200 mL) and the organic layer separated. The aqueous layer was then extracted with DCM (3 x 150 mL), and the combined layers were dried over $MgSO_4$ and concentrated under reduced pressure to afford a pale brown solid. The crude product was recrystallised with water to give thiopheneboronic acid (**40**) as a white solid. (11.9 g, 78 %, melting point 125 - 127^{o}C).

Terthiophene-OEG-BOC (41)

A solution of dibromothiophene-OEG-BOC (**39**) (1 equiv.) and (2-thiophene) boronic acid (**40**) (3 equiv.) in DME (14 mL) was degassed for 20 min, under Ar. Similarly, an aqueous solution of Na_2CO_3 (1 M, 10.0 mL) was also degassed for 20 min under Ar. Then to the solution of DME, $Pd(PPh_3)_4$ (94 mg, 0.08 mmol, 6 mol %) and Na_2CO_3 solution were added and the resulting mixture was heated at 60^{o} C under Ar for 6 h. The reaction mixture was concentrated and then diluted with DCM (20 mL) and separated. The organic residue was washed with water (2 x 20 mL), dried over $MgSO_4$ and concentrated in *vacuo* to give a yellow solid. Crude product was separated by FCC eluting Hex/EtOAc (4:1) to afford the desired product (**41**) as bright yellow solid.

Terthiophene-OEG-NH_2 (42)

A solution of terthiophene-OEG-BOC derivative (**41**) (100 mg, 0.168 mmol, 1 eq.) in TFA (2 mL) was stirred at rt for 3 h. Solvent was removed in *vacuo* and the resulting product (**42**) taken to the next reaction without further purification.

^{1}H NMR (500 MHz, $CDCl_3$) δ 3.00 (brt, *J* = 5.4 Hz, 2H), 3.45-3.55 (m, 8H), 3.60 (brt, , *J* = 5.4 Hz, 2H), 6.99 (dd, *J* = 3.7, 5.2 Hz, 1H), 7.02 (dd, *J* = 4.1, 5.4 Hz, 1H), 7.15 (dd, *J* = 1.1, 3.5 Hz, 1H), 7.22 (dd, *J* = 1.1, 5.1 Hz, 1H), 7.28 (dd, *J* = 1.1, 3.5 Hz, 1H), 7.34 (s, 1H), 7.15 (d, *J* = 1.1 Hz, 1H)

^{13}C NMR (125 MHz, $CDCl_3$): δ 39.3, 39.7, 67.0, 69.7, 70.1, 70.2, 124.5, 124.9, 125.3, 127.6, 127.7, 128.0, 128.3, 133.6, 133.9, 134.9, 135.9, 136.4, 164.5.

HRMS (EI): MH_+, found 495.1440. $C_{23}H_{31}N_2O_4S_3$ requires 495.1438.

Terthiophene-OEG-COOH (22)

To the solution of terthiophene-OEG amine derivative (**42**) (40 mg, 0.0809 mmol, 1 equiv.) in 10 mL toluene was added succinic anhydride (8 mg, 0.0809 mmol, 1 equiv.) and the mixture was refluxed under an atmosphere of nitrogen for 1 h. The reaction mixture was diluted with DCM and water. The organic layer was separated and dried over magnesium sulphate and the solvent removed in *vacuo*. The residue was purified by flash column chromatography with silica, eluting with DCM/MeOH/HOAc 10/1/0.1, to afford the desired product (35 g, 73 %) as a yellow solid.

^{1}H NMR (500 MHz, $CDCl_3$) δ 1.62-1.72 (m, 4H), 2.37-2.41 (m, 2H), 2.53-2.57 (m, 2H), 3.24 (q, *J* = 5.7 Hz, 2H), 3.34-3.50 (m, 14H), 4.96 (brt, *J* = 5.3 Hz, NH), 6.80 (brt, *J* = 5.3 Hz, NH), 6.95 (dd, *J* = 3.7, 5.1 Hz, 1H), 7.00 (dd, *J* = 3.7, 5.3 Hz, 1H), 7.10 (dd, *J* = 1.1, 3.6 Hz, 1H), 7.18 (dd, *J* = 1.1, 5.2 Hz, 1H), 7.23 (dd, *J* = 1.1, 3.5 Hz, 1H), 7.29 (s, 1H), 7.31 (dd, *J* = 1.1, 5.2 Hz, 1H)

^{13}C NMR (125 MHz, $CDCl_3$): δ 28.6, 28.9, 30.3, 30.8, 38.0, 38.3, 69.6, 69.9, 70.0, 70.1, 70.3, 70.4, 124.4, 124.9, 125.3, 127.7, 127.8, 128.0, 128.4, 133.5, 134.3, 134.6, 135.9, 136.4, 164.2, 172.7, 174.8.

HRMS (EI): MH+, found 595.1601. $C_{27}H_{35}N_2O7S_3$ requires 595.1604.

Electrochemistry

Cyclic voltammograms of the background electrolyte (0.1M TBAP in acetonitrile) are shown below. The electrochemistry was carried out in the purpose-built set-up with an SPR chip as the working electrode. Figure 70 shows a background voltammogram with a scan speed of 5 V/s (coating speed) and Figure 71 the background with a scan speed of 100 mV/s (post-coating speed).

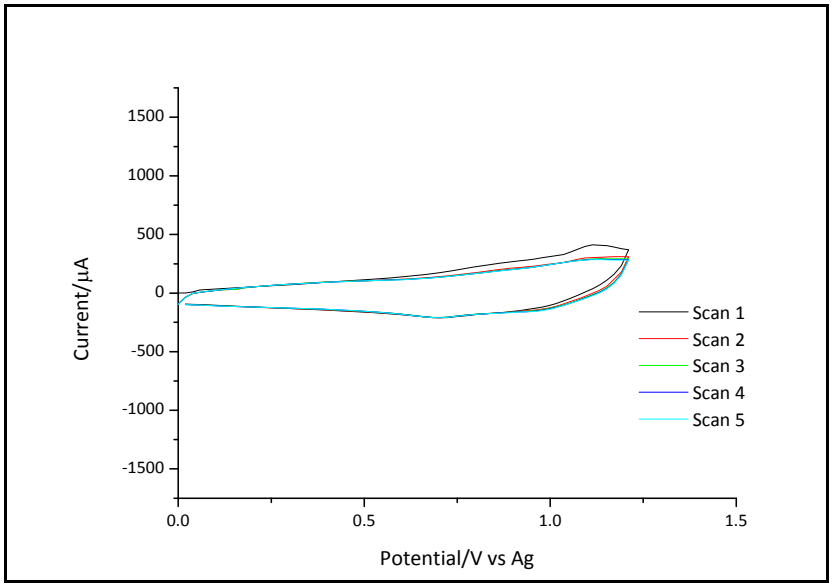

Figure 70: Background cyclic voltammogram of supporting electrolyte 0.1 M TBAP in acetonitrile on a gold surface. Potential limits 0/+1.2 V. 5 cycles. Scan rate 5 V/s. Stainless steel counter electrode.

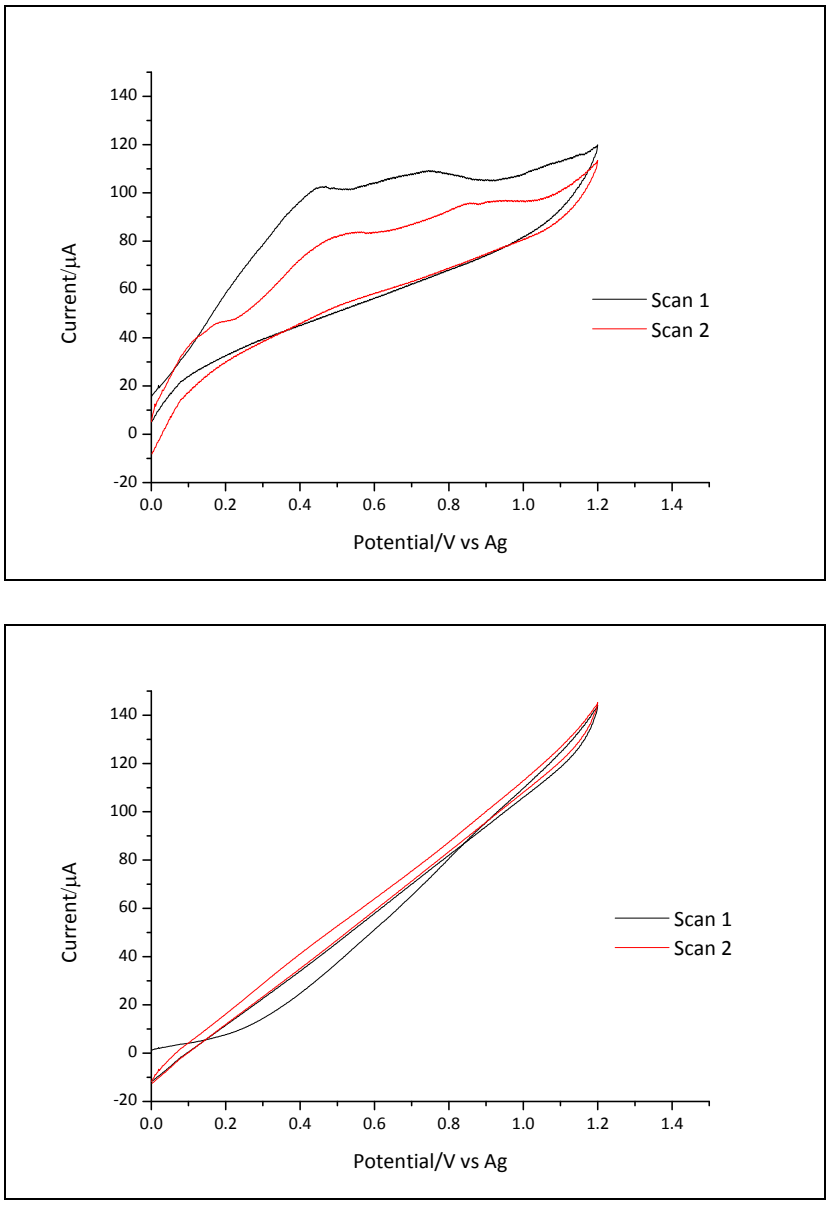

Figure 71: Cyclic voltammograms of supporting electrolyte 0.1 M TBAP in acetonitrile. Potential limits 0/+1.2 V. 5 cycles. Scan rate 100 mV/s. Stainless steel counter electrode.

References

1. Routledge, E.J., et al., *Identification of Estrogenic Chemicals in STW Effluent. 2. In Vivo Responses in Trout and Roach.* Environmental Science and Technology, 1998. **32**(11): p. 1559-1565.
2. Carlsen, E., et al., *Declining semen quality and increasing incidence of testicular cancer: is there a common cause?* Environmental health perspectives, 1995. **103 Suppl 7**: p. 137-9.
3. Sharpe, R.M., *Natural and anthropogenic environmental estrogens: the scientific basis for risk assessment. Environmental estrogens and male infertility.* Pure and Applied Chemistry, 1998. **70**(9): p. 1685-1701.
4. Williams, R.J., et al., *Steroid Estrogens Profiles along River Stretches Arising from Sewage Treatment Works Discharges.* Environmental Science and Technology, 2003. **37**(9): p. 1744-1750.
5. Routledge, E.J., et al., *Some alkyl hydroxy benzoate preservatives (parabens) are estrogenic.* Toxicology and applied pharmacology, 1998. **153**(1): p. 12-9.
6. Lintelmann, J., et al., *Endocrine disruptors in the environment (IUPAC technical report).* Pure and Applied Chemistry, 2003. **75**(5): p. 631-681.
7. Racz, L. and R.K. Goel, *Fate and removal of estrogens in municipal wastewater.* Journal of Environmental Monitoring, 2010. **12**(1): p. 58-70.
8. Lopez de Alda, M.J. and D. Barcelo, *Determination of steroid sex hormones and related synthetic compounds considered as endocrine disrupters in water by fully automated on-line solid-phase extraction-liquid chromatography-diode array detection.* Journal of Chromatography, A, 2001. **911**(2): p. 203-210.
9. Salvador, A., et al., *On-line solid-phase extraction with on-support derivatization for high-sensitivity liquid chromatography tandem mass spectrometry of estrogens in influent/effluent of wastewater treatment plants.* Journal of Chromatography A, 2007. **1145**(1–2): p. 102-109.

10. Viglino, L., et al., *Analysis of natural and synthetic estrogenic endocrine disruptors in environmental waters using online preconcentration coupled with LC-APPI-MS/MS.* Talanta, 2008. **76**(5): p. 1088-1096.
11. Lefebvre, K.A. and A. Robertson, *Domoic acid and human exposure risks: A review.* Toxicon, 2010. **56**(2): p. 218-230.
12. Garthwaite, I., *Keeping shellfish safe to eat: a brief review of shellfish toxins, and methods for their detection.* Trends Food Sci. Technol., 2001. **11**(7): p. 235-244.
13. Jasperse, J.A. *Marine toxins and New Zealand shellfish. Proceedings of a workshop on research issues.* 1993. Wellington, New Zealand: The Royal Society of New Zealand.
14. Munday, R., et al., *Comparative toxicity to mice of domoic acid and isodomoic acids A, B and C.* Toxicon, 2008. **52**(8): p. 954-956.
15. Quilliam, M.A. and J.L.C. Wright, *The amnesic shellfish poisoning mystery.* Analytical Chemistry, 1989. **61**(18): p. 1053A-1054A, 1056A, 1058A-1060A.
16. Jeffery, B., et al., *Amnesic shellfish poison.* Food and Chemical Toxicology, 2004. **42**(4): p. 545-557.
17. Campas, M., B. Prieto-Simon, and J.-L. Marty, *Biosensors to detect marine toxins: Assessing seafood safety.* Talanta, 2007. **72**(3): p. 884-895.
18. Rhodes, L., C. Scholin, and I. Garthwaite, *Pseudo-nitzschia in New Zealand and the role of DNA probes and immunoassays in refining marine biotoxin monitoring programmes.* Natural Toxins, 1998. **6**(3-4): p. 105-111.
19. Van Dolah, F.M., *Marine algal toxins: origins, health effects, and their increased occurrence.* Environ. Health Perspect. Suppl., 2000. **108**(1): p. 133-141.
20. Hallegraeff, G.M., *A review of harmful algal blooms and their apparent global increase*.* Phycologia, 1993. **32**(2): p. 79-99.
21. Yu, F.-Y., et al., *Development of a Sensitive Enzyme-Linked Immunosorbent Assay for the Determination of Domoic Acid in Shellfish.* Journal of Agricultural and Food Chemistry, 2004. **52**(17): p. 5334-5339.

22. Tsao, Z.-J., et al., *Development of a Monoclonal Antibody against Domoic Acid and Its Application in Enzyme-Linked Immunosorbent Assay and Colloidal Gold Immunostrip.* Journal of Agricultural and Food Chemistry, 2007. **55**(13): p. 4921-4927.
23. Kania, M. and B. Hock, *Development of monoclonal antibodies to domoic acid for the detection of domoic acid in blue mussel (Mytilus edulis) tissue by ELISA.* Analytical Letters, 2002. **35**(5): p. 855-868.
24. Zhou, Y., et al., *Development of a novel antibody probe useful for domoic acid detection.* Biosensors and Bioelectronics, 2009. **24**(10): p. 3159-3163.
25. Dubois, M., et al., *Development of ELISAs for detecting domoic acid, okadaic acid, and saxitoxin and their applicability for the detection of marine toxins in samples collected in Belgium.* Food Addit. Contam., Part A, 2010. **27**(6): p. 859-868.
26. Garthwaite, I., et al., *Polyclonal antibodies to domoic acid, and their use in immunoassays for domoic acid in sea water and shellfish.* Natural Toxins, 1998. **6**(3/4): p. 93-104.
27. Garthwaite, I., et al., *Integrated enzyme-linked immunosorbent assay screening system for amnesic, neurotoxic, diarrhetic, and paralytic shellfish poisoning toxins found in New Zealand.* Journal of AOAC International, 2001. **84**(5): p. 1643-8.
28. Quilliam, M.A., et al., *High-performance liquid chromatography of domoic acid, a marine neurotoxin, with application to shellfish and plankton.* Int. J. Environ. Anal. Chem., 1989. **36**(3): p. 139-54.
29. Wright, J.L.C., et al., *Identification of domoic acid, a neuroexcitatory amino acid, in toxic mussels from eastern Prince Edward Island.* Canadian Journal of Chemistry, 1989. **67**(3): p. 481-490.
30. Lawrence, J.F., et al., *Liquid chromatographic determination of domoic acid in shellfish products using the paralytic shellfish poison extraction procedure of the Association of Official Analytical Chemists.* Journal of Chromatography, 1989. **462**: p. 349-56.

31. Quilliam, M.A., M. Xie, and W.R. Hardstaff, *Rapid extraction and cleanup for liquid chromatographic determination of domoic acid in unsalted seafood.* Journal of AOAC International, 1995. **78**(2): p. 543-54.

32. Mafra Jr, L.L., et al., *Analysis of trace levels of domoic acid in seawater and plankton by liquid chromatography without derivatization, using UV or mass spectrometry detection.* Journal of Chromatography A, 2009. **1216**(32): p. 6003-6011.

33. Mackenzie, A.L., et al., *Domoic Acid and the New-Zealand Greenshell Mussel (Perna-Canaliculus)*. Toxic Phytoplankton Blooms in the Sea, ed. T.J. Smayda and Y. Shimizu. Vol. 3. 1993. 607-612.

34. Maroulis, M., et al., *Determination of domoic acid in mussels by HPLC with post-column derivatization using 4-chloro-7-nitrobenzo-2-oxa-1,3-diazole (NBD-Cl) and fluorescence detection.* Journal of Chromatography B, 2008. **876**(2): p. 245-251.

35. Sun, T. and W.H. Wong, *Determination of Domoic Acid in Phytoplankton by High-Performance Liquid Chromatography of the 6-Aminoquinolyl-N-hydroxysuccinimidyl Carbamate Derivative.* Journal of Agricultural and Food Chemistry, 1999. **47**(11): p. 4678-4681.

36. Ciminiello, P., et al., *Hydrophilic interaction liquid chromatography/mass spectrometry for determination of domoic acid in Adriatic shellfish.* Rapid Commun. Mass Spectrom., 2005. **19**(14): p. 2030-2038.

37. Thibault, P., et al., *Mass spectrometry of domoic acid, a marine neurotoxin.* Biomed. Environ. Mass Spectrom., 1989. **18**(6): p. 373-86.

38. Regueiro, J., et al., *Sensitive determination of domoic acid in shellfish by on-line coupling of weak anion exchange solid-phase extraction and liquid chromatography–diode array detection–tandem mass spectrometry.* Food Chemistry, 2011. **129**(2): p. 672-678.

39. Wang, Z., et al., *Determination of domoic acid in seawater and phytoplankton by liquid chromatography–tandem mass spectrometry.* Journal of Chromatography A, 2007. **1163**(1–2): p. 169-176.

40. Zhao, J.-Y., P. Thibault, and M.A. Quilliam, *Analysis of domoic acid isomers in seafood by capillary electrophoresis.* ELECTROPHORESIS, 1997. **18**(2): p. 268-276.

41. Nguyen, A.L., J.H.T. Luong, and C. Masson, *Capillary electrophoresis for detection and quantitation of domoic acid in mussels.* Anal. Lett., 1990. **23**(9): p. 1621-34.

42. Van Dolah, F.M., et al., *A microplate receptor assay for the amnesic shellfish poisoning toxin, domoic acid, utilizing a cloned glutamate receptor.* Analytical Biochemistry, 1997. **245**(1): p. 102-105.

43. Nylander, C., B. Liedberg, and T. Lind, *Gas detection by means of surface plasmon resonance.* Sens. Actuators, 1982. **3**(1): p. 79-88.

44. Liedberg, B., C. Nylander, and I. Lundstroem, *Surface plasmon resonance for gas detection and biosensing.* Sensors and Actuators, 1983. **4**(2): p. 299-304.

45. Wood, R.W., *On a remarkable case of uneven distribution of light in a diffraction grating spectrum.* Philosophical Magazine, 1902. **4**(19-24): p. 396-402.

46. Wood, R.W., *Diffraction gratings with controlled groove form and abnormal distribution of intensity.* Philosophical Magazine, 1912. **23**(133-8): p. 310-317.

47. Rayleigh, L., *Note on the remarkable case of diffraction spectra described by Prof. Wood.* Philosophical Magazine, 1907. **14**(79-84): p. 60-65.

48. Fano, U., *The theory of anomalous diffraction gratings and of quasi-stationary waves on metallic surfaces (Sommerfeld's waves).* Journal of the Optical Society of America, 1941. **31**(3): p. 213-222.

49. Ritchie, R.H., et al., *Surface-Plasmon Resonance Effect in Grating Diffraction.* Physical Review Letters, 1968. **21**(22): p. 1530-1533.

50. Otto, A., *EXCITATION OF NONRADIATIVE SURFACE PLASMA WAVES IN SILVER BY METHOD OF FRUSTRATED TOTAL REFLECTION.* Zeitschrift Fur Physik, 1968. **216**(4): p. 398-&.

51. Kretschmann, E. and H. Raether, *Radiative decay of nonradiative surface plasmons excited by light.* Z. Naturforsch. A, 1968. **23**(12): p. 2135-6.

52. Malmqvist, M., *Biospecific interaction analysis using biosensor technology.* Nature, 1993. **361**(6408): p. 186-187.

53. Rich, R.L. and D.G. Myszka, *Survey of the year 2007 commercial optical biosensor literature.* J. Mol. Recognit., 2008. **21**(6): p. 355-400.

54. Mitchell, J.S. and Y. Wu, eds. *Affinity constants for small molecules from SPR competition experiments*. Methods in Molecular Biology (Totowa, NJ, United States). Vol. 627. 2010. 113-129.

55. Chinowsky, T.M., et al., *Portable 24-analyte surface plasmon resonance instruments for rapid, versatile biodetection.* Biosensors & Bioelectronics, 2007. **22**(9-10): p. 2268-2275.

56. Zhan, S., et al., *Study on design and application of fully automatic miniature surface plasmon resonance concentration analyzer.* Sensors and Actuators, B Chemical, 2011. **B153**(2): p. 427-433.

57. Kawazumi, H., et al., *Compact surface plasmon resonance (SPR) immunosensor using multichannel for simultaneous detection of small molecule compounds.* Sensors and Actuators, B Chemical, 2005. **B108**(1-2): p. 791-796.

58. Sjoelander, S. and C. Urbaniczky, *Integrated fluid handling system for biomolecular interaction analysis.* Anal. Chem., 1991. **63**(20): p. 2338-45.

59. Loefaes, S. and B. Johnson, *A novel hydrogel matrix on gold surfaces in surface plasmon resonance sensors for fast and efficient covalent immobilization of ligands.* Journal of the Chemical Society, Chemical Communications, 1990(21): p. 1526-8.

60. Loefas, S., et al., *Methods for site controlled coupling to carboxymethyldextran surfaces in surface plasmon resonance sensors.* Biosensors & Bioelectronics, 1995. **10**(9/10): p. 813-22.

61. *Biacore Sensor Surface Handbook*. BR-1005-71 AB 05/2008 ed. 2008. 100.

62. Johnsson, B., S. Loefaas, and G. Lindquist, *Immobilization of proteins to a carboxymethyldextran-modified gold surface for biospecific interaction analysis in surface plasmon resonance sensors.* Anal Biochem, 1991. **198**(2): p. 268-77.

63. Salchert, K., et al., *Immobilization of an anticoagulant benzamidine derivative: Effect of spacer arms and carrier hydrophobicity on thrombin binding.* Acta Biomaterialia, 2005. **1**(4): p. 441-449.

64. Weimer, B.C., M.K. Walsh, and X. Wang, *Influence of a poly-ethylene glycol spacer on antigen capture by immobilized antibodies.* Journal of Biochemical and Biophysical Methods, 2000. **45**(2): p. 211-219.

65. Cao, T., et al., *Investigation of spacer length effect on immobilized Escherichia coli pili-antibody molecular recognition by AFM.* Biotechnology and Bioengineering, 2007. **98**(6): p. 1109-1122.

66. Herforth, C., et al., *Polymer-bound reagents for the introduction of spacer-modified biotin labels.* Bioorganic & Medicinal Chemistry, 2004. **12**(11): p. 2895-2902.

67. Watanabe, H., et al., *Biomimetic Engineering of Modular Bispecific Antibodies for Biomolecule Immobilization.* Langmuir, 2011. **27**(16): p. 9656-9661.

68. Wu, Y., et al., *Evaluation of progesterone-ovalbumin conjugates with different length linkers in enzyme-linked immunosorbant assay and surface plasmon resonance-based immunoassay.* Steroids, 2002. **67**(7): p. 565-572.

69. Mitchell, J.S., et al., *Technical Note: Protein conjugate-based immunoassay of whole milk progesterone.* J. Dairy Sci., 2004. **87**(9): p. 2864-2867.

70. Bieniarz, C., et al., *Extended Length Heterobifunctional Coupling Agents for Protein Conjugations.* Bioconjugate Chem., 1996. **7**(1): p. 88-95.

71. Van Weemen, B.K. and A.H.W.M. Schuurs, *The influence of heterologous combinations of antiserum and enzyme-labeled estrogen on the characteristics of estrogen enzyme-immunoassays.* Immunochemistry, 1975. **12**(8): p. 667-670.

72. Tanaka, T., M. Yanagi, and A. Kubodera, *Bridge-heterologous chemiluminescence enzyme-linked immunosorbent assay of estriol 3-sulfate in pregnancy plasma.* Steroids, 1998. **63**(10): p. 516-522.

73. Nara, S., et al., *Influence of hydrophobic and hydrophilic spacer-containing enzyme conjugates on functional parameters of steroid immunoassay.* Anal. Biochem., 2008. **373**(1): p. 18-25.

74. Hosoda, H., N. Kawamura, and T. Nambara, *Studies on steroids. CLXVI. Effect of bridge heterologous combination on sensitivity in enzyme immunoassay for cortisol.* Chem. Pharm. Bull., 1981. **29**(7): p. 1969-74.

75. Hatzidakis, G., A. Stefanakis, and E. Krambovitis, *Comparison of different antibody-conjugate derivatives for the development of a sensitive and specific progesterone assay.* J. Reprod. Fertil., 1993. **97**(2): p. 557-61.

76. Mitchell, J.S., et al., *Sensitivity enhancement of surface plasmon resonance biosensing of small molecules.* Anal. Biochem., 2005. **343**(1): p. 125-135.

77. Yuan, J., et al., *Sensitivity enhancement of SPR assay of progesterone based on mixed self-assembled monolayers using nanogold particles.* Biosensors & Bioelectronics, 2007. **23**(1): p. 144-148.

78. Jiang, X., et al., *Sensitive determination of estriol-16-glucuronide using surface plasmon resonance sensing.* Steroids, 2009. **74**(10-11): p. 819-24.

79. Jiang, X., et al., *Determination of estriol 16-glucuronide in human urine with surface plasmon resonance and lateral flow immunoassays.* Analytical Methods, 2010. **2**(4): p. 368-374.

80. Mitchell, J.S., et al., *Estrogen conjugation and antibody binding interactions in surface plasmon resonance biosensing.* Steroids, 2006. **71**(7): p. 618-631.

81. Mitchell, J.S. and T.E. Lowe, *Ultrasensitive detection of testosterone using conjugate linker technology in a nanoparticle-enhanced surface plasmon resonance biosensor.* Biosensors & Bioelectronics, 2009. **24**(7): p. 2177-2183.

82. Mitchell, J.S., T.E. Lowe, and J.R. Ingram, *Rapid ultrasensitive measurement of salivary cortisol using nano-linker chemistry coupled with surface plasmon resonance detection.* Analyst (Cambridge, U. K.), 2009. **134**(2): p. 380-386.

83. Yuan, J., et al., *Surface Plasmon Resonance Assay for Chloramphenicol.* Analytical Chemistry (Washington, DC, United States), 2008. **80**(21): p. 8329-8333.

84. Yuan, J., et al., *Surface plasmon resonance assay for chloramphenicol without surface regeneration.* Anal. Biochem., 2009. **390**(1): p. 97-99.

85. Yuan, J., et al., *Surface plasmon resonance biosensor for the detection of ochratoxin A in cereals and beverages.* Analytica Chimica Acta, 2009. **656**(1–2): p. 63-71.

86. Frens, G., *Controlled nucleation for the regulation of the particle size in monodisperse gold suspensions.* Nature (London), Phys. Sci., 1973. **241**(105): p. 20-2.

87. Lyon, L.A., M.D. Musick, and M.J. Natan, *Colloidal Au-Enhanced Surface Plasmon Resonance Immunosensing.* Anal. Chem., 1998. **70**(24): p. 5177-5183.

88. Lyon, V.A., et al., *Surface plasmon resonance of colloidal Au-modified gold films.* Sensors and Actuators, B Chemical, 1999. **B54**(1-2): p. 118-124.

89. Lyon, L.A., D.J. Pena, and M.J. Natan, *Surface Plasmon Resonance of Au Colloid-Modified Au Films: Particle Size Dependence.* Journal of Physical Chemistry B, 1999. **103**(28): p. 5826-5831.

90. Lee, K.-S. and M.A. El-Sayed, *Gold and Silver Nanoparticles in Sensing and Imaging: Sensitivity of Plasmon Response to Size, Shape, and Metal Composition.* Journal of Physical Chemistry B, 2006. **110**(39): p. 19220-19225.

91. Mitchell, J., *Small molecule immunosensing using surface plasmon resonance.* Sensors, 2010. **10**: p. 7323-7346.

92. Mustafa, D.E., et al., *Surface Plasmon Coupling Effect of Gold Nanoparticles with Different Shape and Size on Conventional Surface Plasmon Resonance Signal.* Plasmonics, 2010. **5**(3): p. 221-231.

93. Matsui, J., et al., *SPR Sensor Chip for Detection of Small Molecules Using Molecularly Imprinted Polymer with Embedded Gold Nanoparticles.* Anal. Chem., 2005. **77**(13): p. 4282-4285.

94. Driskell, J.D., R.J. Lipert, and M.D. Porter, *Labeled Gold Nanoparticles Immobilized at Smooth Metallic Substrates: Systematic Investigation of Surface Plasmon Resonance and Surface-Enhanced Raman Scattering.* The Journal of Physical Chemistry B, 2006. **110**(35): p. 17444-17451.

95. Hong, X. and E.A.H. Hall, *Contribution of gold nanoparticles to the signal amplification in surface plasmon resonance.* Analyst, 2012. **137**(20): p. 4712-4719.

96. Morel, A.-L., et al., *Optimized immobilization of gold nanoparticles on planar surfaces through alkyldithiols and their use to build 3D biosensors.* Colloids and Surfaces B: Biointerfaces, 2010. **81**(1): p. 304-312.

97. Ko, S., et al., *Directed self-assembly of gold binding polypeptide-protein A fusion proteins for development of gold nanoparticle-based SPR immunosensors.* Biosensors and Bioelectronics, 2009. **24**(8): p. 2592-2597.

98. Huang, X., et al., *A gold nanoparticle labeling strategy for the sensitive kinetic assay of the carbamate–acetylcholinesterase interaction by surface plasmon resonance.* Talanta, 2009. **78**(3): p. 1036-1042.

99. Law, W.-C., et al., *Nanoparticle enhanced surface plasmon resonance biosensing: application of gold nanorods.* Opt. Express, 2009. **17**(21): p. 19041-19046.

100. Gu, J.H., et al., *Enhancement of the sensitivity of surface plasmon resonance biosensor with colloidal gold labeling technique.* Supramolecular Science, 1998. **5**(5–6): p. 695-698.

101. Buckle, P.E., et al., *The resonant mirror: a novel optical sensor for direct sensing of biomolecular interactions part II: applications.* Biosensors and Bioelectronics, 1993. **8**(7–8): p. 355-363.

102. He, L., et al., *Colloidal Au-Enhanced Surface Plasmon Resonance for Ultrasensitive Detection of DNA Hybridization.* Journal of the American Chemical Society, 2000. **122**(38): p. 9071-9077.

103. Lee, J.-H., et al., *Signal enhancement of surface plasmon resonance based immunosensor using gold nanoparticle-antibody complex for beta -amyloid (1-40) detection.* Journal of Nanoscience and Nanotechnology, 2009. **9**(12): p. 7155-7160.

104. Tanaka, R., et al., *A novel enhancement assay for immunochromatographic test strips using gold nanoparticles.* Analytical and Bioanalytical Chemistry, 2006. **385**(8): p. 1414-1420.

105. Zhu, J., et al., *Development of an immunochromatographic assay for the rapid detection of bromoxynil in water.* Environmental Pollution, 2008. **156**(1): p. 136-142.

106. Nagatani, N., et al., *Gold nanoparticle-based novel enhancement method for the development of highly sensitive immunochromatographic test strips.* Science and Technology of Advanced Materials, 2006. **7**(3): p. 270-275.

107. Verheijen, R., et al., *Development of a one step strip test for the detection of sulfadimidine residues.* Analyst (Cambridge, United Kingdom), 1998. **123**(12): p. 2437-2441.

108. Ulman, A., *Formation and Structure of Self-Assembled Monolayers.* Chemical Reviews (Washington, D. C.), 1996. **96**(4): p. 1533-1554.

109. Nuzzo, R.G. and D.L. Allara, *Adsorption of bifunctional organic disulfides on gold surfaces.* Journal of the American Chemical Society, 1983. **105**(13): p. 4481-3.

110. Baccar, H., et al., *Surface plasmon resonance immunosensor for bacteria detection.* Talanta, 2010. **82**(2): p. 810-814.

111. Larsson, A., et al., *A novel biochip technology for detection of explosives–TNT: Synthesis, characterisation and application.* Sensors and Actuators B: Chemical, 2006. **113**(2): p. 730-748.

112. Kim, S.J., et al., *A simple and versatile self-assembled monolayer based surface plasmon resonance immunosensor for highly sensitive detection of 2,4-D from natural water resources.* Sensors and Actuators B: Chemical, 2008. **130**(1): p. 281-289.

113. Altintas, Z., et al., *Surface plasmon resonance based immunosensor for the detection of the cancer biomarker carcinoembryonic antigen.* Talanta, 2011. **86**(0): p. 377-383.

114. Liu, X., et al., *Enhanced optical immuosensor (sic) based on surface plasmon resonance for determination of transferrin.* Talanta, 2006. **68**(3): p. 1026-1031.

115. Sasaki, S., R. Nagata, and I. Karube, *Novel surface plasmon resonance sensor chip functionalized with organic silica compounds for antibody attachment.* Analytica Chimica Acta, 1998. **368**(1-2): p. 71-76.

116. Jeon, B.-J., M.-H. Kim, and J.-C. Pyun, *Application of a functionalized parylene film as a linker layer of SPR biosensor.* Sensors and Actuators, B Chemical, 2011. **B154**(2): p. 89-95.

117. Guedon, P., et al., *Characterization and Optimization of a Real-Time, Parallel, Label-Free, Polypyrrole-Based DNA Sensor by Surface Plasmon Resonance Imaging.* Anal. Chem., 2000. **72**(24): p. 6003-6009.

118. Kim, H.-C., et al., *Detection of C-reactive protein on a functional poly(thiophene) self-assembled monolayer using surface plasmon resonance.* Ultramicroscopy, 2008. **108**(10): p. 1379-1383.

119. Albers, W.M., et al., *Structural and functional characteristics of chimeric avidins physically adsorbed onto functionalized polythiophene thin films.* ACS Applied Materials & Interfaces, 2012: p. Ahead of Print.

120. Kim, H.-C., et al., *A reactive polythiophene for protein immobilization.* Polymers for Advanced Technologies, 2009. **20**(3): p. 298-302.

121. Lepinay, S., et al., *In-situ polymerized molecularly imprinted polymeric thin films used as sensing layers in surface plasmon resonance sensors: Mini-review focused on 2010-2011.* Chem. Pap., 2012. **66**(5): p. 340-351.

122. Wulff, G., *Molecular imprinting in crosslinked materials with the aid of molecular templates - a way towards artificial antibodies.* Angew. Chem., Int. Ed. Engl., 1995. **34**(17): p. 1812-32.

123. Henry, O.Y.F., D.C. Cullen, and S.A. Piletsky, *Optical interrogation of molecularly imprinted polymers and development of MIP sensors: a review.* Analytical & Bioanalytical Chemistry, 2005. **382**(4): p. 947-956.

124. Pernites, R., et al., *Electropolymerization molecularly imprinted polymer (E-MIP) SPR sensing of drug molecules: Pre-polymerization complexed terthiophene and carbazole electroactive monomers.* Biosensors & Bioelectronics, 2011. **26**(5): p. 2766-2771.

125. Sharma, P.S., et al., *Electrochemically synthesized polymers in molecular imprinting for chemical sensing.* Analytical and Bioanalytical Chemistry, 2012. **402**(10): p. 3177-3204.

126. Seydack, M., *Immunoassays: basic concepts, physical chemistry and validation.* Springer Series on Fluorescence, 2008. **6**(Standardization and Quality Assurance in Fluorescence Measurements II): p. 401-428.

127. Makin, H.L.J. and D.B.E. Gower, *Steroid Analysis, 2nd ed*. 2010.

128. Wang, J. and H.S. Zhou, *Aptamer-Based Au Nanoparticles-Enhanced Surface Plasmon Resonance Detection of Small Molecules.* Analytical Chemistry (Washington, DC, United States), 2008. **80**(18): p. 7174-7178.

129. Henseleit, A., et al., *A compact and rapid aptasensor platform based on surface plasmon resonance.* Engineering in Life Sciences, 2011. **11**(6): p. 573-579.

130. Lee, S.J., et al., *ssDNA Aptamer-Based Surface Plasmon Resonance Biosensor for the Detection of Retinol Binding Protein 4 for the Early Diagnosis of Type 2 Diabetes.* Analytical Chemistry (Washington, DC, United States), 2008. **80**(8): p. 2867-2873.

131. Sheehan, J.C., P.A. Cruickshank, and G.L. Boshart, *Convenient synthesis of water-soluble carbodiimides.* Journal of Organic Chemistry, 1961. **26**: p. 2525-8.

132. Sheehan, J.C., J. Preston, and P.A. Cruickshank, *Rapid synthesis of oligopeptide derivatives without isolation of intermediates.* Journal of the American Chemical Society, 1965. **87**(11): p. 2492-3.

133. Davies, C., *Concepts.* Immunoassay Handbook, (2nd Edition), 2001: p. 78-110.

134. Choi, J.-W., et al., *Ultra-sensitive surface plasmon resonance based immunosensor for prostate-specific antigen using gold nanoparticle-antibody complex.* Colloids and Surfaces, A Physicochemical and Engineering Aspects, 2008. **313+314**: p. 655-659.

135. Pieper-Fuerst, U., W.F.M. Stoecklein, and A. Warsinke, *Gold nanoparticle-enhanced surface plasmon resonance measurement with a highly sensitive quantification for human tissue inhibitor of metalloproteinases-2.* Analytica Chimica Acta, 2005. **550**(1-2): p. 69-76.

136. Abuchowski, A., et al., *Alteration of immunological properties of bovine serum albumin by covalent attachment of polyethylene glycol.* Journal of Biological Chemistry, 1977. **252**(11): p. 3578-81.

137. Savoca, K.V., et al., *Preparation of a non-immunogenic arginase by the covalent attachment of polyethylene glycol.* Biochimica et Biophysica Acta (BBA) - Protein Structure, 1979. **578**(1): p. 47-53.

138. Otsuka, H., Y. Nagasaki, and K. Kataoka, *PEGylated nanoparticles for biological and pharmaceutical applications.* Advanced Drug Delivery Reviews, 2003. **55**(3): p. 403-419.

139. Li, L., et al., *Protein Adsorption on Oligo(ethylene glycol)-Terminated Alkanethiolate Self-Assembled Monolayers: The Molecular Basis for Nonfouling Behavior.* Journal of Physical Chemistry B, 2005. **109**(7): p. 2934-2941.

140. Yu, Q., et al., *Anti-fouling bioactive surfaces.* Acta Biomaterialia, 2011. **7**(4): p. 1550-1557.

141. Prime, K. and G. Whitesides, *Self-assembled organic monolayers: model systems for studying adsorption of proteins at surfaces.* Science, 1991. **252**(5009): p. 1164-1167.

142. Harder, P., et al., *Molecular Conformation in Oligo(ethylene glycol)-Terminated Self-Assembled Monolayers on Gold and Silver Surfaces Determines Their Ability To Resist Protein Adsorption.* The Journal of Physical Chemistry B, 1998. **102**(2): p. 426-436.

143. Ostuni, E., et al., *A Survey of Structure−Property Relationships of Surfaces that Resist the Adsorption of Protein.* Langmuir, 2001. **17**(18): p. 5605-5620.

144. Frens, G., *Controlled nucleation for the regulation of the particle size in monodisperse gold suspensions.* Nature (London), Physical Science, 1973. **241**(105): p. 20-2.

145. Turkevich, J., P.C. Stevenson, and J. Hillier, *The nucleation and growth processes in the synthesis of colloidal gold.* Discuss. Faraday Soc., 1951. **No. 11**: p. 55-75.

146. Henderson, K.M., et al., *Concentrations of oestrone sulphate in milk during pregnancy in dairy cows* Proceedings of the New Zealand Society of Animal Production, 1992. **52**: p. 17-20.

147. Elder, P.A., L. Manley, and J.G. Lewis, *Use of monoclonal antibody to estrone 3-glucuronide in an enzyme-linked immunosorbent assay (ELISA).* Journal of Steroid Biochemistry, 1990. **36**(5): p. 439-43.

148. Kumar, S., J. Aaron, and K. Sokolov, *Directional conjugation of antibodies to nanoparticles for synthesis of multiplexed optical contrast agents with both delivery and targeting moieties.* Nat. Protoc., 2008. **3**(2): p. 314-320.

149. Carroll, F.I., et al., *The Synthesis of Haptens and Their Use for the Development of Monoclonal Antibodies for Treating Methamphetamine Abuse.* Journal of Medicinal Chemistry, 2009. **52**(22): p. 7301-7309.

150. Yu, Q., et al., *Detection of low-molecular-weight domoic acid using surface plasmon resonance sensor.* Sensors and Actuators, B: Chemical, 2005. **B107**(1): p. 193-201.

151. Lotierzo, M., et al., *Surface plasmon resonance sensor for domoic acid based on grafted imprinted polymer.* Biosensors & Bioelectronics, 2004. **20**(2): p. 145-152.

152. Kim, S.J., et al., *Novel miniature SPR immunosensor equipped with all-in-one multi-microchannel sensor chip for detecting low-molecular-weight analytes.* Biosensors & Bioelectronics, 2007. **23**(5): p. 701-707.

153. Traynor, I.M., et al., *Immunobiosensor detection of domoic acid as a screening test in bivalve molluscs: comparison with liquid chromatography-based analysis.* Journal of AOAC International, 2006. **89**(3): p. 868-872.

154. Le Berre, M. and M. Kane, *Biosensor-based assay for domoic acid: comparison of performance using polyclonal, monoclonal, and recombinant antibodies.* Analytical Letters, 2006. **39**(8): p. 1587-1598.

155. Kawatsu, K., Y. Hamano, and T. Noguchi, *Production and characterization of a monoclonal antibody against domoic acid and its application to enzyme immunoassay.* Toxicon, 1999. **37**(11): p. 1579-1589.

156. Perrin, D.D. and W.L.F. Armarego, *Purification of Laboratory Chemicals. 3rd Ed*. 1988: Pergamon Press. 391 pp.

157. Lawrence, J.F., et al., *Liquid chromatographic determination of domoic acid in shellfish products using the paralytic shellfish poison extraction procedure of the association of official analytical chemists.* Journal of Chromatography A, 1989. **462**(0): p. 349-356.

158. Sugimoto, R., et al., *Preparation of soluble polythiophene derivatives utilizing transition metal halides as catalysts and their property.* Chemistry Express, 1986. **1**(11): p. 635-8.

159. Hassan, N., et al., *Rheological properties of ovalbumin hydrogels as affected by surfactants addition.* International Journal of Biological Macromolecules, 2011. **48**(3): p. 495-500.

160. Hanna, G.F. and J.F. Foster, *Streaming orientation studies on denatured proteins. IV. Denaturation of ovalbumin with surface-active ions.* Journal of Physical Chemistry, 1953. **57**: p. 614-17.

161. Vashist Sandeep, K., *A method for regenerating gold surface for prolonged reuse of gold-coated surface plasmon resonance chip.* Anal Biochem, 2012. **423**(1): p. 23-5.

162. Liedberg, B., I. Lundstroem, and E. Stenberg, *Principles of biosensing with an extended coupling matrix and surface plasmon resonance.* Sensors and Actuators, B Chemical, 1993. **B11**(1-3): p. 63-72.

163. Löfås, S., et al., *Bioanalysis with surface plasmon resonance.* Sensors and Actuators B: Chemical, 1991. **5**(1–4): p. 79-84.

164. Hosoda, H., S. Miyairi, and T. Nambara, *Studies on steroids. Part CLV. Synthesis of corticosteroid haptens possessing the bridge at the C-4 position.* Chemical & Pharmaceutical Bulletin, 1980. **28**(4): p. 1294-9.

165. Yoshida, H., et al., *Synthesis of 11alpha -hydroxyprogesterone haptens.* Steroids, 1989. **53**(6): p. 727-38.

166. Hosoda, H., et al., *Studies on steroids. CLXXIV. Synthesis of haptens for use in immunoassays of Delta 4-3-keto steroids.* Chemical & Pharmaceutical Bulletin, 1982. **30**(1): p. 202-5.